AFCRL-69-0152

Distribution of this document is unlimited. It may be released to the Clearinghouse, Department of Commerce, for sale to the general public

AD 687751

128

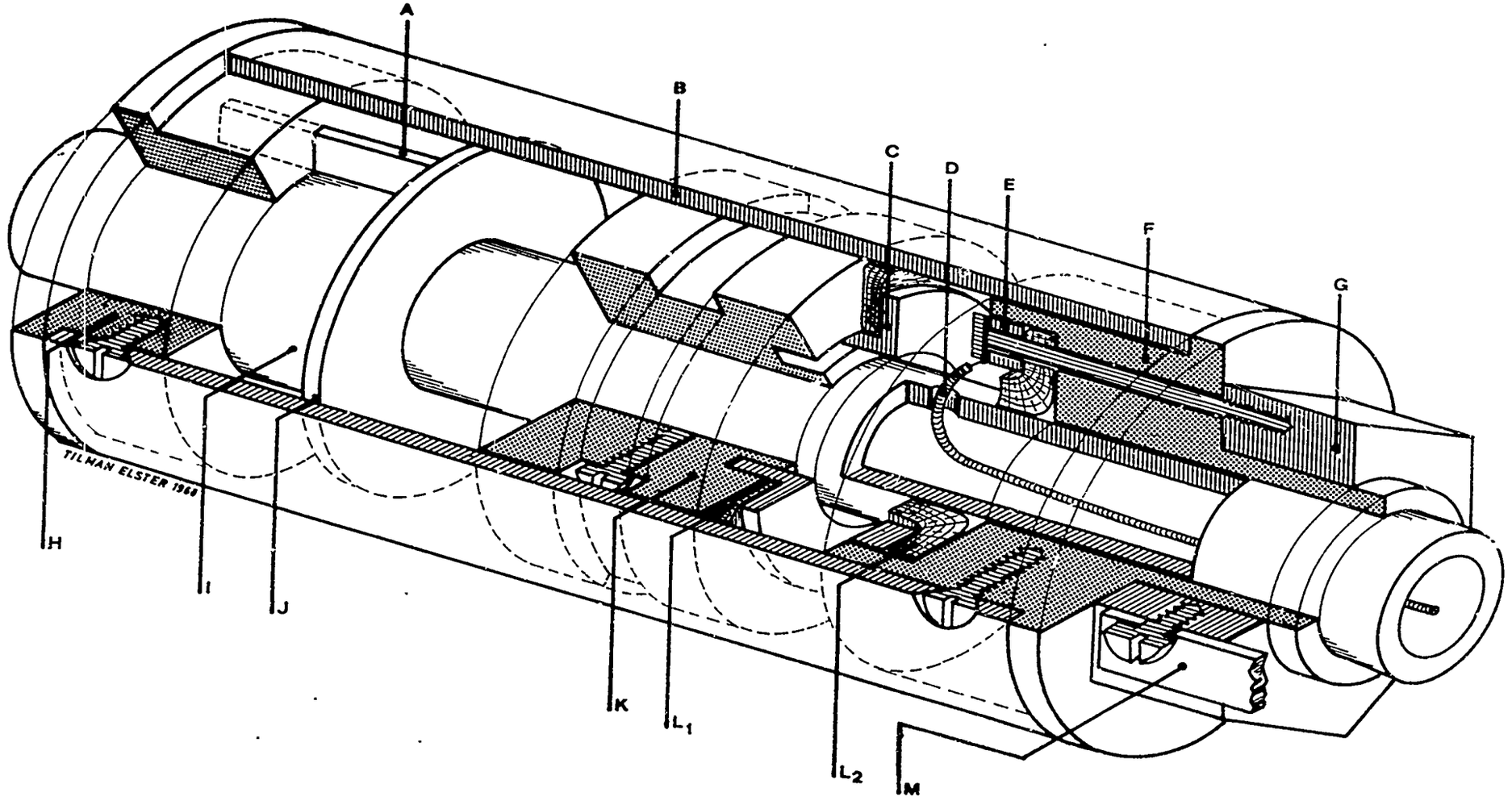

Fig.: 5.1

CONTRACT 61(052)-902 31 December 1968

AFCRL-69-0152

FINAL SCIENTIFIC REPORT

for

CONTRACT 61(052)-902

ON THE PROPAGATION OF VLF WAVES IN SOLIDS AND LIQUIDS

Univ. Doz. Dr. W. BITTERLICH
VLF PROJECT INNSBRUCK
AUSTRIA

THIS RESEARCH HAS BEEN SPONSORED IN PART BY THE
UNITED STATES GOVERNMENT UNDER CONTRACT 61(052)-902.

PREFACE

The present report is a final report, a summary of the research work done in the years 1966, 1967 and 1968 under Contract No. 61(052)-902, which was the second period of contract since fall 1960. It is not intended, however, to summarize all the work and results in abstract form, but to report mainly the work of 1968. The tables of contents of the Annual Reports of 1966 and 1967 as well as a list of the titles of scientific reports shall give a review of the entire period of contract.

The main program of the research work of 1968 was the examination of helical antennas, the propagation of electromagnetic waves of medium frequencies through the interior of the earth and the influence of electric rock parameters on the directivity pattern of antennas and also on the wave propagation. Further studies are concerned with the determination of rock conductivity and dielectric constant from field diagram measurements. The present report is wound off with newly commenced geophysical studies on the electrical conduction mechanism in rock and a contacting probe as well as an examination of problems of recording atmospheric noise signals. Those whose interest does not concentrate on the scientific studies are recommended to read the chapter "What happened in 1968".

The fact that so much work could be done is entirely due to my co-workers, because an obstinate disease forced me to reduce my work to advisory activity only. I wish to thank my co-workers and ALL PERSONS WHO ASSISTED US in our work. I want to express my special gratitude to the following firms for their great help:

Montanwerke Brixlegg, Direktor Dipl. Ing. P. Kettner
Mitterberger Kupferbergbau, Direktor Dipl. Ing. S. Biangardi
Siemens Bauelementewerk - München, Balanstraße

Tiroler Wasserkraftwerke, Jenbach, Dir. Dr. Ing. H. Wagensonner
Innerebner u. Mayer, Solbad Hall, Tirol
Jenbacher Werke.

May the work of our team be successful also in the future.

Wolfram Bitterlich

Innsbruck, December 1968.

VLF Team 1968

Contractor, head of team: Univ. Doz. Dr. Wolfram BITTERLICH

Office: Frau Beate BITTERLICH
" Herta HOWORKA

Scientific Collaborators: Dr. Norbert NESSLER
Hans WÖBKING

Thesis Graduates: Walter GRADL
Christoff GRISSEMANN
Walter KELLNER
Raphael LUKAVEC

Technical Assistance: Tilman ELSTER

ABSTRACT

In continuation of the studies on small, self-resonant helical antennas, impedance, current distribution and antenna characteristics of various antenna types were measured in air and in water.

Two methods of determining the conductivity and dielectric constant of a dissipative medium with a graphical evaluation were described as examples of applying antenna diagram measurements on frame antennas.

Radio communcation between the mines of Schwaz and St. Gertraudi was reached with a 1600 m^2 frame antenna, using a new low-noise receiving amplifier.

Preliminary geoelectrical examinations of ores were made and a measuring probe was constructed for bore hole examinations.

TABLE OF CONTENTS

TABLE OF CONTENTS

(continued) page

LIST OF FIGURES

LIST OF FIGURES

(continued)

1. MEASURED PROPERTIES OF SMALL SELF-RESONANT HELICAL ANTENNAS AT LOW FREQUENCIES FOR APPLICATION IN DISSIPATIVE MEDIA

PREFACE

The use of a wire wound on a carrier in the form of a helix as a transmitting and receiving antenna in the VLF and LF region was suggested in 1962 by the head of the VLF project. In 1964, a small transmitter was built with a helical antenna 2 m long and 6 cm in diameter, which was operated in water. This antenna had a real input resistance at 110 kHz. The propagation measurements which were observed by visitors of the AFCRL Cambridge, Mass. were highly promising so that the construction of a much larger antenna was begun in the mine of St. Gertraudi in June 1965.

The experimental examinations such as impedance and propagation measurements were made by W. Bitterlich and C. Wörz. G. Tinhofer worked on the theory of this antenna type. Numerous unsolved problems made it necessary to continue the work on this antenna type, the results being described in the present scientific report. The essential parts of this paper were presented at the '68 International IEEE/G-AP Symposium in Boston, Mass.

1.1. Introduction

When electromagnetic waves propagate through lossy media such as the earth's crust, there occurs not only an unfortunate shortening of the wavelength, but also an exponential attenuation which increases with the distance from the radiation source. Both effects lead to a rapid decrease in field strength at larger distances and make necessary the

use of low frequencies, if large distances are to be bridged.

Since, however, the available space in such cases is usually limited, only short electric or small magnetic dipoles are commonly used.

On the whole, helical antennas which are small compared to the wavelength and which have numerous turns, represent a combination of these two antenna types permitting theoretically an optimum utilization of a cylindrical cavity. Such antennas radiate in the so-called "normal mode", which naturally is not quite as effective as the "beam mode". Owing to problems of space, the latter cannot be attained at low frequencies.

1.2. Impedance measurement

For optimum application of an antenna, however, it is necessary to know the input impedance as dependent on the frequency and other parameters. Since there existed no adequate theory, various helical antennas were constructed with convenient size, whose typical behavior will be shown on two examples.

At first, the behavior of the antennas in air was examined in a laboratory of Innsbruck University, then the antennas were transferred into an old mine near St. Gertraudi (25 miles east of Innsbruck) to be examined in a cavity, at first in air and then in water. The rock in this area electrically is almost homogeneous. The mine is free of rails and other metal installations with the exception of one gallery containing rails which lead to the surface of the mountain so that transportation of heavier measuring devices is possible. A small laboratory installed half a mile inside the mountain is permanently dryed and heated with 3 kws to keep the relative humidity of the air low.

Thus, transmitters and other electronic apparatus can be repaired and left there for several weeks without being damaged by the relative humidity of the mine which is always 100%.

The most important instruments for measuring the antenna impedances and the electrical properties of the used fresh water were the impedance bridge 716-L by General Radio for a frequency range of 1-100 kHz, and for the subsequent frequency range up to 15 MHz the R-L-C bridge LE 300/A1 by Hatfield (GB). The bridges are powered by suitable battery-fed frequency generators (a powerful generator with low output impedance for frequencies between 440 kHz and 16 MHz was specially constructed by the author) and balanced to zero by the selective μv meters

TF 2330 Marconi (20 Hz - 50 kHz, bandwidth: 7 Hz)
SPM-2 Wandel u. Goltermann (4-600 kHz, bandwidth: 200 Hz)
Type2006 Brüel u. Kjaer (100 kHz - 230 MHz, bandwidth: 2,5 kHz).

Frequency is controlled by "small wonder" 100A Monsanto Counter, power-supplied by a battery and a specially constructed DC-changer.

Fig. 1.1 shows the relative electric "permittivity" of the used water, measured with a small cylindrical capacitor described in Ref. [1]. $\varepsilon_{relative}$ and the frequency in a range of 1 - 1000 kHz are plotted in a log-log scale. The conductivity (mhos/m) which is written right above the curve, changes comparatively little in this frequency range. The increase in ε at low frequencies is explained by polarization effects at the electrodes which occur in a somewhat different form also on the antennas, but not during the free propagation of electromagnetic waves.

Generally, the mutual capacity of two parallel

planes of equal surface areas in a lossy medium is given by (see Refs. [7], [8])

$$C = \frac{\varepsilon_o \varepsilon_r^o \cdot A}{d} + \frac{\varepsilon_\omega \cdot A}{d^2}$$

d ... distance between the electrodes

ε_o ... Dielectric constant of free space

ε_r^o ... relative dielectric constant of the medium under test for conductivity $\sigma \to$ zero (for water $\varepsilon_r^o \approx 80$)

A ... surface area of one electrode

ε_ω ... is a function of the frequency, conductivity of the medium, electrode material, temperature, chemical composition of the medium which causes the conductivity, and the surface quality of the electrodes.

A cylindrical capacitor is somewhat more complicated to describe, because of the difference between the surface area of the two electrodes. Therefore Fig. 1.1 can only give a rough information of the frequency dependence of

$$\varepsilon_r^o + \varepsilon_\omega = \varepsilon_r$$

but gives some idea of what one has to expect putting a bare wire antenna in such a medium.

Now to the antennas themselves.

The first antenna of this series consisted of 200 meters of "insulated" copper wire, 1,5 mm in diameter, which was wound on a carrier of impregnated wood, 2m long, in such a way that the length of one turn was 1 m, that means the antenna had 200 turns and a pitch of 1 cm. The antenna was fed in the middle. (At this point the insulation should be mentioned. It was found that in water the insulation of the wire was good for nothing. The water penetrated very rapidly into the insulation material and finally reached the copper wire. During this time a continuous change of the input

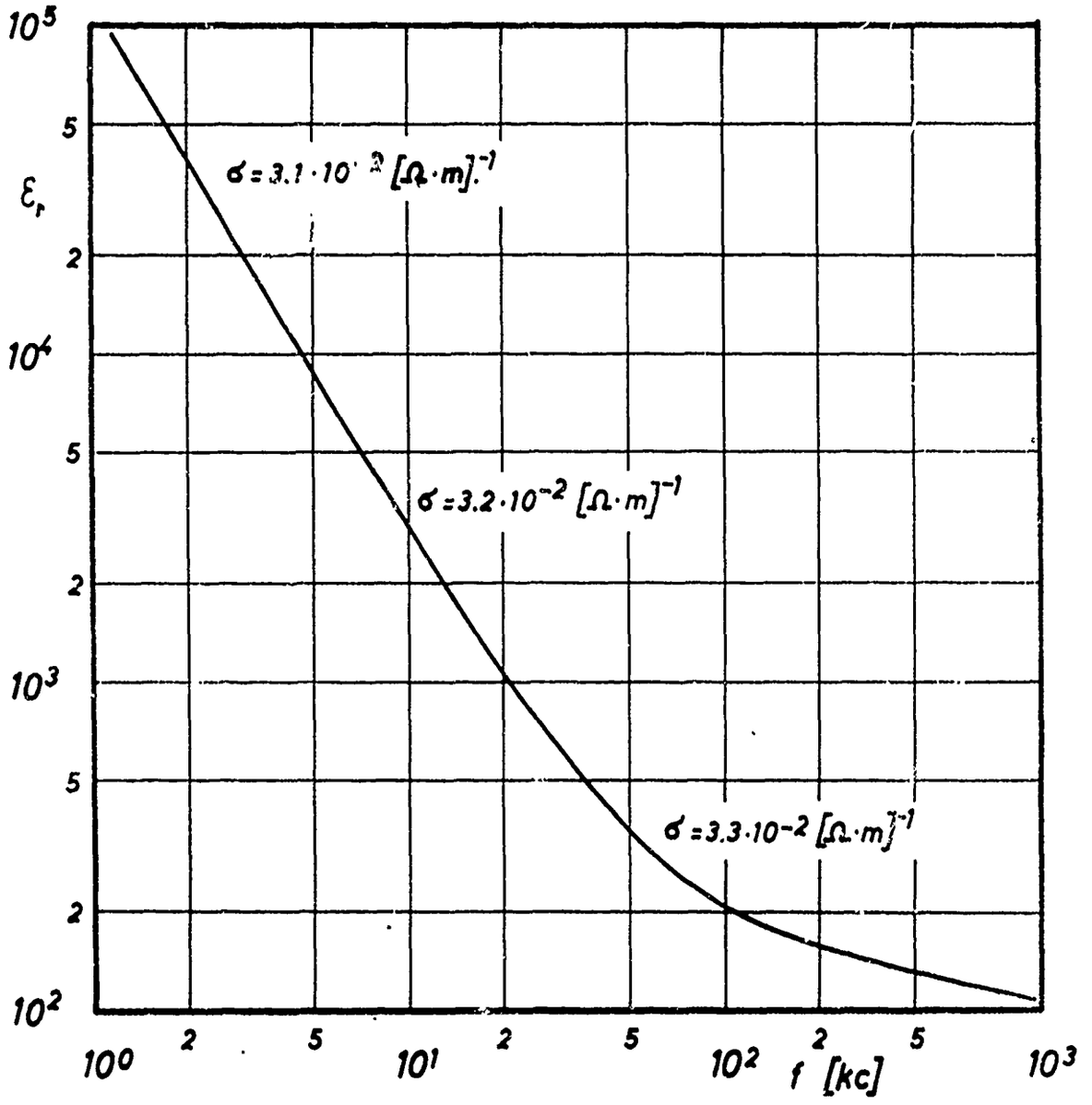
10^5
5
ε_r
2
10^4
5
2
10^3
5
2
10^2
$\sigma = 3.1 \cdot 10^{-2}$ [Ω·m]$^{-1}$
$\sigma = 3.2 \cdot 10^{-2}$ [Ω·m]$^{-1}$
$\sigma = 3.3 \cdot 10^{-2}$ [Ω·m]$^{-1}$
10^0 2 5 10^1 2 5 10^2 2 5 10^3
f [kc]

FIG. 1.1

impedance was observed. After a "saturation time" of about one hour the input impedance was stable so that the wire acted nearly as a bare one.)

Fig. 1.2 shows the input impedance of this antenna measured in air. The scale for the real and imaginary parts as abscissa is quadratic, whereas the scale for the frequency as ordinate is linear. Between 1,1 and 1,4 MHz, the antenna has the two lowest resonance points. The first one at 1,151 MHz is a series resonance with 66 ohms input resistance, the second one at 1,312 MHz is a non-harmonic parallel resonance with an input resistance of 15 kohms.

These values remain the same when the antenna is set up in the mine, if the cavity in which it is located has a diameter of at least twice the maximum antenna dimension. If the cavity is smaller, the resonant frequencies decrease slightly, whereas the input resistance at series resonance increases considerably.

These properties can be explained on a network model which is correct at least in the neighborhood of the lowest resonant frequency and below.

The phase velocity along the axis is then given by

$$v_{axis} = \frac{1}{\sqrt{\bar{L}_1 \cdot \bar{C}_1}} \quad \left[\frac{m}{sec}\right] \qquad (1.1)$$

where $\bar{L}_1$ is the mean inductivity per unit length, given by (see Ref. [2])

$$\bar{L}_1 = \frac{\mu_o \cdot \cot^2 \psi}{4\pi} \quad \left[\frac{H}{m}\right] \qquad (1.2)$$

μ_o ... $4\pi \cdot 10^{-7}$ $\left[\frac{H}{m}\right]$

ψ ... pitch angle

C_1, the mean capacity per unit length so far can only be measured at frequencies that are very low as compared to the first resonant frequency (condition: The antenna must be carefully dried, because even little humidity leads to an increase in C_1 at lower frequencies due to polarization effects.)

From formula (1.1) the first resonant frequency can be calculated as

$$f_r = \frac{v_{axis}}{\lambda_{axis}} \quad [Hz]$$

where λ_{axis} is twice the axial length of the antenna. This of course is valid for both air and water as surrounding media.

The input resistance at the lowest resonant frequency can be calculated from the expression of an open-end transmission line (see for example Ref. [3]) as follows:

$$R_e(0) = \bar{Z} \cdot \frac{e^{2\beta l} - e^{-2\beta l} - 2i \sin(2\alpha l)}{e^{2\beta l} + e^{-2\beta l} - 2\cos(2\alpha l)} \quad \text{if } \beta \ll \alpha \Rightarrow \bar{Z} \approx \bar{Z} \quad (1.3)$$

where

$$\alpha = \frac{2\pi}{\lambda}$$

$$\beta = \frac{\bar{R}_1}{2\bar{Z}} + \frac{\bar{G}_1 \cdot \bar{Z}}{2}$$

λ = wavelength along the helix axis
$\bar{Z}$ = mean characteristic impedance
$\bar{R}_1$ = mean series resistance per unit length
$\bar{G}_1$ = mean shunt conductance per unit length

for $l = \frac{\lambda}{4}$ (first resonance frequency) follows

$-2i \sin(2\alpha l) = -2i \sin \pi = 0$ and

$-2 \cos(2\alpha l) = -2 \cos \pi = +2$

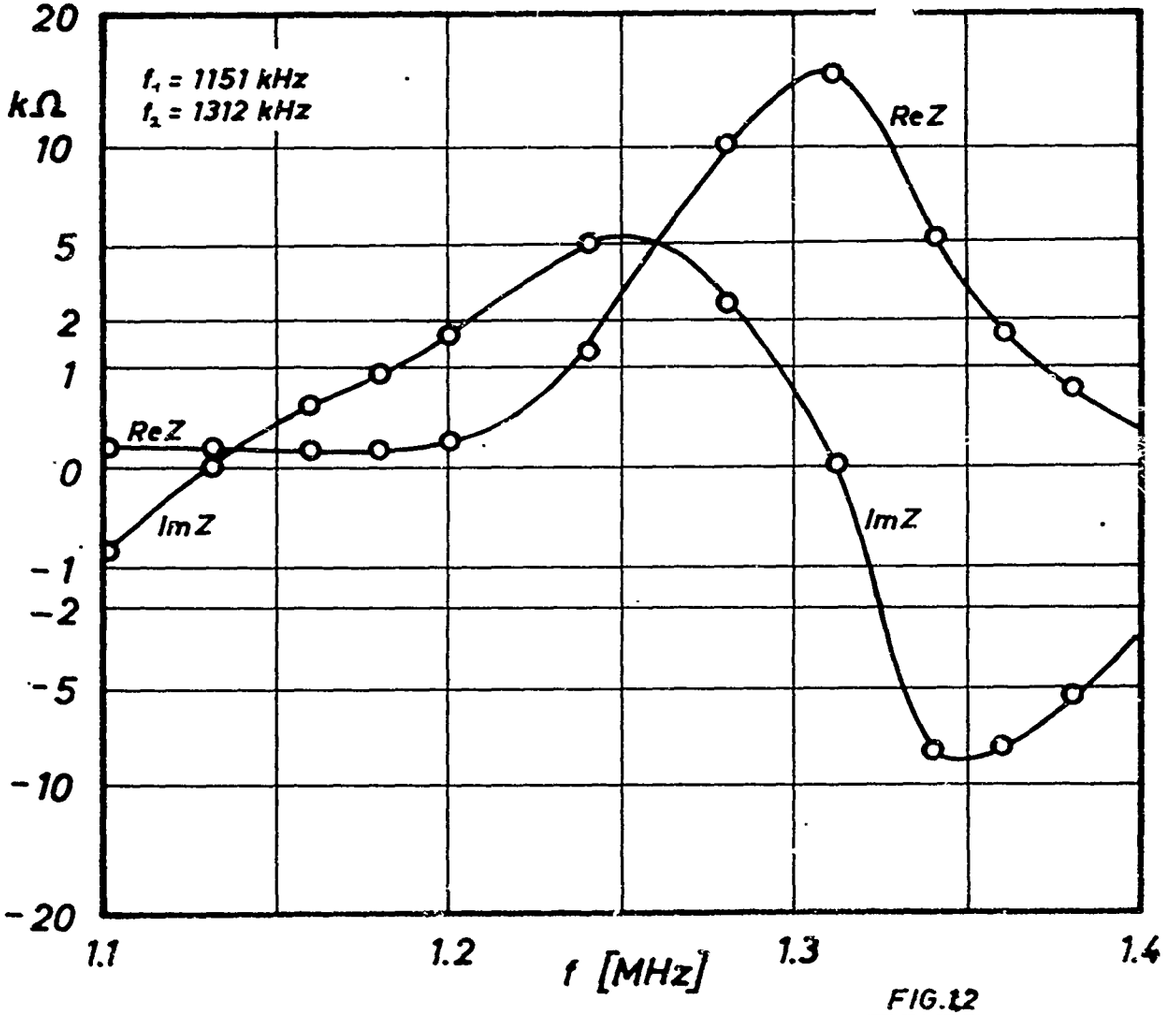
20
kΩ
10
5
2
1
0
-1
-2
-5
-10
-20
f_1 = 1151 kHz
f_2 = 1312 kHz
ReZ
ImZ
ReZ
ImZ
1.1
1.2
f [MHz]
1.3
1.4

FIG.12

so that formula (1.3) writes as

$$R(0) = Z \cdot \frac{\sinh(2\beta l)}{\cosh(2\beta l)+1} \quad (l = \frac{\lambda}{4}) \qquad (1.4)$$

For $(2\beta l) < 0,2$ (usually the case for these antennas in air) and a maximum error of 1/2% ($2\beta l < 0,3$ error $< 1\%$)
($2\beta l < 1$ error $< 8,1\%$)
formula (1.4) can be written as

$$R_e(0) = Z \cdot \beta l \qquad (1.5)$$

and finally substituting for β:

$$R_e(0) = \frac{Z^2 G_1 l}{2} + \frac{R_1 \cdot l}{2} \qquad (1.6)$$

The electric data of the antenna described at first are the following

$\bar{L}_1 = 10^{-3}$ [H/m]
$\bar{C}_1 = 4,8 \cdot 10^{-11}$ [F/m]
$\cot\psi = 100$
$\bar{v}_{axis} = 4,56 \cdot 10^{6}$ [m/sec]
$\bar{v}_{wire} = 4,56 \cdot 10^{8}$ [m/sec]

the phase velocity factor p

$$p = \frac{\bar{v}_{wire}}{c_o} = 1,52 \quad (c_o = \text{velocity of light in free space})$$

This is very different from the behavior of antennas operating in the beam mode which have a $p \leqslant 1$.

$$\bar{Z} = \sqrt{\frac{\bar{L}_1}{\bar{C}_1}} = 1,45 \quad k\Omega$$

In equation (1.6), the first term on the right side represents the dielectric losses caused by the carrier material and of the environment, respectively. The second term gives the ohmic wire losses.

Since $\bar{R}_1$ is only 2 ohms and $\underline{l}$ is 1 meter, whereas the input resistance is 66 ohms, it follows that the majority of losses are dielectric losses that can be reduced by reducing $\bar{Z}$, for example by increasing the capacitance.

For this reason and mainly because of the reduction in resonant frequency, tests have been made with the antennas being submerged in water.

Fig. 1.3 shows the obtained impedance curve for the antenna in water: Here, the ordinate is the real part and the abscissa is the imaginary part of the input resistance, frequency being the parameter. The first resonance has decreased to 49 kHz which corresponds to a relative ε of 550. Despite the conductivity of water (given in Fig. 1.1), the input resistance increased to no more than 71 ohms.

Since the resonant frequencies for this antenna for both cases in air and in water were too high owing to attenuation in rock and in water, and since there were no suitable transmitters and receivers available for these frequencies, new antennas were built.

The most recent and most interesting antenna is shown in Fig. 1.4: On a carrier made of six hard PVC tubes, there are 772 turns of insulated copper wire, 1,5 mm in diameter, mounted in six chambers. One turn again has a length of 1 meter, the total length of the antenna axis being again 2 meters. The picture was taken in the mine of St. Gertraudi and shows also the stand on which the antenna is mounted and the battery-powered transmitter made by W. Kellner, member of the VLF-team.

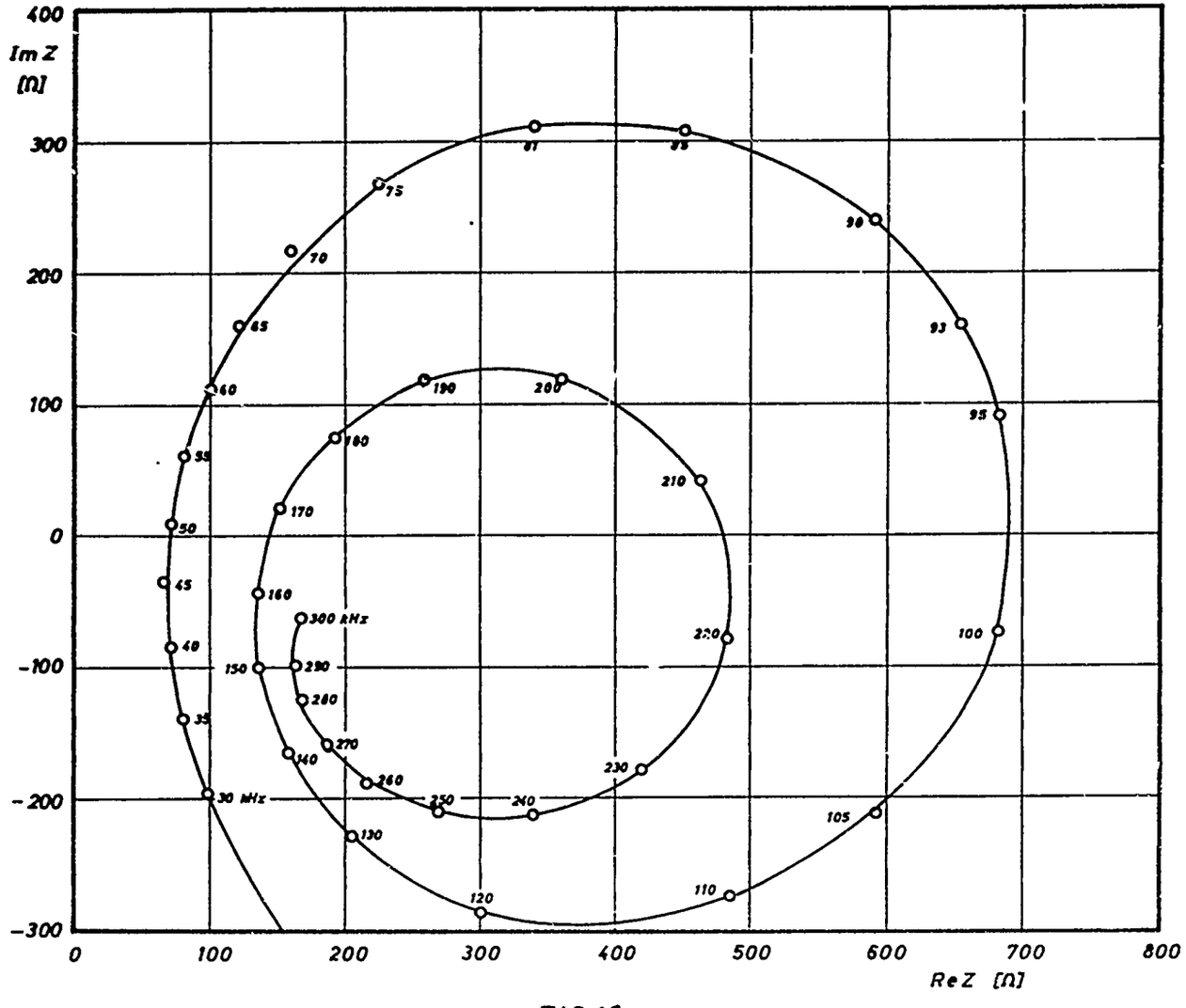
400
Im Z
[Ω]
300
200
100
0
-100
-200
-300
0
100
200
300
400
500
600
700
800
Re Z [Ω]
300 kHz
30 MHz
50
45
40
35
55
60
65
70
75
81
85
90
93
95
100
105
110
120
130
140
150
160
170
180
190
200
210
220
230
240
250
260
270

FIG.13

Fig. 1.5 gives the input impedance of this antenna in air, with the first resonance at 294 kHz with 85 ohms input resistance. The antenna has a Q of 126 and a bandwidth of 2,3 kHz. The dielectric losses are again much higher than the ohmic losses which are only 8 ohms.

Furthermore, this antenna has the following data:

$$\bar{L}_1 = 14{,}7 \quad [\mathrm{mH/m}]$$

$$\bar{C}_1 = 50 \quad [\mathrm{pF/m}]$$

$$\cot \psi = 384$$

$$v_{axis} = 1{,}17 \cdot 10^6 \ \mathrm{m/sec}$$

$$v_{wire} = 4{,}5 \cdot 10^8 \ \mathrm{m/sec}$$

$$p = \frac{v_{wire}}{c_o} = 1{,}5$$

$$\bar{Z} = 17{,}2 \ \mathrm{k\Omega}$$

This antenna was also put into the water chamber in the mine of St. Gertraudi.

Fig. 1.6 presents a map of the central part of the mine. It shows Basin I and the pumping station P from where the water is transferred into the water chamber called "Mabuse" through 180 m of special rubber hose having a clear width of 100 mm. "Mabuse" has a capacity of 10.000 gallons and can be filled or emptied within one hour if necessary. Point A indicates the source from which Basin I is permanently filled. The underground laboratory is located 45 m south of point P. Basin II increases the storage capacity during dry-weather periods. For more detailed information please see Ref. [1] pp 3-5.

Fig. 1.7 shows the antenna in the water chamber which is completely filled with water during the measurements.

Fig. 1.8 gives the impedance curve of the antenna in this situation. The lowest resonance lies at 5,50 kHz which means a relative ε of 2850. The input resistance in this case is 122 ohms, which is somewhat more than under "ideal conditions" in air. The bandwidth of 1,5 kHz yields a Q of 3,66. The characteristic impedance $\bar{Z}$ is no more than 322 ohms (at 5,5 kHz only because $\bar{C}_2$ is a function of frequency due to the polarization effects). This low $\bar{Z}$ explains the relatively low input resistance, although damping by conductivity is quite high (β = 0,377, $2\beta l$ = = 0,755). (The error using formula (1.5) instead of formula (1.4) is still smaller than 5 per cent).

1.3 Current distribution

Equally important as the impedance behavior of an antenna is the current distribution. The main difficulty when measuring the current distribution of small self-resonant helical antennas is their capacitive sensitivity. This fact represents a serious limitation for the accuracy of measurements. However, an accuracy of less than 10% could be realized using the Hewlett-Packard AC-Current Probe Type 456 A in connection with one of the selective µv-meters with high input impedance.

The current distribution at resonant frequencies is a cosine or a sine function which, as far as the field strength is concerned, is an advantage of about 27% as compared to the linear current drop of a short wire of the same length as the helix axis and equal input current.

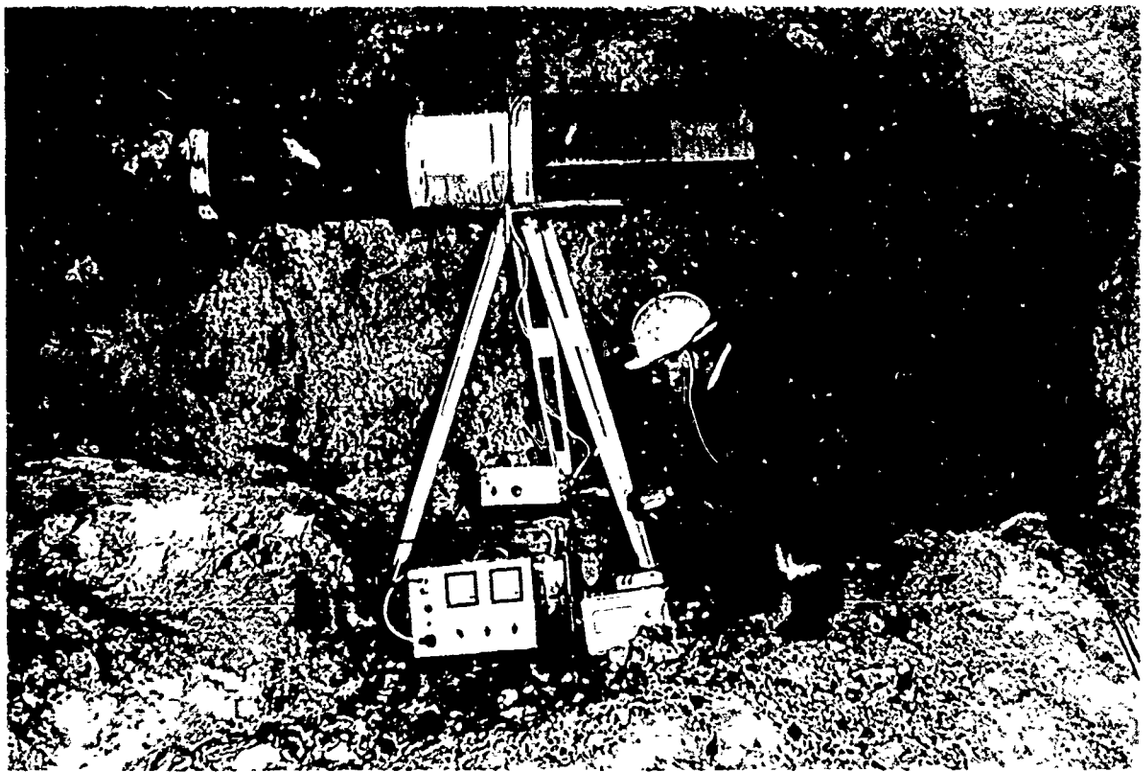

BILD I (Fig. 1.4)

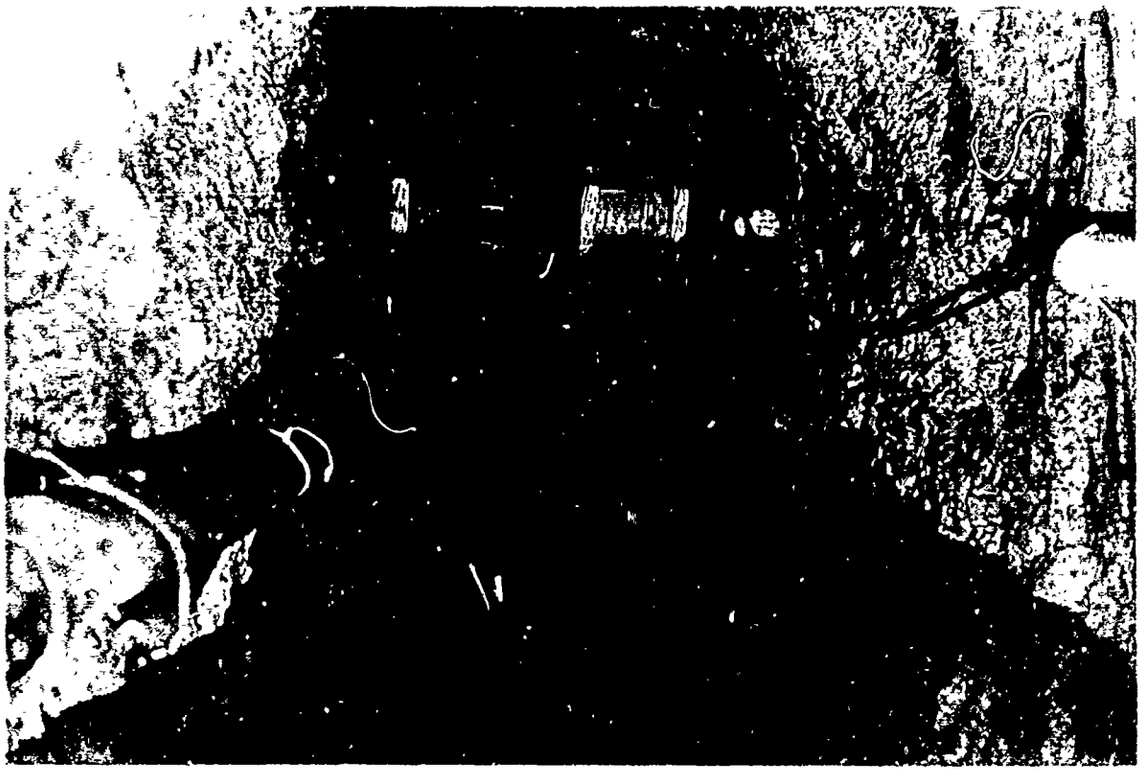

BILD II (Fig. 1.7)

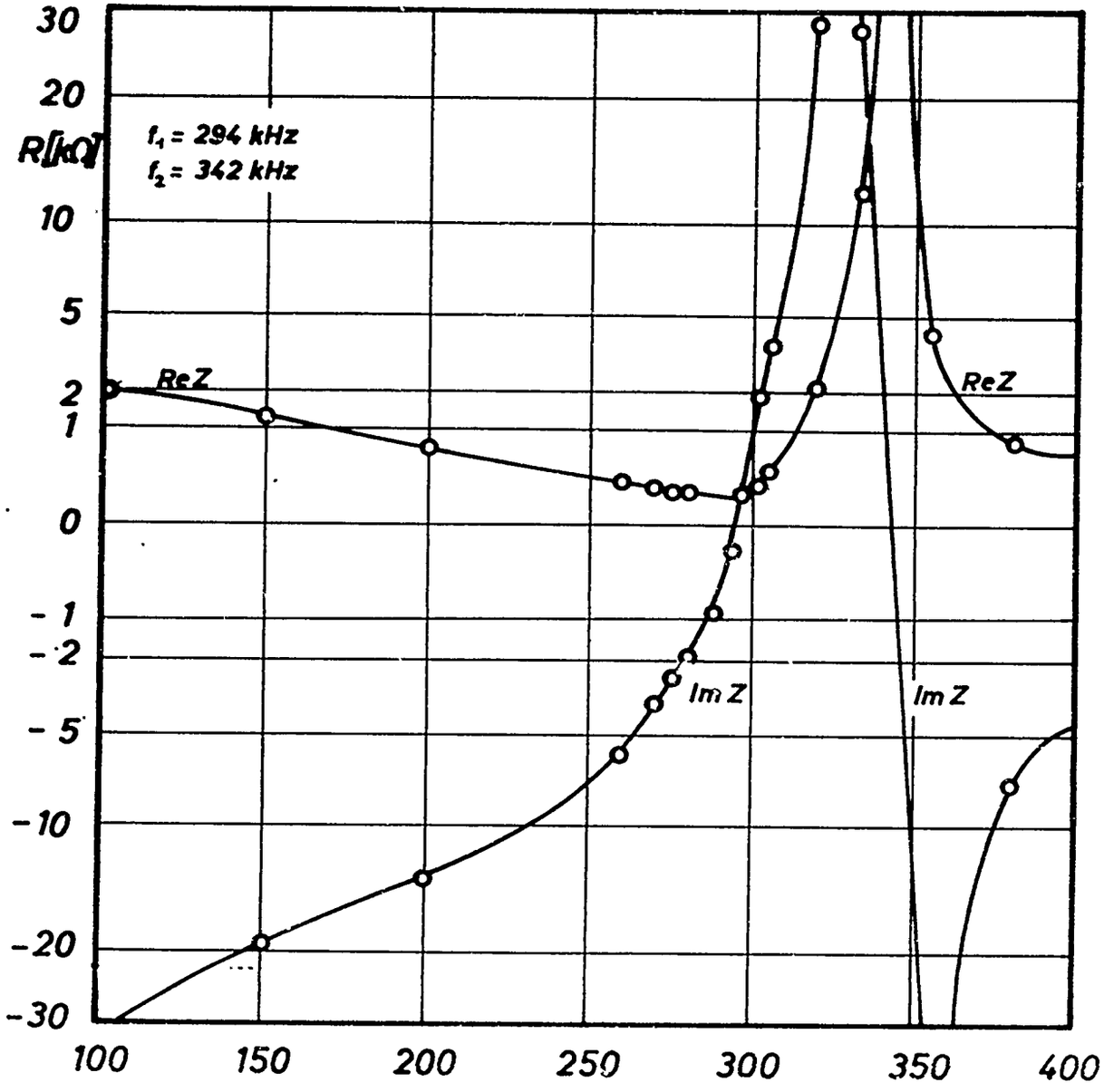
30
20
R[kΩ]
10
5
2
1
0
-1
-2
-5
-10
-20
-30
f1 = 294 kHz
f2 = 342 kHz
ReZ
ReZ
ImZ
ImZ
100
150
200
250
300
350
400
f [kHz]

FIG.1.5

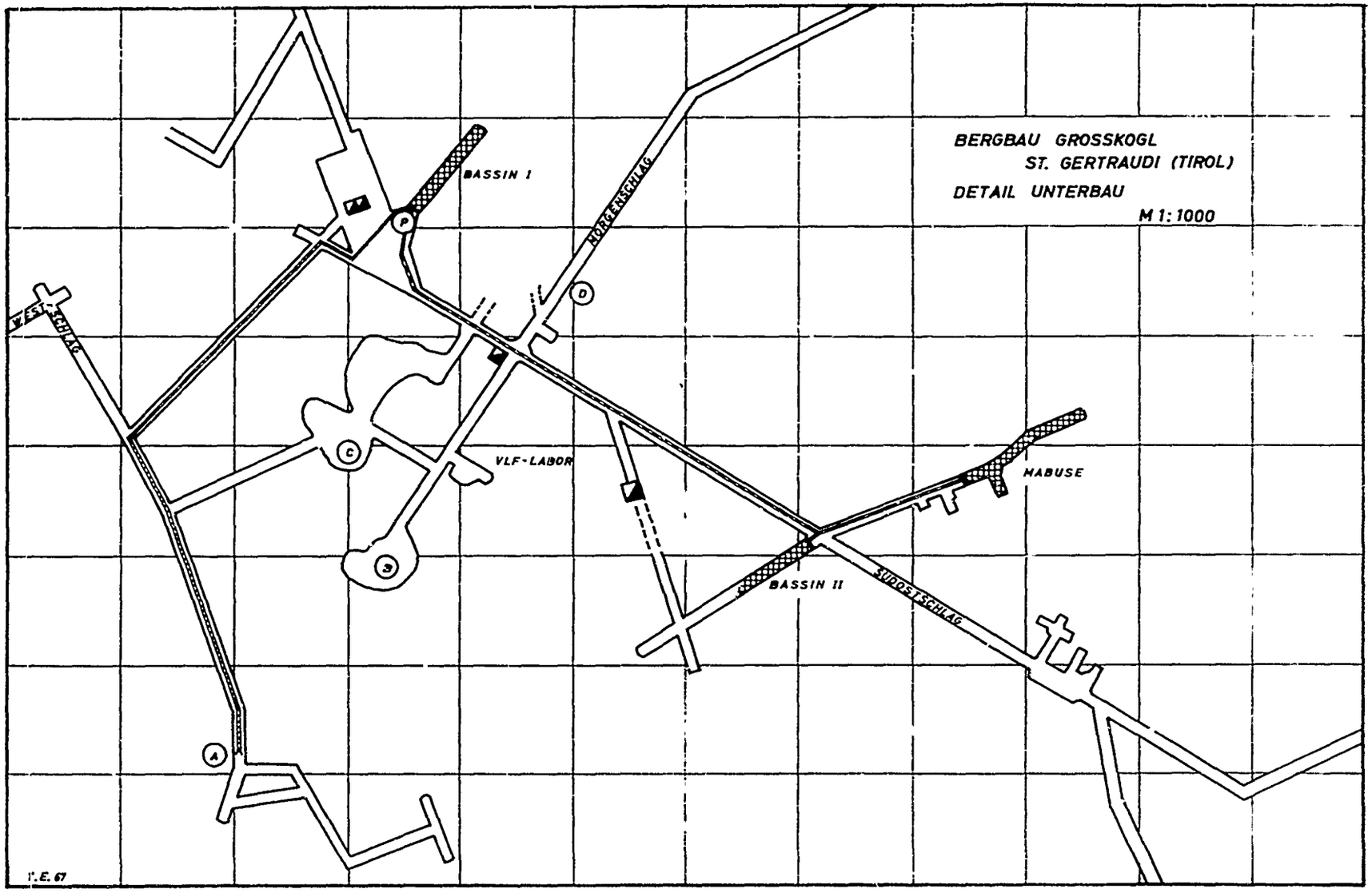
BERGBAU GROSSKOGL
ST. GERTRAUDI (TIROL)
DETAIL UNTERBAU
M 1:1000
BASSIN I
HORIZONTSCHLAG
WESTSCHLAG
VLF-LABOR
MABUSE
BASSIN II
SUDOSTSCHLAG
A
B
C
D
P
T.E. 67

FIG.16

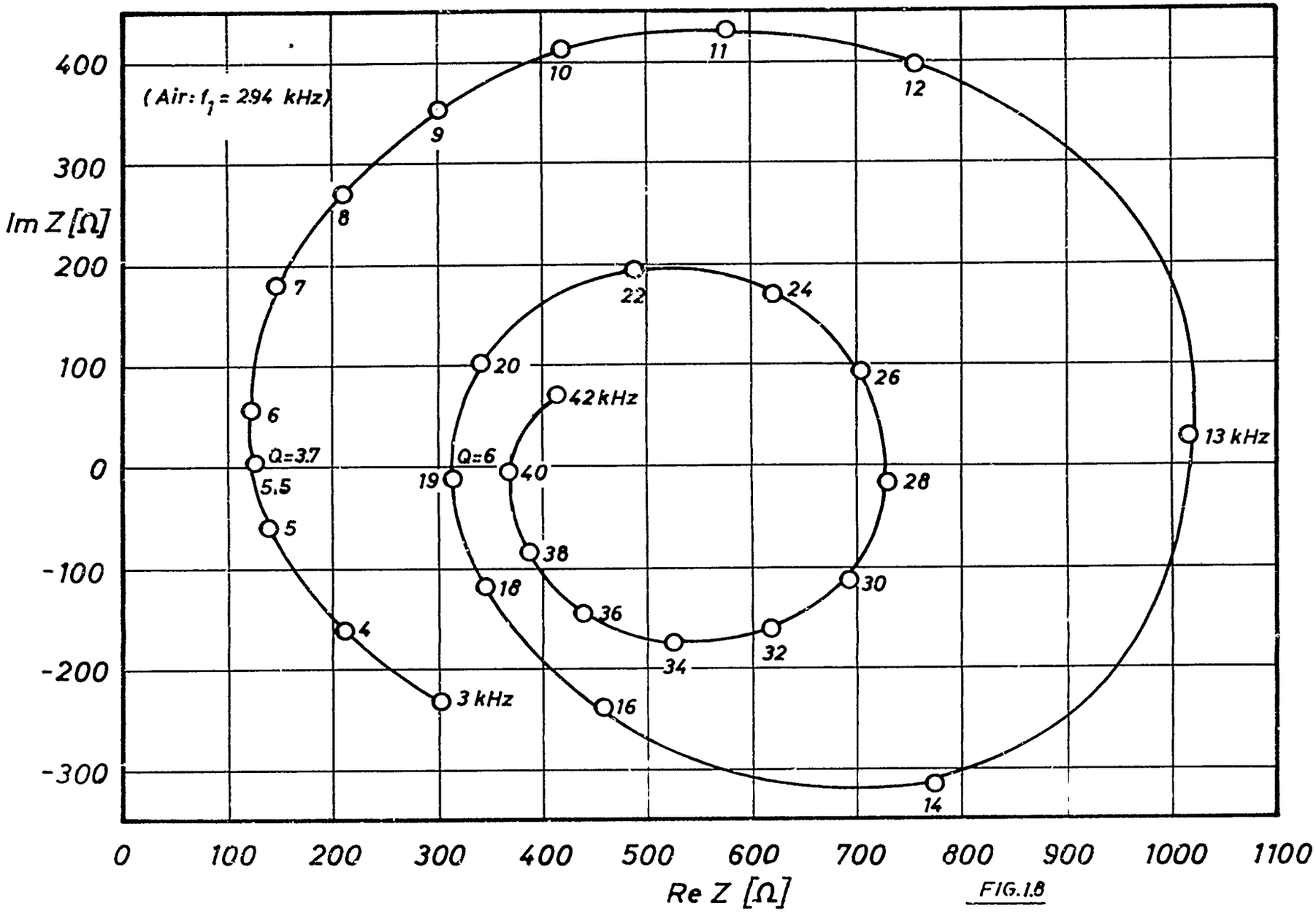
(Air: f_1 = 294 kHz)
400
300
200
100
0
-100
-200
-300
Im Z [Ω]
0
100
200
300
400
500
600
700
800
900
1000
1100
Re Z [Ω]
3 kHz
4
5
5.5
Q=3.7
6
7
8
9
10
11
12
13 kHz
14
16
18
19
Q=6
20
22
24
26
28
30
32
34
36
38
40
42 kHz

FIG.1.8

1.4 Field strength measurements

Before starting propagation measurements in a mine, the correctness of the mining chart has to be checked. Therefore, a completely new survey of the mine was made during the installation work. Thus, a number of discrepancies between the old mining charts and the actual distances could be eliminated.

Let us now discuss the fields of these antennas. It is sufficient to measure either the electric or the magnetic field strength components. Decision was taken in favor of the magnetic components, because magnetic antennas (e.g., small ferrite rod antennas) are easier to balance and have no capacitive sensitivity. As mentioned at the beginning, these helical antennas represent a combination of one electric and one magnetic dipole both having the direction of the helix axis. This gives three components of induction (see Ref. [4],[5],[6]):

$$B_r = \frac{1}{2\pi}\mu_o(I\cdot n\cdot A)_{eff}\cdot \cos\vartheta \frac{e^{i(\omega t-Kr)}}{r^3}\ (1 + iKr) \qquad (1.7)$$

$$B_\vartheta = \frac{1}{4\pi}\mu_o(I\cdot n\cdot A)_{eff}\cdot \sin\vartheta \frac{e^{i(\omega t-Kr)}}{r^3}\ (1-K^2r^2+ iKr) \qquad (1.8)$$

$$B_\varphi = \frac{1}{4\pi}\mu_o(I\cdot l)_{eff}\cdot \sin\vartheta \frac{e^{i(\omega t-Kr)}}{r^2}\ (1 + iKr) \qquad (1.9)$$

B ... in $\left[\frac{vs}{m^2}\right]$

μ_o ... $4\pi\cdot 10^{-7}$ [H/m]

I ... current [a]

n ... number of turns

A ... cross section area [m^2]

ω ... angular frequency

t ... time

ϑ ... angle between antenna axis and radius vector from the antenna to the point of observation

r ... transmitter to receiver distance

K ... complex propagation constant

$K = K_1 - iK_2$

K_1... phase constant

K_2... attenuation constant

$$K_1 = \frac{2\pi}{\lambda} = \frac{\omega}{c_o}\sqrt{\frac{\varepsilon_r\mu_r}{2}}\sqrt{1+\sqrt{1+\left(\frac{\sigma}{\omega\varepsilon\varepsilon_o}\right)^e}} \quad [m^{-1}] \qquad (1.10)$$

$$K_2 = \frac{\omega}{c_o}\sqrt{\frac{\varepsilon_r\mu_r}{2}}\sqrt{-1+\sqrt{1+\left(\frac{\sigma}{\omega\varepsilon\varepsilon_o}\right)^2}} \quad [m^{-1}] \qquad (1.11)$$

$\omega = 2\pi f$ ... angular frequency

c_o = phase velocity of light in free space

ε_r, μ_r ... relative dielectric constant, relative magnetic permeability of the medium ($\mu_r = 1$ in our case, except for the ferrite rod antennas)

σ = electric conductivity in mhos/m

ε_o = electric permittivity in free space = $8{,}86 \cdot 10^{-12}$ [F/m]

The index "eff" in formulas (1.7) - (1.9) means that the current distribution has to be taken into account. In our case this means the factor $2/\pi$ by which the magnetic moments must be multiplied.

Formulas (1.7) - (1.9) indicate that B_r and B_φ are in phase, both having a phase difference with respect to B_ϑ which depends on the frequency, distance and qualities of the medium. For details in theory and measuring technique, please see Ref. [9] and [10].

Formulas (1.8) and (1.9) can be simplified for the far field (with good accuracy for $k_1 r > 5$) which leads to the following expressions:

$$|B_\vartheta| = \frac{\mu_o (I \cdot n \cdot A)_{eff}}{4\pi} \sin\vartheta \, \frac{e^{-K_2 r}}{r} (K_1^2 + K_2^2) \qquad (1.12)$$

$$|B_\varphi| = \frac{\mu_o (I \cdot l)_{eff}}{4\pi} \sin\vartheta \, \frac{e^{-K_2 r}}{r} \sqrt{K_1^2 + K_2^2} \qquad (1.13)$$

So the ratio between the absolute values of the far field components of an electric dipole (B_φ) and that of a magnetic dipole (B_ϑ) can be written as:

$$\left| \frac{B_\varphi}{B_\vartheta} \right| = \frac{(I_{el} \cdot l)_{eff}}{(I_m \cdot n \cdot A)_{eff} \sqrt{K_1^2 + K_2^2}} \qquad (1.14)$$

As $\sqrt{K_1^2 + K_2^2} = \sqrt{K^2} = |K|$ in rock has an order of magnitude of 10^{-2} to 10^{-3} in the frequency region under question, it follows that the product $(I_m \cdot n \cdot A)_{eff}$ has to be two to three orders of magnitude higher than $(I_{el} \cdot l)_{eff}$.

This formula could easily be proved with our helical antennas, because we have the same currents and current distributions for both field strength components ($I_{el} = I_m$; index "eff" means $2/\pi$ in both cases). Formula (1.14) writes then as follows:

$$\left| \frac{B_\varphi}{B_\vartheta} \right|_{helix} = \frac{l_{axis}}{n \cdot A \cdot |K|} \qquad (1.15)$$

The phase angle between B_φ and B_ϑ is then given by

$$\tan\delta = \frac{K_1}{K_2} = \sqrt{\frac{1 + \sqrt{1 + \left(\frac{\sigma}{\omega\varepsilon\varepsilon_o}\right)^2}}{-1 + \sqrt{1 + \left(\frac{\sigma}{\omega\varepsilon\varepsilon_o}\right)^2}}} \qquad (1.16)$$

So δ generally lies between 45° (ideal conductor, $\frac{\sigma}{\omega\varepsilon\varepsilon_o} \to \infty$)

and 90° (ideal insulator; $\frac{\sigma}{\omega\varepsilon\varepsilon_0} \neq 0$). Ref. [9] Fig. 1.2 gives the exact phase difference curves as dependent on $p = \frac{K_2}{K_1}$ and $K_1 r$.

The fields of the second described antenna have been measured in the mine at the lowest resonance frequency for both cases: antenna in air and antenna in water.

In the case of the antenna in a cavity in air, the electrical quantities to be substituted in formulas (1.7)-(1.9) are the following:

$$
\begin{aligned}
I &= 0{,}6 \quad [A] \\
n &= 772 \\
A &= 0{,}081 \quad [m^2] \\
l &= 2 \quad [m] \\
\omega &= 2\pi \cdot 294 \cdot 10^3 \ [Hz] \\
K_1 &= 1{,}76 \cdot 10^{-2} [m^{-1}] \\
K_2 &= 0{,}532 \cdot 10^{-2} \ [m^{-1}] \\
\varphi &\ldots 0^{\circ} \ldots 90^{\circ}
\end{aligned}
$$

At this frequency, the measured amplitude and phase values in the near field are consistent with theory within 5%. At distances > 300 m they are not consistent owing to geological disturbances. The maximum distance covered at 294 kHz was 600 m through rock, the transmitter power being 60 watts. It was possible to match the antenna and transmission line very carefully to the battery-powered transmitter made by W. Kellner.

At the receiver side, a ferrite rod antenna of 48cm length was used as well as a bearing head in connection with a FET-preamplifier (see Fig.1.9) and the selective µV-meter 2006 [Brüel & Kjaer]. The maximum field strength at 600 m distance was $2{,}0 \cdot 10^{-14}$ [vs/m], the noise level being still somewhat

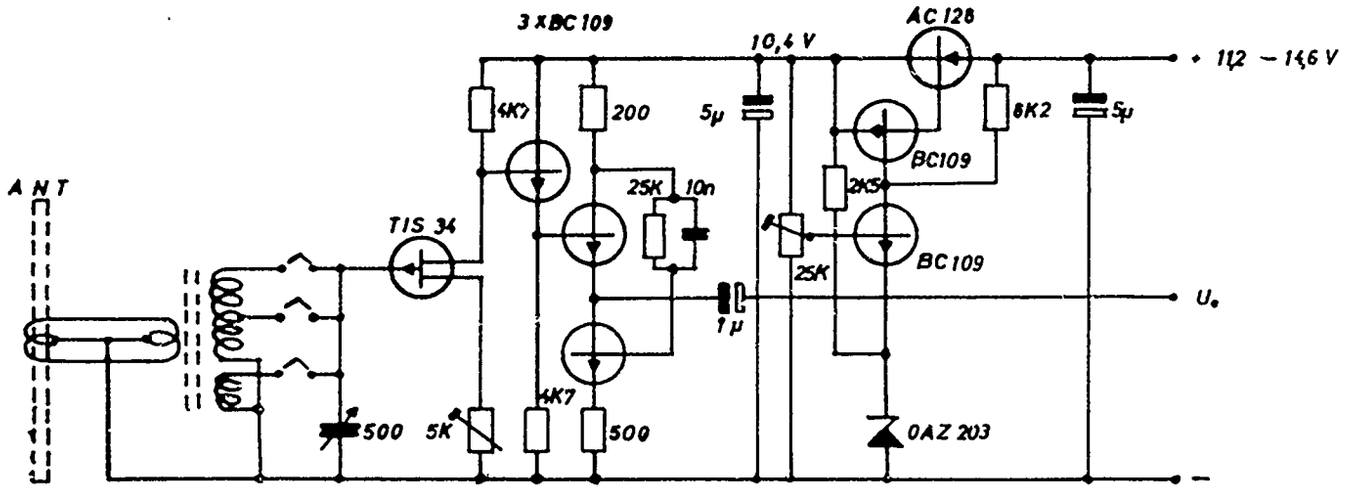
3 x BC 109
10,4 V
AC 128
+ 11,2 – 14,6 V
4K7
200
5µ
8K2
5µ
BC109
2K5
25K
10n
ANT
TIS 34
BC 109
25K
Ua
1µ
4K7
500
5K
500
OAZ 203
–

FIG.19

more than half this value. The angle φ was approximately 90 degrees.

With the antenna being in the water chamber, the following quantities are different:

$$I = 0{,}8 \ [A]$$
$$\omega = 2\pi \cdot 5{,}5 \cdot 10^3 \ [Hz]$$
$$K_1 \approx 1{,}5 \cdot 10^{-3} \ [m^{-1}] = K_2$$

The maximum distance bridged at 5,5 kHz was 1,6 km through rock, a distance given by the size of the mine. The transmitter power was ≈ 160 watts, the "transmitter" being a McIntosh stereo-amplifier operated by an RC generator.

The receiving device was a twin ferrite rod antenna 1 m long, a FET preamplifier for the frequency region between 3 kHz and 25 kHz constructed by Univ. Doz. Dr. W. Ritterlich (see Ref. [11]) and the Marconi μV meter TF 2330 with 7 Hz bandwidth. The field strength at 1,6 km distance was $6{,}4 \cdot 10^{-13}$ $[vs/m^2]$ the noise level being $\sim 4{,}6 \cdot 10^{-14}$ $[vs/m^2]$ (3mv) with peaks of $\sim 5 \cdot 10^{-13}$ $[vs/m^2]$ about every second. Enlarging the distance in air, additional 400 m can be bridged. Greater distances could be reached with a phase-locked amplifier.

In both cases, the maximum distance was not confined by the internal noise of the receiving system, but by atmospheric and industrial noise produced in the neighborhood of the mine. These noises cover a very wide frequency region and distance so that for example medium sized thunderstorms at a distance of 100 km make these measurements completely impossible.

1.5. Calibration of the receiving devices

The receiving devices were calibrated in accordance with the National Bureau of Standards, Ref. [12]. However, one has to realize the length of the ferrite rod receiving antenna and the $1/r^3$ decrease of the near field produced by the calibration coil leading to a smaller effective distance than the two antenna centers geometrically have. This can be calculated easily, since the mean value of a function $\overline{F(x)}$ times the region of integration (x_2-x_1) equals

$$\int_{x_1}^{x_2} F(x)dx.$$

Mathematically expressed:

$$\int_{x_1}^{x_2} F(x)\,dx = \overline{F(x)}\,(x_2-x_1) \qquad (1.17)$$

In our case, $F(x)$ is C/x^3 where C is the field constant depending on the calibration coil dimensions and the current in it, x is the distance of the center of the calibration coil, x_2 and x_1 are the distances from the far end and the near end respectively, of the receiving antenna to the center of the calibration coil.

Formula (1.17) can thus be written as:

$$C\int_{x_1}^{x_2} \frac{dx}{x^3} = -\frac{1}{2}\,C\,\left(\frac{1}{x_2^2}-\frac{1}{x_1^2}\right) = \frac{C}{\bar{x}^3}\,(x_2-x_1)$$

and $\bar{x}$ the " effective"(medium) distance is then:

$$\bar{x} = \left[\frac{2(x_2-x_1)}{\left(\frac{1}{x_1^2}-\frac{1}{x_2^2}\right)}\right]^{1/3} \quad [m]. \qquad (1.18)$$

The formula for the field strength in the near field of a calibration coil is in accordance with Ref.[12]:

$$|B| = \frac{\mu_o \cdot I \cdot r_1^2}{2R_o^3} (1 + \beta^2 R_o^2)^{1/2} \left[vs/m^2\right]$$

I ... circulating current in the calibration coil [A]

r_1 ... radius of the calibration coil [m]

R_o^2 ... $d^2 + r_1^2 + r_2^2$ [m²]

r_2 ... radius of the receiving antenna to be calibrated [m]

d ...center to center distance of the two antennas [m]

β ... $\frac{2\pi}{\lambda_o}$ [m^{-1}]

λ_o ... wavelength in free space [m]

For d^2 we have to substitute $\bar{x}^2$ calculated from formula (1.18). Furthermore $(1 + \beta^2 R_o^2)^{1/2}$ is nearly 1 up to 1 MHz (error smaller than 1%) since the maximum distance used is 7 meters, r_1 being 0,2 meters, r_2 being negligibly small.

1.6. The problem of comparing antennas in dissipative media.

Sometimes one wants to compare different antenna types or different antennas of the same type to optimize some transmitting or receiving problems. Therefore the author would like to point out some of the fundamental facts and problems occurring when antennas are used in a lossy medium and for the purpose of comparison. In this case one should make sure that:

1) The surrounding medium has the same properties in all cases in question (In addition the same method of measurement of these properties should be used!)

2) The frequency is the same in all cases.
3) The cavity in the lossy medium has the same size and shape.
4) The antennas have approximately the same size. This of course is a very critical point. The problem is how to compare geometrically a long and straight wire and a circular loop for instance. Perhaps one should count the volume occupied by rotating the antennas in all directions.
5) In this cavity, temperature, medium, pressure and humidity are kept constant in all cases, since these circumstances can change the properties, especially of small antennas, by powers of ten. (This was experimentally proved during our work).
6) The antennas operate under the same electrical power condition (very essential not only when using magnetic cores).

In addition it must be mentioned that many quantities defined in air such as radiation resistance, power-radiation factor and therefore also efficiency (see for example Ref.[13]) are not defined in a lossy medium.

The reason is the following: In air or in vacuo, the radiation resistance is defined by volume-integration over the pointing vector in the far field of the antenna. Dividing this integral by the square of some maximum current along the antenna one obtains the radiation resistance. This integral is volume-independent in vacuo as long as one integrates around the radiation source. This of course is not so in a lossy medium, furthermore there is no "radiation field" in such a medium, strictly speaking.

In air, parts of the near field energy come back to the antenna producing the capacitive and inductive properties of the antenna and the Q factor. In a lossy medium nearly

all the energy is consumed in the extreme near field where there exist the highest field strengths. Therefore it is clear that even if a thing as the radiation resistance could be defined in such a medium: the meaning would be very poor.

In such a situation the only things one is able to compare are the electric or magnetic field-strength components and their phase-correct combinations produced by some antenna at some frequency under certain conditions at a certain distance. A theoretical approach to this problem was made by Dr. G. Tinhofer, Innsbruck, Ref. [14] in the frame of the VLF Project Univ. Doz. Dr. W. Bitterlich. It was found that for given electric and magnetic moments and medium data there exists an optimum frequency for a certain distance. However, the problem is much more complicated, because nothing is said about how the moments can be produced best at this frequency, furthermore the frequency dependence of the medium properties and the noise level distribution had to be neglected.

However, the radiation resistance and efficiency of these antennas working in free space can be easily calculated. (Ref. [13]). This shall now be done for the second described antenna at 294 kHz:

The radiation resistance of the electric dipole component is:

$$\underline{R_e} = 20\,(l_{eff} \cdot K_{1_{air}})^2 = \underline{1{,}2 \cdot 10^{-4}\ \Omega}\ .$$

The magnetic dipole component gives:

$$\underline{R_m} = 20\left[(n \cdot F)_{eff} K_{1_{air}}^2\right]^2 = \underline{4{,}32 \cdot 10^{-5}\ \Omega}$$

The total antenna efficiency is therefore:

$$\underline{e} = \frac{R_m + R_e}{R_{input}} = \frac{4{,}32 \cdot 10^{-5} + 1{,}2 \cdot 10^{-4}}{85} = \underline{1{,}92 \cdot 10^{-6}} \quad .$$

As the antenna has a real input impedance of suitable value it can easily be matched to a transmission line and a transmitter. Therefore a coupling efficiency of nearly 0,5 can be reached without difficulties.

This is one of the advantages of this antenna type. Even higher efficiencies could be obtained with a completely dry antenna (in air) or with a surrounding medium of high ε without the conductivity of the used water (for example glycerin).

Of course this antenna type has a series of disadvantages, e.g., the capacitive sensitivity and the cavity condition mentioned at the beginning of the paper. But these properties are inherent to all small antennas of high efficiency or high Q.

On the whole, this antenna type seems to be quite reasonable having advantages which other equally-sized antenna types for transmitting purposes do not have, without having some of the less interesting qualities of pure electric or magnetic dipoles discussed in Ref. [13].

2. MEASUREMENT OF THE CONDUCTIVITY AND DIELECTRIC CONSTANT OF A WEAKLY CONDUCTIVE HOMOGENEOUS MEDIUM BY WAVE PROPAGATION

2.1. Introduction

For the ideal case of an isotropic, homgeneous and unbounded medium, the field strength formulas for this special case were derived in a well-known manner from Maxwell's equations [6].

For practical and theoretical considerations [15], magnetic dipoles were used for the transmitter and receiver of such waves. On the transmitter side, they were materialized almost exclusively by non-ferrous frame coils of various dimensions, whereas on the receiver side ferrite rod antennas proved favorable.

2.2. Theoretical considerations

Of all the field formulas, only the magnetic component is of interest in this connection for understanding the above-mentioned method.

The following relations are valied for this special case

$$\vec{H}_r = 2\,m \exp(-ik^*r)\cos\varphi\left(\frac{1}{r^3} + \frac{ik^*}{r^2}\right)$$

$$\vec{H}_\vartheta = 0 \qquad (2.1)$$

$$\vec{H}_\varphi = m \exp(-ik^*r)\sin\varphi\left(\frac{1}{r^3} + \frac{ik^*}{r^2} + \frac{k^{*2}}{r}\right)$$

where $m = n \cdot I \cdot F$ = magnetic moment of the transmitting frame

φ = angle between the axis of the transmitting dipole (= axis of the transmitting frame) and the radius vector with respect to the point of measurement

r = distance between transmitter and point of measurement

k^* = complex wave number containing the material constants ε, σ, μ and the frequency $\omega = 2\pi f$.

$$k^* = \sqrt{\omega^2 \varepsilon \varepsilon_o \mu \mu_o} \sqrt{1 - \frac{i\sigma}{\omega \varepsilon_o \varepsilon}} = k_1 - ik_2 \quad . \quad (2.2)$$

Calculating the amounts of the parts of components that depend on the distance only, we obtain

$$H_0 = 2 \exp(-k_2 r) \left\{ \frac{1}{r^6} + \frac{2k_2}{r^5} + \frac{k_1^2 + k_2^2}{r^4} \right\}^{1/2} \quad (2.3a)$$

for $\vartheta = 0^\circ$ in correspondence with the first Gaussian position and

$$H_{90} = \exp(-k_2 r) \left\{ \frac{1}{r^6} + \frac{2k_2}{r^5} + \frac{3k_2^2 - k_1^2}{r^4} + \frac{2k_2(k_1^2 + k_2^2)}{r^3} + \right.$$

$$\left. + \frac{(k_1^2 + k_2^2)^2}{r^2} \right\}^{1/2} \quad (2.3b)$$

for $\vartheta = 90^\circ$ in accordance with the second Gaussian position.

The induction voltage at the point of reception which is proportional to the field strength, is found to be

$$U_{ind} \sim |\vec{H}| \sim \left\{ H_0^2 \cos^2 \vartheta + H_{90}^2 \sin^2 \vartheta \right\}^{1/2} \quad (2.4)$$

In all formulas, the conductivity σ and the dielectric constant ε occur as essential rock parameters in the wave number (k_1) and attenuation constant (k_2).

Hence results the demand for a measurement of these quantities which is as simple as possible and sufficiently accurate.

The measurement on suitably shaped laboratory specimens which at first appeared well suited, proved to be

problematic, since essential factors such as humidity and porosity change when producing the specimen.

The present method permits measurement immediately through rock by means of wave propagation. The basic idea of this measurement lies in the fact that the rock parameters influencing and changing the wave propagation, are made accessible to measurement by this very change. The principle of this measurement furthermore contains an averaging of the parameters ε and σ over the region penetrated by the waves, which is of great advantage for application to propagation measurements as compared to measurements on locally taken laboratory specimens.

Further considerations are based on measurements of directivity patterns giving in a well-known manner the radiation characteristics of a magnetic dipole as dependent on the parameters ϑ at constant σ or r. Fig. 2.1 shows two diagrams for constant σ and variable distance r as parameters. Fig. 2.2 shows two directivity patterns for constant distance and variable σ, with the field strength H or a quantity proportional to it (e.g., inductance B or induced voltage U) being plotted radially at the point of observation.

In all four families of curves, one can see the change in the curve shape from a horizontal eight (near field) at low conductivity or small distance via approximately annular (transition zone) to a vertical eight (far field) at high conductivity or great distance.

Mathematical analysis of these curves yields the parameter representation

$$x = H \cos\vartheta = \left\{ H_0^2 \cos^2\vartheta + H_{90}^2 \sin^2\vartheta \right\}^{1/2} \cos\vartheta$$

$$y = H \sin\vartheta = \left\{ H_0^2 \cos^2\vartheta + H_{90}^2 \sin^2\vartheta \right\}^{1/2} \sin\vartheta \qquad (2.5)$$

and after eliminating the parameter ϑ a four-degree

equation is obtained. The shape of the antenna directivity pattern is determined only by the relation of

$$G = H_0/H_{90} \quad . \tag{2.6}$$

Thus, the quantity G is the ratio of the field strength at the point of observation for the two Gaussian positions.

Explicit calculation of the expressions for k_1 and k_2 from Eq. (2.2) yields

$$k_1 = \sqrt{\frac{1}{2}\omega^2\mu_0\varepsilon\varepsilon_0}\sqrt{1+\sqrt{1+\left(\frac{\sigma}{\omega\varepsilon\varepsilon_0}\right)^2}} \tag{2.7}$$

$$k_2 = \sqrt{\frac{1}{2}\omega^2\mu_0\varepsilon\varepsilon_0}\sqrt{-1+\sqrt{1+\left(\frac{\sigma}{\omega\varepsilon\varepsilon_0}\right)^2}} \quad . \tag{2.8}$$

If $\frac{\sigma}{\omega\varepsilon\varepsilon_0} \gg 1$, the second root of the two equations can be simplified, yielding

$$k_1 \doteq k_2 \doteq \sqrt{\frac{\omega\mu_0\sigma}{2}} \quad . \tag{2.9}$$

This simplification corresponds to a neglection of the displacement current, the dielectric constant ε no longer occurs in the formulas [6]. The parameter σ which is decisive for propagation, can be determined by measuring one single quantity, e.g., G. For greater details and boundaries for the applicability of this method see Ref. [17] and [18].

2.3. Conditions of measurement

If the two parameters ε and σ are to be measured, the frequency must be chosen so high that $\frac{\sigma}{\omega\varepsilon\varepsilon_0} \sim 1$, i.e.,

Antennendiagramm

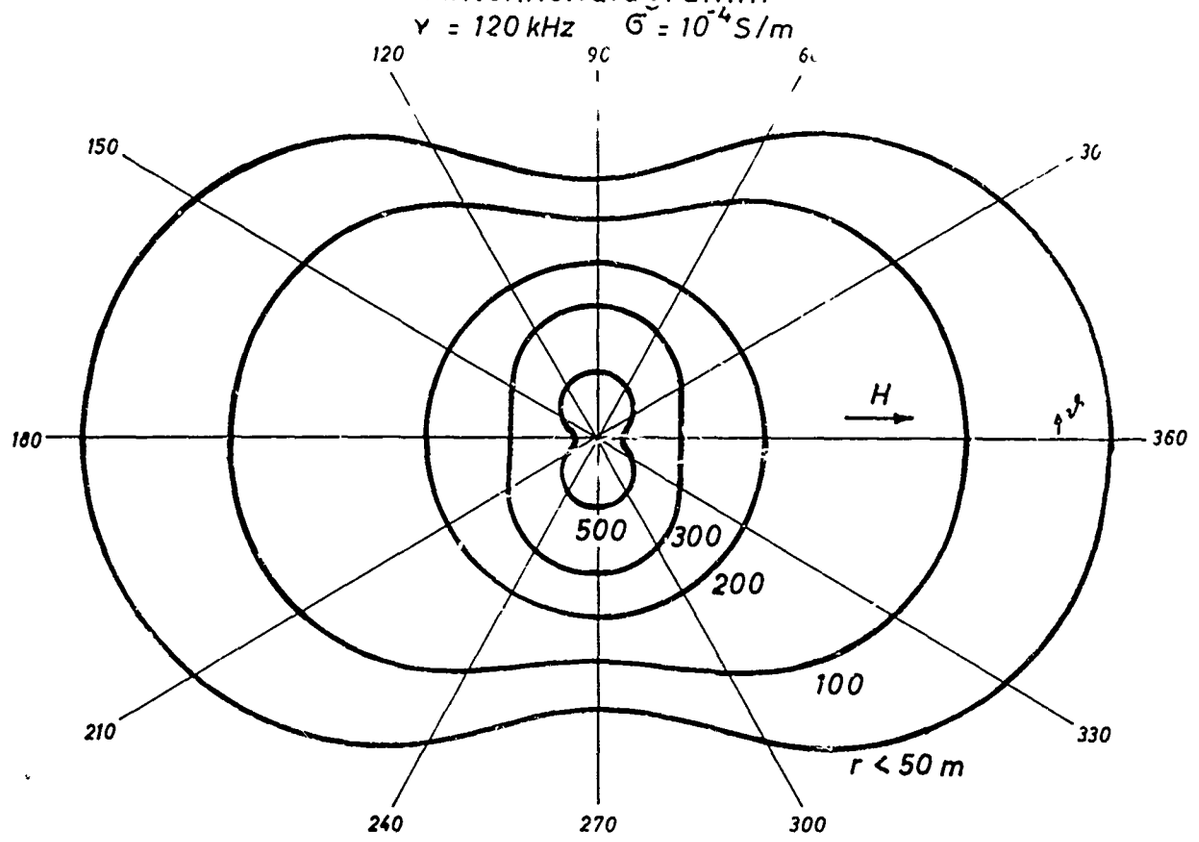

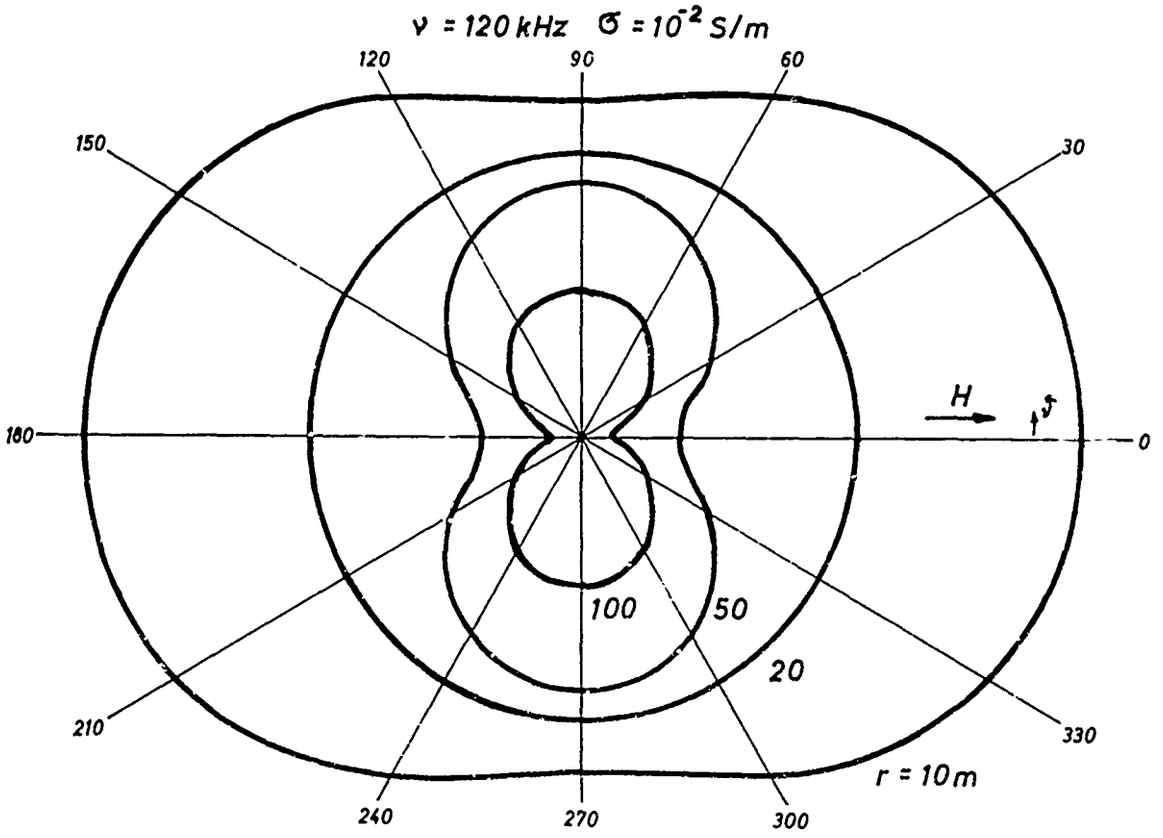

Fig.: 2.1

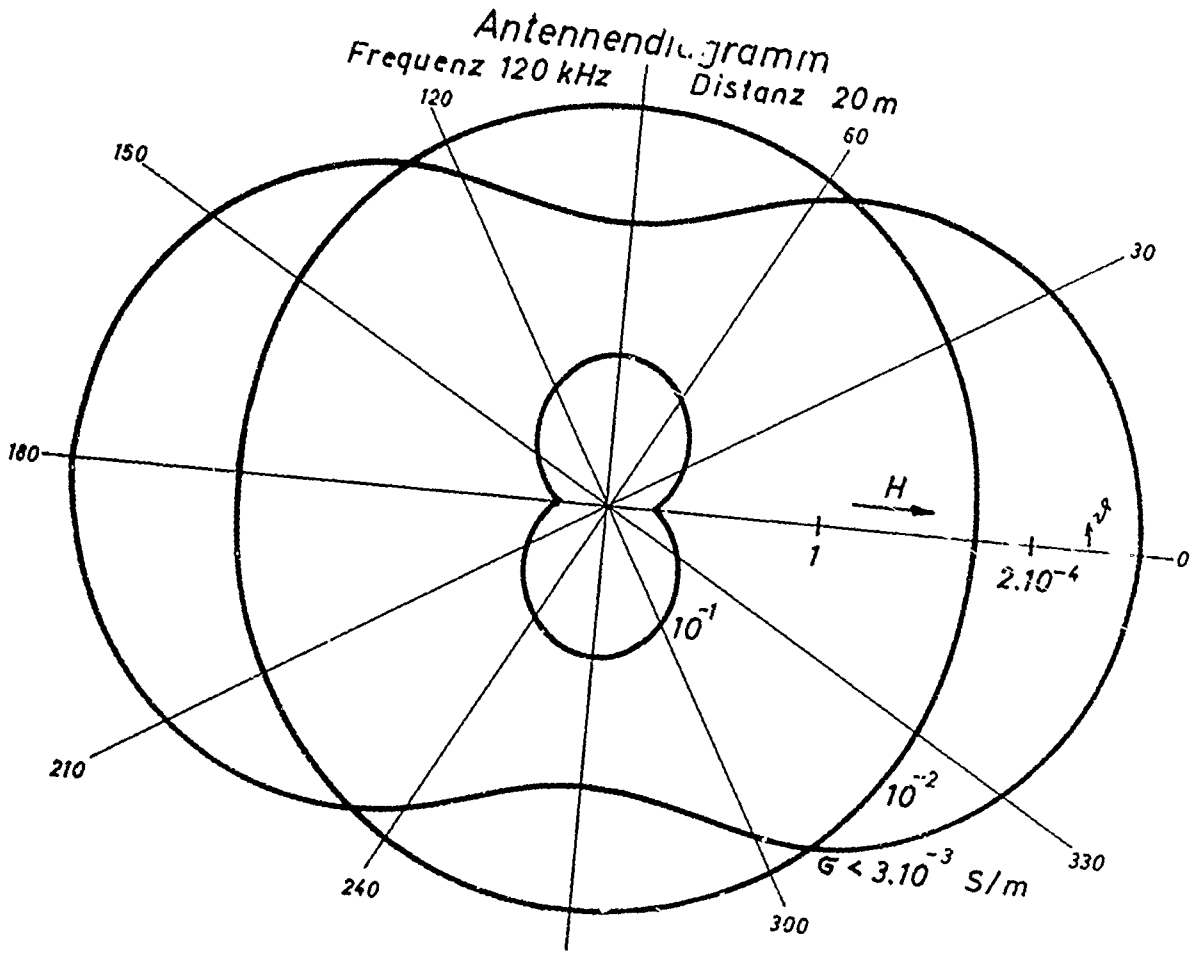
Antennendiagramm
Frequenz 120 kHz
Distanz 20 m
120
60
150
30
180
H
1
2.10⁻⁴
0
10⁻¹
210
10⁻²
330
240
G < 3.10⁻³ S/m
300

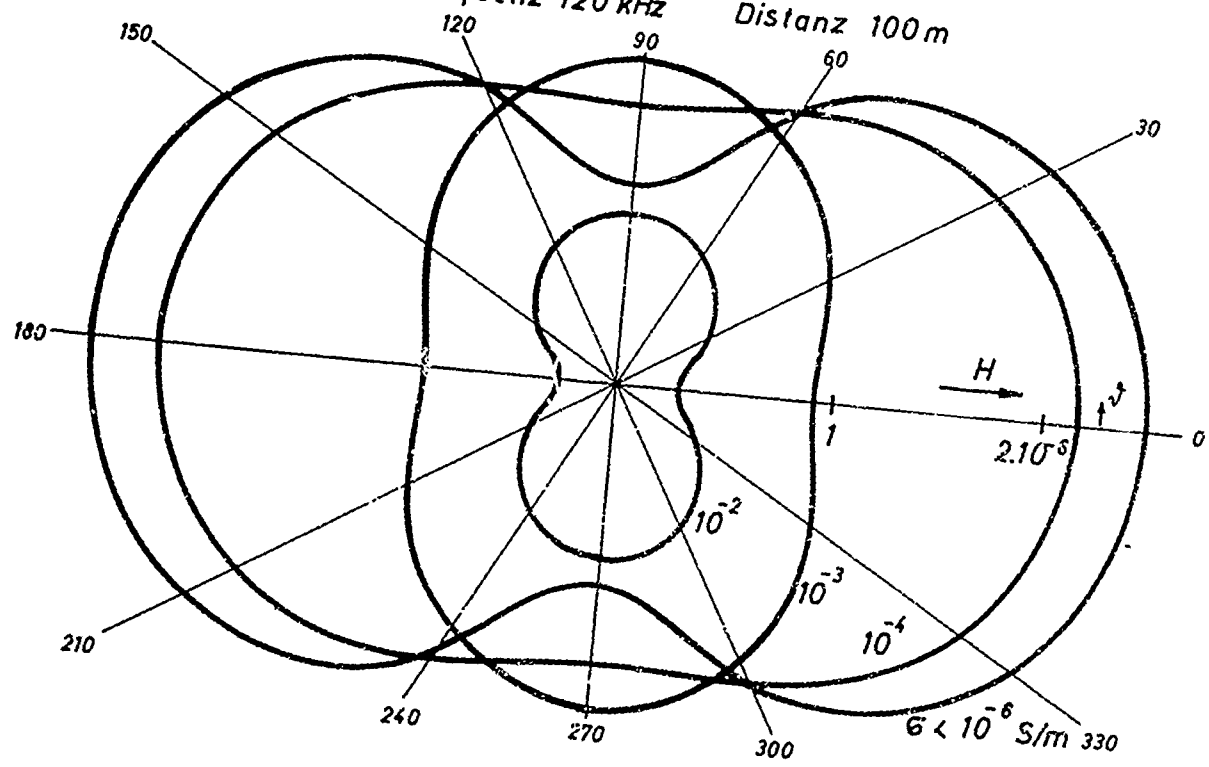
Frequenz 120 kHz
Distanz 100 m
150
120
90
60
30
180
H
1
2.10⁻⁶
0
10⁻²
10⁻³
210
10⁻⁴
240
270
300
G < 10⁻⁶ S/m
330

Fig.: 2.2

that both, the conduction current and the displacement current contribute to wave propagation.

The other extreme case of $\frac{\sigma}{\omega \varepsilon \varepsilon_0} \ll 1$ does not yield anything new for the $\sigma - \varepsilon$ measurement, since both unknowns are still contained even after simplification of the expressions for k_1 and k_2. The experimental materialization of this approximation requires either extremely low conductivity or a frequency that lies right in the MHz region. The applicability of the formulas for the VLF region for such high frequencies still remains to be checked.

The direct calculation of the quantities ε and σ from the Eqs. (2.3), (2.7) and (2.8) theoretically is possible always with two independent quantities being given (e.g., H_{90} and G). The given formulas, however, are far too complicated for a direct calculation, since the unknown quantities are contained in the power and also in the exponential expressions.

2.4. Graphical determination of ε and σ

A much simpler method is the graphical determination of ε and σ by means of families of curves, with the attainable accuracy being adaptable to the requirements and the accuracy of measurement.

For obtaining the necessary families of curves, a large field of field strength values was computed at Innsbruck University, About 35.000 figure values on about 180 pages shall be published separately.

Plotting the pairs of G and H_0 values as dependent on the variable parameters σ and ε and the fixed parameters r (distance) and ω (frequency) on a diagram, we obtain Fig. 2.3

and 2.6. The latter are only a small part of all possible and possibly necessary families of curves.

Each family of curves here corresponds to a certain frequency and distance of measurement. Theoretically, a measuring frequency and distance suitable for any imaginable combination of ε and σ can be found so that curves for the parameters to be separated are far enough apart from each other. Then the trumpet shape of Fig. 2.3 - 2.6 is obtained. The region of measurement that can be evaluated in practice, is due to the technical limitations of the measuring instruments, e.g., by the signal-to-noise ratio or by the transmitter power as shall be discussed later.

The conductivity σ and the dielectric constant ε are determined so that the measured values of H_{90} and $G = H_0/H_{90}$ of a suitable point of measurement are plotted in the corresponding diagram, from which the rock parameters ε and σ can be read directly or by interpolation.

2.5. Accuracy of measurement

Naturally it is possible to estimate the accuracy of measurement for ε and σ in accordance with the laws of usual calculation of errors. The accuracy of the parameters is easy to determine in connection with the table of errors computed at Innsbruck University. This table contains the deviation factors of the quantities H_0, H_{90} and G for a parameter change of +50% for the same parameter region as above. These table values are those factors by which the field strength value at constant parameters would have to be multiplied in order to yield the value of parameter deviation.

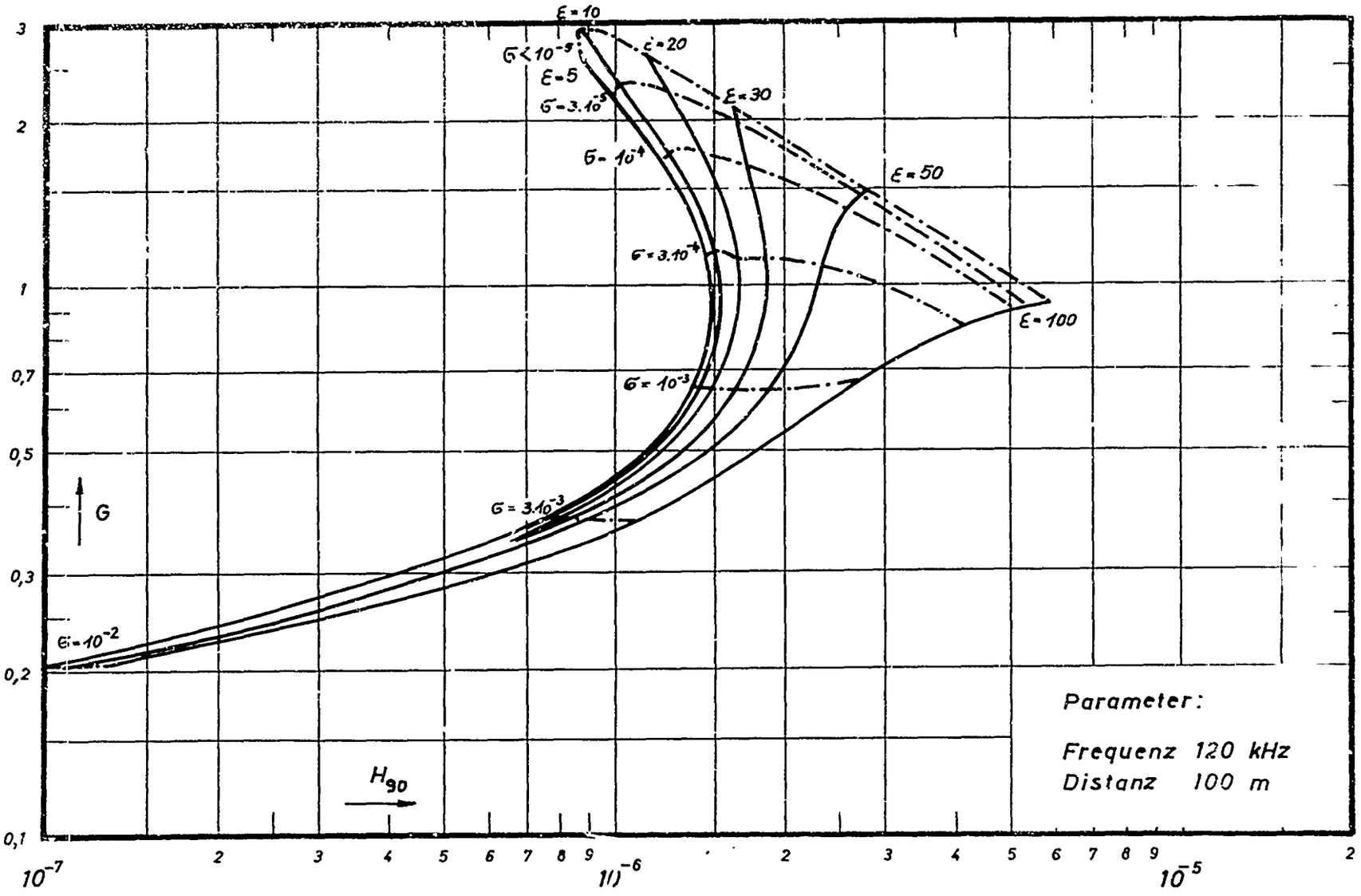
ε = 10
σ < 10⁻⁹
ε = 5
σ = 3.10⁻⁵
ε = 20
ε = 30
σ = 10⁻⁴
ε = 50
σ = 3.10⁻⁴
ε = 100
σ = 10⁻³
σ = 3.10⁻³
σ = 10⁻²
G
H90
Parameter:
Frequenz 120 kHz
Distanz 100 m
3
2
1
0,7
0,5
0,3
0,2
0,1
10⁻⁷
10⁻⁶
10⁻⁵

Fig.: 2.3

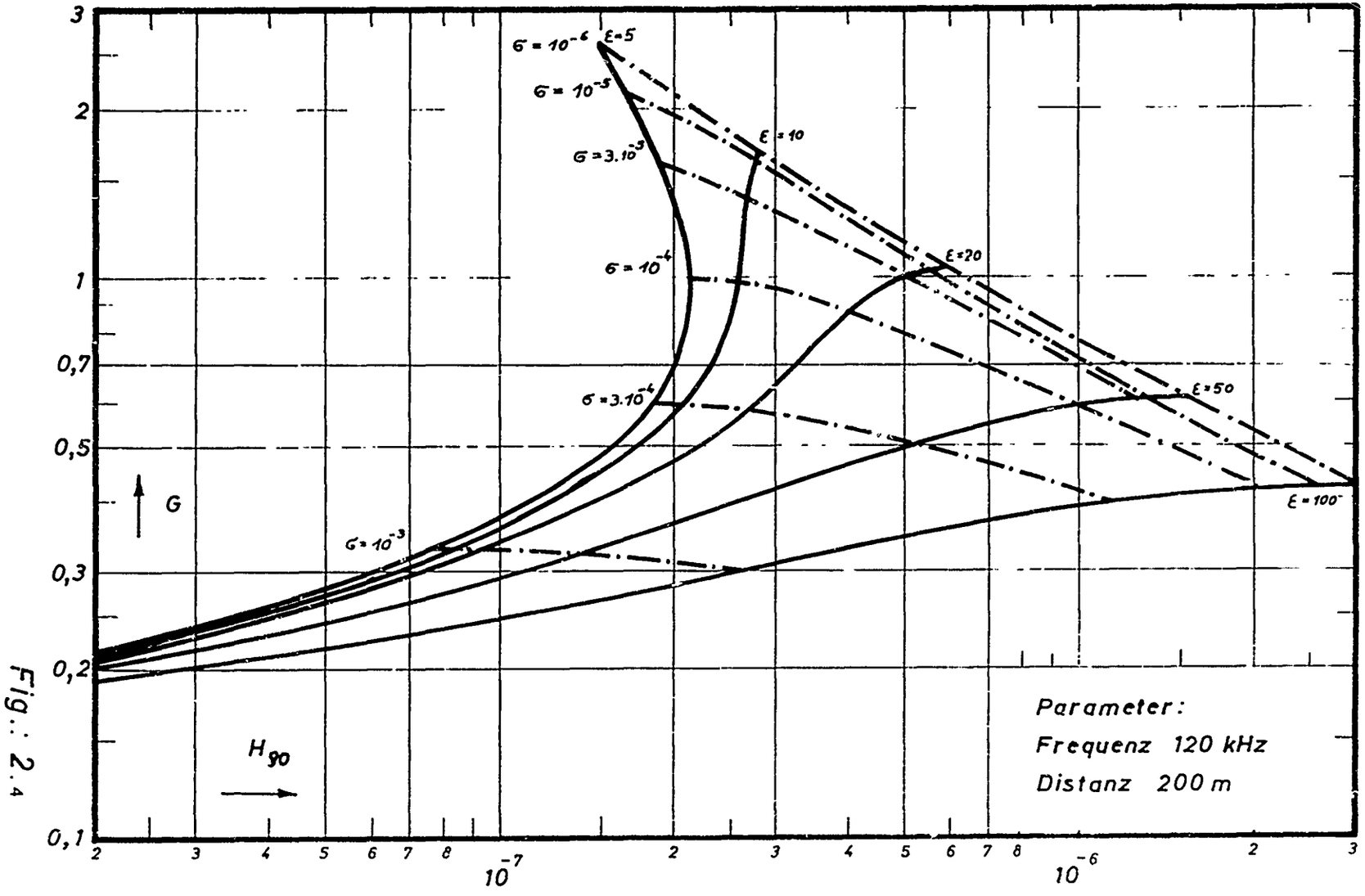
3
2
1
0,7
0,5
0,3
0,2
0,1
G
H_{90}
10^{-7}
10^{-6}
2 3 4 5 6 7 8
$\sigma = 10^{-6}$
$\sigma = 10^{-5}$
$\sigma = 3.10^{-5}$
$\sigma = 10^{-4}$
$\sigma = 3.10^{-4}$
$\sigma = 10^{-3}$
$\varepsilon = 5$
$\varepsilon = 10$
$\varepsilon = 20$
$\varepsilon = 50$
$\varepsilon = 100$
Parameter:
Frequenz 120 kHz
Distanz 200 m

Fig.: 2.4

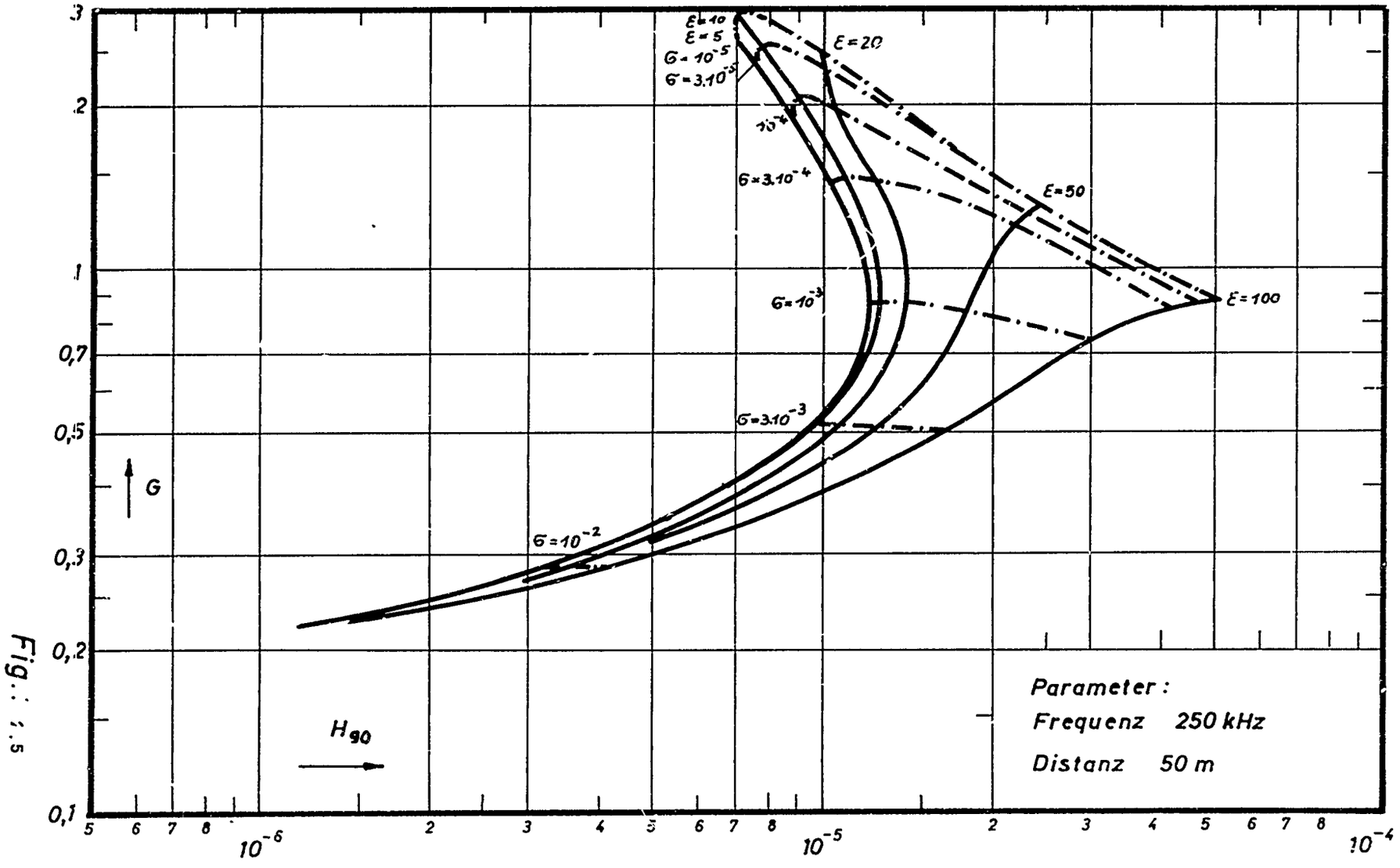
ε=10
ε=5
G=10⁻⁵
G=3.10⁻⁵
10⁻⁴
G=3.10⁻⁴
ε=20
ε=50
ε=100
G=10⁻³
G=3.10⁻³
G=10⁻²
G
H90
Parameter :
Frequenz 250 kHz
Distanz 50 m
0,1
0,2
0,3
0,5
0,7
1
2
3
5 6 7 8
10⁻⁶
2 3 4 5 6 7 8
10⁻⁵
2 3 4 5 6 7 8
10⁻⁴

Fig. 1.5

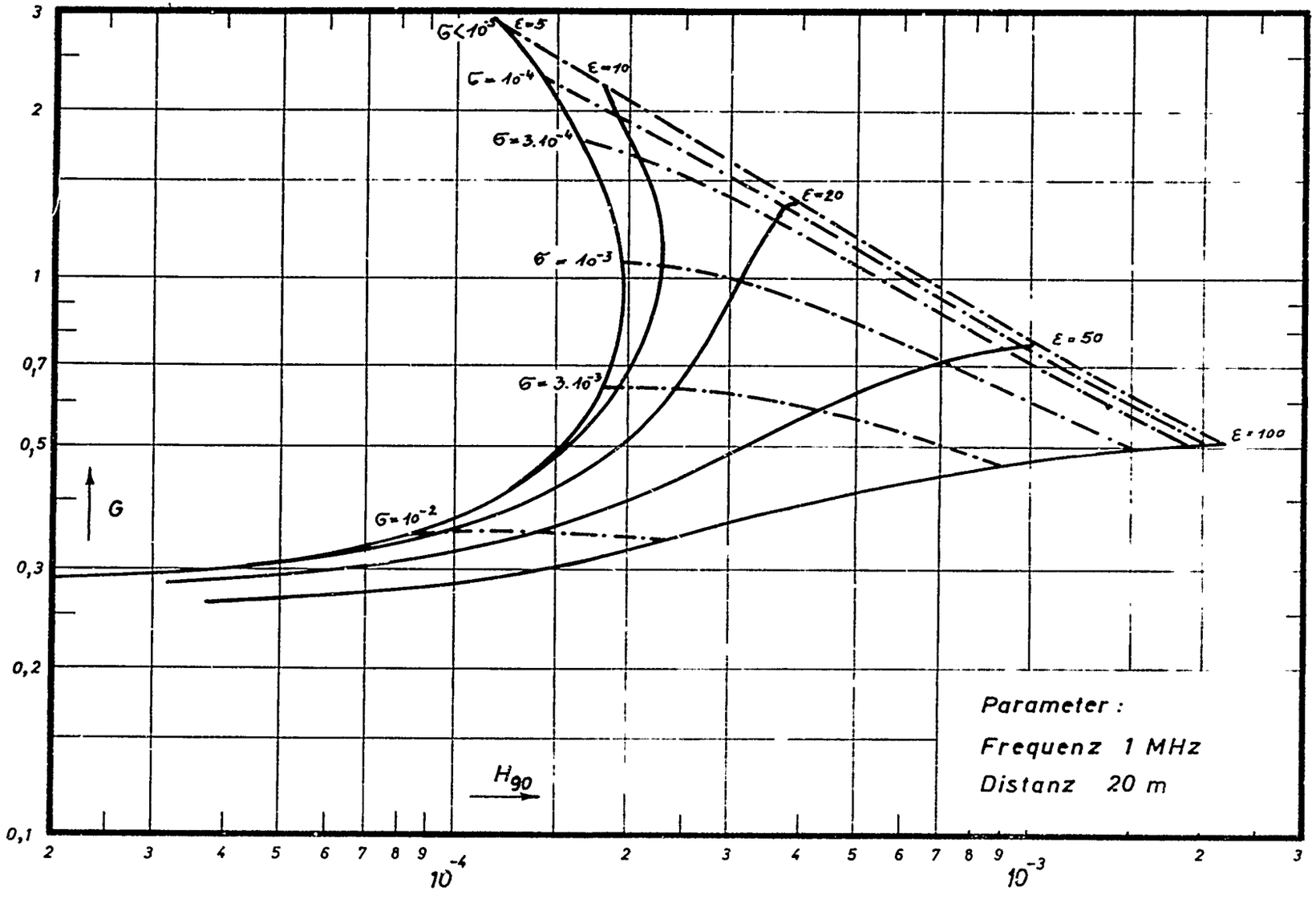
σ<10⁻⁵
ε=5
σ=10⁻⁴
ε=10
σ=3.10⁻⁴
ε=20
σ=10⁻³
ε=50
σ=3.10⁻³
ε=100
σ=10⁻²
G
H90
Parameter :
Frequenz 1 MHz
Distanz 20 m
3
2
1
0,7
0,5
0,3
0,2
0,1
2 3 4 5 6 7 8 9
10⁻⁴
2 3 4 5 6 7 8 9
10⁻³
2 3

Fig.: 2.6

The following relations are valid:

$$\Delta H_0^{\sigma} = \frac{H_0(\sigma + \Delta\sigma, \varepsilon)}{H_0} \qquad \Delta H_0^{\varepsilon} = \frac{H_0(\sigma, \varepsilon + \Delta\varepsilon)}{H_0}$$

$$\Delta H_{90}^{\sigma} = \frac{H_{90}(\sigma + \Delta\sigma, \varepsilon)}{H_{90}} \qquad \Delta H_{90}^{\varepsilon} = \frac{H_{90}(\sigma, \varepsilon + \Delta\varepsilon)}{H_{90}}$$

$$\Delta G^{\sigma} = \frac{G(\sigma + \Delta\sigma, \varepsilon)}{G} \qquad (2.10)$$

$$\Delta G^{\varepsilon} = \frac{G(\sigma, \varepsilon + \Delta\varepsilon)}{G}$$

By means of the above values, the following quantities are obtained for the points of measurement to be examined:

$$\Delta e = 100 \{\max|(\Delta H_{90}^{\varepsilon}, \Delta G^{\varepsilon}) - 1|\}\% \qquad (2.11)$$

$$\Delta s = 100 \{\max|(\Delta H_{90}^{\sigma}, \Delta G^{\sigma}) - 1|\}\%$$

which take into account the quantities G or H_{90} decisive for the accuracy of $\varepsilon(\Delta e)$ and $\sigma(\Delta s)$ measurements. In the diagrams Fig. 2.3 through Fig. 2.5, the relation can be seen from the position of the families of curves for constant σ and ε relative to the ordinate (G) or abscissa (H_{90}). In Fig. 2.3, for example, the quantity H_{90} (in contrast to the quantity G) in the neighborhood of the approximately horizontal curve for $\sigma = 10^{-3}$ (S/m) is no criterium for distinguishing various σ values.

If we assume the quantities G and H_{90} to have a measuring accuracy of Δm, and if linear interpolation is permitted, which will be the case for a small region, the errors for ε and σ will be as follows:

$$\Delta\varepsilon = 50\,\frac{\Delta m}{\Delta e}\ \%$$
$$\Delta\sigma = 50\,\frac{\Delta m}{\Delta s}\ \% \qquad (2.12)$$

2.6. Example of measurement

For checking this method experimentally, the above-mentioned series of measurements was made with an existing device working at 120 kHz. Table 2.1 gives only those values the corresponding curves for which are described in the present report.

TABLE 2.1

r	H_{90}	G
100 m	$1{,}4 \cdot 10^{-6}$	1,4
200 m	$2{,}5 \cdot 10^{-7}$	0,75

The quantities for H_{90} were converted into the "reduced" field strengths given in Eqs. (2.3a,b) by means of the calibration factors specific for the measuring instrument. The magnetic moment of the transmitting dipole here will be m = 1 (cf. Eq. (2.1)) and the voltage U induced in the receiving antenna must be converted to field strength values by the calibration factor.

The diagrams (Fig. 2.3 and Fig. 2.4) thus yield the values

$$\sigma \doteq 2 \cdot 10^{-4}\ \text{S/m}$$
$$\varepsilon \doteq 12 \quad .$$

For determining the accuracy of measurement, the table of deviation factors will be used from which the values for $\varepsilon = 10$ (by approximation for $\varepsilon = 12$) and $\sigma = 3 \cdot 10^{-4}$ S/m (by approximation for $\sigma = 2 \cdot 10^{-4}$ S/m) are taken in accordance with Table 2.2.

TABLE 2.2

r	ΔH_{90}^{σ}	$\Delta H_{90}^{\varepsilon}$	ΔG^{σ}	ΔG^{ε}
100 m	1,033	1,049	0,835	1,006
200 m	0,71	1,18	0,82	0,994

From Eqs. (2.11) and (2.12), the limits of errors are determined for a measuring distance of 100 m on the basis of a measuring accuracy of $\Delta m = 10$ %:

$$\Delta\sigma = 30\ \%$$
$$\Delta\varepsilon = 100\ \%.$$

For a distance of 200 m, the corresponding figures are

$$\Delta\sigma = 26\ \%$$
$$\Delta\varepsilon = 28\ \%.$$

In accordance with the curves, the accuracy of measurement increases with the distance, but cannot be increased arbitrarily, since the accuracy of the original values of H_{90} and G decreases as the distance increases, because of the decreasing signal-to-noise ratio.

A better and more effective possibility of increasing the accuracy of measurement can be seen in Figs. 2,5 and 2.6. At a frequency of 1 MHz and at a distance of only 20 m, the splitting up of curves is approximately the same as it is at 120 kHz and 200 m. At such small distances, however,

the cavity must already be taken into account. The selectivity of this method increases about proportionally with frequency, i.e., at constant resolution, the product of frequency and distance is approximately constant.

In this connection it must be taken into account that the method is an integrating one owing to the method of measurement, which summarizes and averages over the more or less considerable fluctuations in the room penetrated by radiation.

For accurate measurements it must furthermore be taken into consideration, that σ and ε both depend on frequency. Information on frequency measurements in this connection are found in [19] and [8] .

2.7. Influence of phase shift between H_0 and H_{90}

Should a special meter for directly determining the required quantities G and H_{90} be not available, the field strength values of H_0 and H_{90} ($G = H_0/H_{90}$) are determined by the method of antenna directivity pattern described at the beginning. The method of measurement and a complete measuring apparatus are described in detail in [18].

When determining the field strengths H_0 and H_{90} it is often necessary that several measurements must be made; and it is not always possible to keep the angle φ exactly 0° or 90°. In this case, the amount of the field strength at the point of observation is given by

$$|\vec{H}| = m \exp(-k_2 r) \left\{ H_0^2 \cos^2 \varphi + H_{90}^2 \sin^2 \varphi \right\}^{1/2} \sim U \quad (2.13)$$

Since H_0 and H_{90} themselves are vectorial quantities, they combine into one vector $\vec{H}$ only if both are in phase. $\vec{H}$ then forms the diagonal in the rectangle spanned out by $\vec{H}_r$ and $\vec{H}_{\varphi}$. ($\vec{H}_r$ and $\vec{H}_{\varphi}$ are the vectors whose amounts are given in Eq. (2.1)). If $\vec{H}_r$ and $\vec{H}_{\varphi}$ are no longer in phase, there results a rotating field ellipse which in analogy with the Lissajous figures is inscribed in the rectangle over $2 \cdot \vec{H}_r$ and $2 \cdot \vec{H}_{\varphi}$. The graphical representation of this fact is given in Fig. 2.8.

The quantities U_1 and U_2 correspond to the large and small axes of the rotating field ellipse and are induced as the voltages in the ferrite rod antenna if the latter is orientated in the respective direction, ψ being the angle of orientation of the direction finding antenna with respect to the radius vector toward the transmitting antenna.

Hereinafter, the influence of the deviation ΔU on the measurement of ε and σ will be estimated.

A rotating field ellipse on the whole will result only if two non-parallel components that are out of phase are added. This yields immediately that an elliptic polarization cannot exist at $\varphi = 0^\circ$ and $\varphi = 90^\circ$ where in accordance with Eq. (2.13) there occurs only the component $\vec{H}_r$ and $\vec{H}_{\varphi}$, respectively.

For φ-values between 0 and 90°, $\vec{H}$ consists of two components: $\vec{H}_r$ and $\vec{H}_{\varphi}$. The ratio

$$\frac{A}{B} = \frac{|\vec{H}_r|}{|\vec{H}_{\varphi}|} = G \cdot \cot \varphi \qquad (2.14)$$

determines the axial ratio of the rectangle in which the rotating field ellipse is inscribed. The axial ratio of U_2/U_1 of the ellipse is a measure for the phase shift between $\vec{H}_r$ and $\vec{H}_{\varphi}$.

If the experimentally determined U_k is compared with the $\vec{H}$ calculated from Eq. (2.13), we find an amplitude error of

$$\Delta U = 100\left(1 - \frac{U_1}{|\vec{H}|}\right) \% \quad . \qquad (2.15)$$

The errors to be expected for some combinations of A/B and U_2/U_1 are calculated in Table 2.3.

TABLE 2.3

U_2/U_1 →	0,1	0,2	0,3	0,5
A/B ↓	ΔU	ΔU	ΔU	ΔU
3	1 %	2 %	6 %	-
2	0,6 %	2 %	5,5 %	12 %
1,5	0,7 %	3 %	6,5 %	10,5 %
1,25	1 %	3,5 %	7,5 %	11,5 %
1,0	2 %	4 %	7,7 %	12,3 %

The table shows that the error for an ellipse with the axial ratio U_2/U_1 being below 0,3 usually will lie withing the measuring accuracy and that intermediate values of ϑ may therefore be used for determining H_0 and H_{90}. H_0 and H_{90} can then be calculated and averaged from several measurements by means of Eq. (2.13).

For the infrequent case of $U_2/U_1 = 0,5$, H_0 and H_{90} must be determined at $\vartheta = 0°$ and $\vartheta = 90°$ as precisely as possible, since here, as mentioned above, only these components will occur and can be measured accurately.

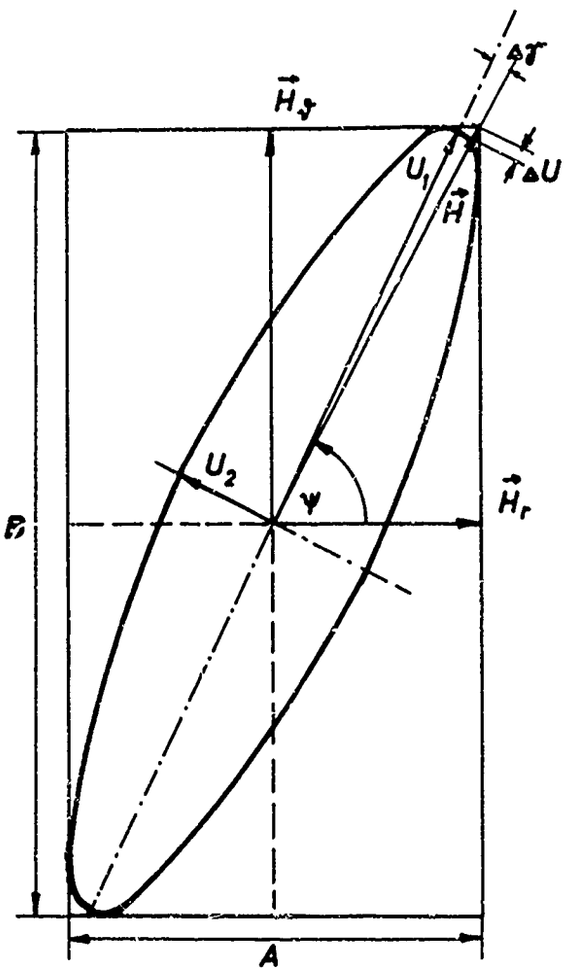

Fig.: 2.8

3. MEASUREMENTS WITH THE LARGE TRANSMITTING ANTENNA SA 9

3.1. Large transmitting frame SA 9

In continuation of measurements over great distances made by Univ. Doz. Dr. W. Bitterlich and Dr. O. Gröbner, studies with the transmitting frame SA 9 have again been made [20]. The transmitting frame SA 9 which has the dimension of 40 x 40 m, 10 turns of 135 mm^2 aluminum conductors is spanned out in suitable galleries and shafts in the mine of Großkogl where it had been set up in 1964 with the same shape it still has. As the antenna has never been serviced up to the present measurements, great difficulties were to overcome before using it again. All supporting inuslators were damp and dirty, some were broken and had to be cleaned or replaced. The nylon ropes used for binding the aluminum cables to the insulators were all damp and partly broken so that some time had to be used for repair work.

Impedance as dependent on frequency could not be measured with the conventional bridge balancing method for reasons which so far have not been fully explained. For getting as clear as possible a picture of the electrical properties of the antenna, the inductance and self-capacitance were determined by the resonance method. The antenna SA 9 can be represented with sufficient approximation as shown in Fig. 3.1. At the transmitter output, and at the end of the Lecher wire, the transmitting antenna is operated as a series resonance circuit in order to obtain a resonance resistance as low as possible, to which the transmitter output can be matched best.

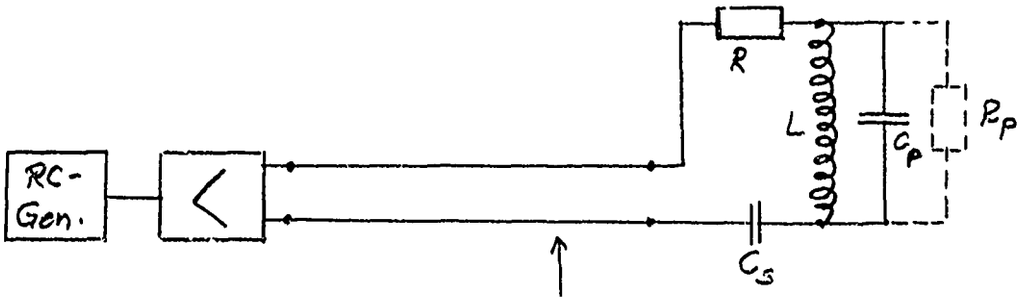

Fig. 3.1

The impedance at the Lecher wire terminals is calculated as follows:

$$\vec{Z} = \vec{R}_R + \vec{R}_\omega + \vec{R}_{L||C_p}$$

$$\vec{Z} = R + \frac{1}{j\omega C_s} + \frac{1}{1/j\omega L + j\omega C_p} \qquad (3.1)$$

$$= R + j\left(\frac{1}{1/\omega L - \omega C_p} - \frac{1}{\omega C_s}\right)$$

At resonance frequency, the imaginary part disappears, i.e., the expression in parenthesis of Eq. 3.1 becomes 0. Hence,

$$\frac{1}{1/\omega L - \omega C_p} = \frac{1}{\omega C_s} \qquad (3.2)$$

or

$$f = \frac{1}{2\pi\sqrt{L(C_p + C_s)}} \quad .$$

If for the graphical representation of various points of measurement we chose the form

$$\frac{1}{f^2} = 4\pi^2 L(C_s + C_p) \qquad (3.3)$$

with $$y = k(x + x_o)$$

the parallel capacitance can be read from the negative abscissa section, whereas the antenna inductance can be calculated from the gradient of the straight line. The actually measured values are listed in Table 3.1 and graphically represented in Fig. 3.2.

TABLE 3.1

f kHz	C_s µF	$1/f^2$
1,18	1000	7.2
1,44	670	4,8
1,85	430	2,93
1,98	395	2,56
2,15	330	2,17
2,44	260	1,68
2,85	192	1,23
3,25	149	0,95
3,35	123	0,89
4,15	88	0,58
5,00	58	0,40
6,7	30	0,223
8,2	20,6	0,149

The inductance for SA 9 calculated from the gradient of the curve in Fig. 3.2 and from the mean value of the individual points of measurement is as follows:

$$L = 18,2 \text{ mH.}$$

The straight line placed optimally through the points of measurement goes through the origin with sufficient accuracy.
This shows that the parallel capacitance is negligibly small.

as compared to the tuning capacitances.

It was assumed that one of the possible reasons for the non-functioning of the bridge method for determining the impedance was the difference (orders of magnitude) of the current intensity and voltages at the antenna on the one hand when operated in resonance with the transmitter and on the other hand with the measuring generator. For studying this possible effect, resonance curves were plotted at ever decreasing voltages and resonance current. The values are listed in Table 3.2. The circuit used for this purpose is shown in Fig. 3.3.

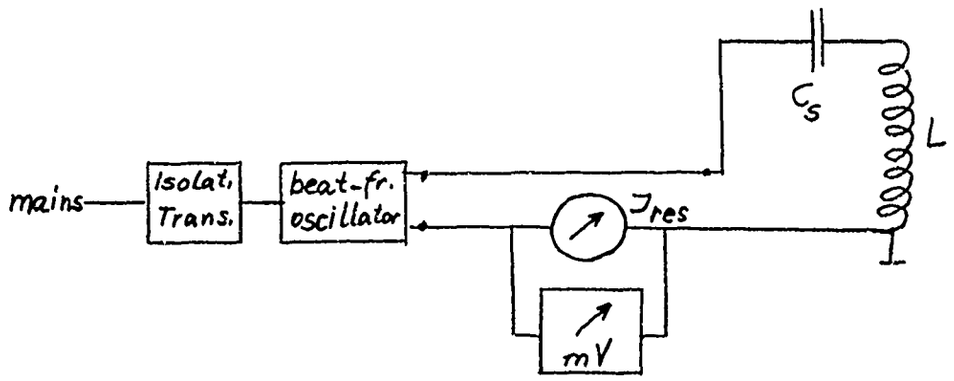

Fig. 3.3

Here it could be seen that the beat-frequency oscillator (Grundig) used as measuring generator, has an output separated from the a-c mains only insufficiently so that in the circuit without an isolating transformer an a-c current flowed through the antenna which made an accurate measurement impossible. The use of an isolating transformer (Grundig) permitted a correct measurement. Another difficulty arose when measuring the current by means of the multi-purpose instrument Unigor 2s (Görz). For the small range of measurement, the too large resistance of this instrument reduced the Q of the antenna such that a direct measurement for currents as small as that was impossible.

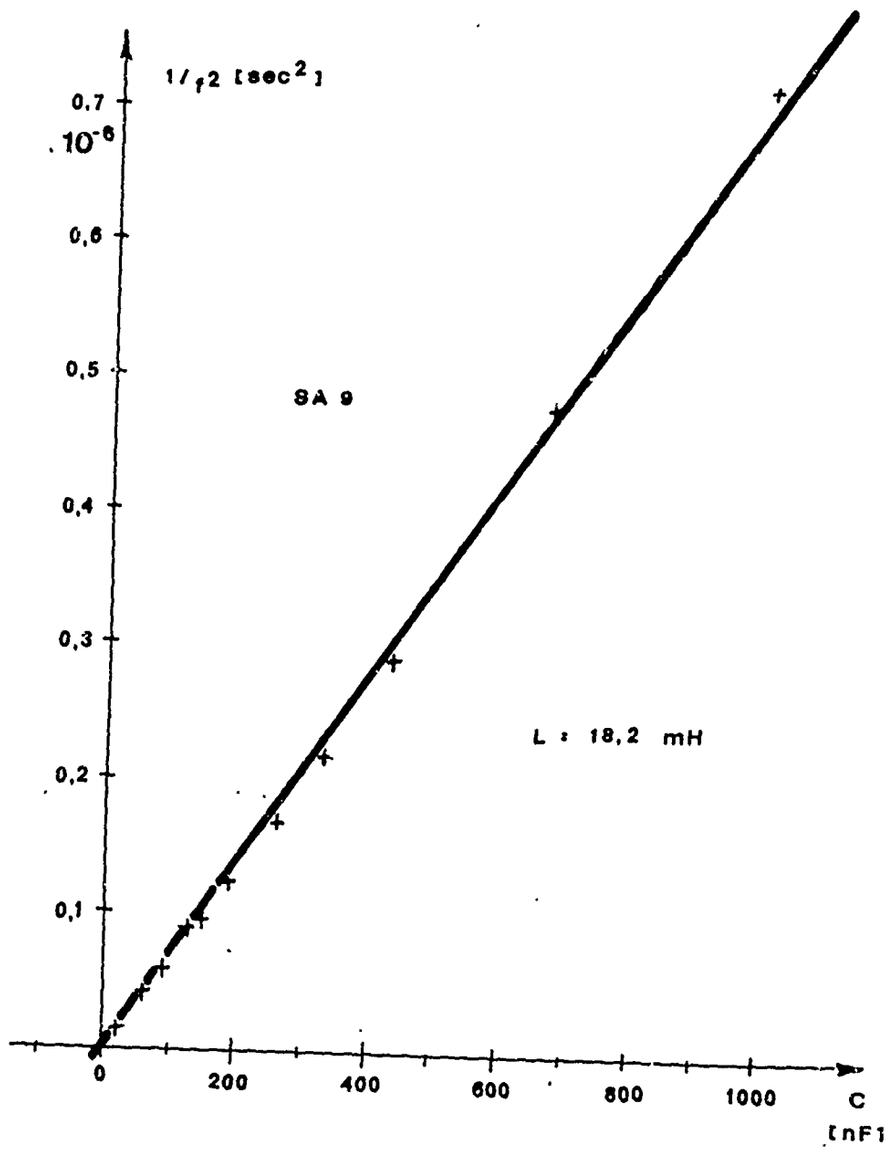
1/f2 [sec2]
0,7
.10-6
0,6
0,5
SA 9
0,4
0,3
L : 18,2 mH
0,2
0,1
0
200
400
600
800
1000
C
[nF]

Fig.: 3.2

At 60 ma, this instrument has a resistance of accurately 1 Ohm so that the voltage drop on this resistance can be measured by means of the selective transmission measuring set (Marconi), the voltage being equal to the current intensity. The current intensities for the last three lines of Table 3.2 have thus been measured. The values of Table 3.2 are voltage values that are standardized to 100% at maximum resonance, giving the drop of the resonance curve to the left and to the right.

TABLE 3.2

I_{res} \ f [kHz] →	2,48	2,50	2,52	2,54	2,56	2,58	2,60
1,35 a	33	43	65	100	95	69	48
0,15 a	34	46	66	100	86	63	37
13 ma	43	57	82	100	86	59	46
1,5 ma	49	63	83	100	83	63	49
103 µa	47	62	85	100	83	62	47

In the first two lines of the table (corresponding to the current intensities of 1,35 a and 0,15 a), the maximum voltage seems to be somewhat unsymmetrical, and the maximum value of voltage would accordingly be more than 100%. The reason for this unsymmetry is to be sought in the resistance of the instrument, as the resistance for these two regions (6 a and 0,6 a) is 0,06 ohms and 0,23 ohms, respectively so that attenuation of the entire circuit for these two regions is much lower. This is expressed in a displacement of maximum voltage toward higher frequencies, and when plotting the curves or comparing the voltage values more precisely, Q is found to be somewhat higher. For the highest resonance current, a Q of about 40 is obtained. By means of this measurement it could be proved that Q and also the antenna inductance are

independent of the applied current or voltage at least over four powers of ten of the current or resonance voltage. The failure of the bridge method thus cannot be explained by referring to currents or voltages owing to galvanic or leadage currents.

For the purpose of explaining the failure of the bridge measurement, it must be examined in how far a loss resistor R_p (cf. Fig. 3.1) to be plotted parallel to the inductance L affects the measurement by making it impossible.

3.2. Feeding the large transmitting antenna SA 9

The large transmitting antenna SA 9 was fed in the same way as in the 1964 examination by means of a transmitting amplifier Type Savage with an output power of 1 kw. The frequency generator was a decadic RC generator (Levell) which in the used frequency region had the required accuracy of frequency and stability. The output transformer of the transmitting amplifier has several circuit variations permitting the output resistance and output voltage at full modulation to be varied. The most favorable output impedance was then determined by experiment.

In the former experiments, oil-soaked paper capacitors of high dielectric strength were used for tuning the transmitting antenna to resonance. The quality of these capacitors, however, was insufficient for guaranteeing continuous operation at high voltage. They got too hot and their quality was thus reduced considerably. For the purpose of attaining a higher resonance power on the antenna, new ceramic capacitors (Rosenthal) were ordered which were able to take the high reactive power without noticeable temperature increase. Since the maximum capacitance of these capacitors was only 6000 pF

owing to their construction, the frequency minimum was 6,2 kHz, the six disk-shaped capacitors having a total capacitance of 35 nF.

For attaining a higher antenna current, the frequency had to be reduced, the capacitance thus being increased. At a frequency of 1,16 kHz, a maximum resonance current of 15 a could be attained (measured by Unigor 2s) and kept constant over a long period of time by means of a mica capacitor (capacitance 1 µF) borrowed from the Austrian Radio Company. During the propagation measurement, however, it was found out that there existed a number of signals close to the transmitting frequency in the neighborhood of the high-voltage lines which are very close in the region to be measured. Probably these are keyed pilot frequencies on the TIWAG lines.

These interfering signals made a measurement over great distances impossible, a somewhat higher transmitting frequency had to be chosen.

After several experiments, a group connection of all existing capacitors was found, yielding a resonant frequency of 2,74 kHz and a resonance current of 12 a which could be kept unchanged for over six hours. The circuit of these capacitors is shown in Fig. 3.4.

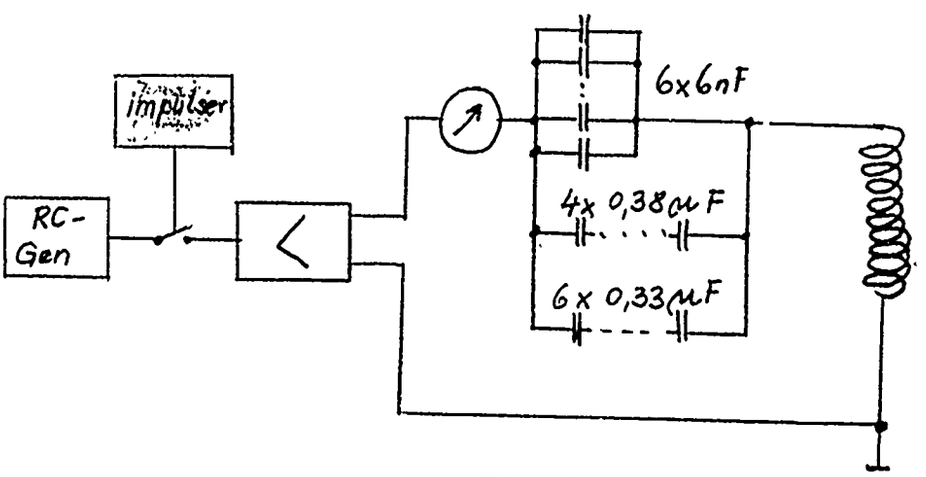

Fig. 3.4

For facilitating the measurement, a previously prepared impulser was connected between the RC generator and transmitter for switching on the signal for 8 secs and off for 2 secs. By means of this regular rhythm, the signal to be measured can clearly be separated from the interfering signal, even with the noise level lying in the same order of magnitude as the signal to be measured. The measurements thus conducted over largest possible distances, are described in detail in the next chapter.

3.3. Measurements with the transmitting antenna SA 9

A propagation measurement around the transmitter site, namely the region of St. Gertraudi - Reith - Großkogl was made with the above-mentioned arrangement (transmitting antenna SA o + ceramic capacitors for tuning to resonance, resonant frequency of 6,7 kHz. The measured values are listed in Table 3.3.

Fig. 3.5 gives these values graphically. A comparison with the antenna diagrams of former studies [15, 18, 21] is possible only up to a certain point, since the conditions for the former directivity patterns are fulfilled only in parts. These are: 1) the distance of the different points of measurement to the transmitting antenna is not the same;

2) The points of measurement lie outside the mountain, on the earth's surface;

3) The distance of penetrated rock is not equally long for all the points.

The last two positions are considerably different from the conditions assumed in theory.

4) The points of measurement do not lie in a plane so that the counting of angles strictly speaking ought to include

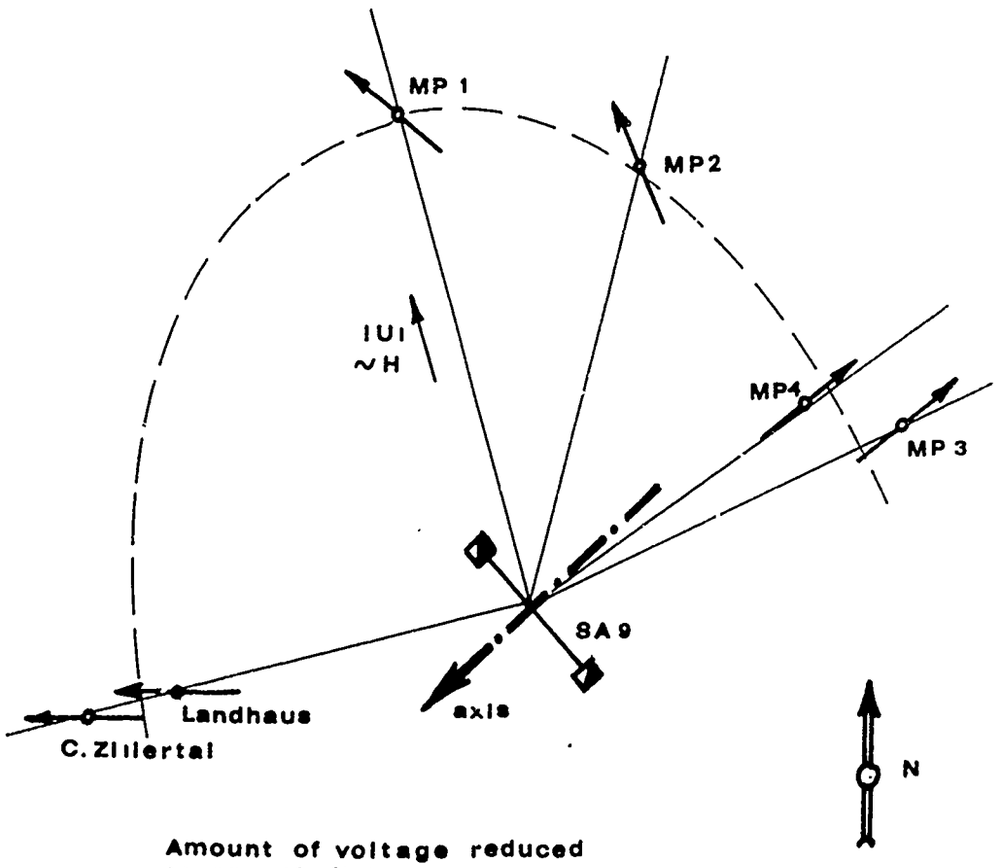
MP 1
MP2
IUI
~H
MP4
MP 3
SA 9
axis
Landhaus
C. Zillertal
N
Amount of voltage reduced
to eaqual distances

Fig.: 3.5

two angles, one in the horizontal direction from the antenna axis, the second one as a vertical deviation from the horizontal. Remarkable is the last point of measurement over a distance of about 3 km (Cafe Zillertal), where a signal-to-noise ratio of 5:1 was attained.

The values of table 3.3 were measured with a receiver which shall be described in detail in the following chapter. The antenna preamplifier was operated without a resonance circuit. This is why the sensitivity is still very low.

TABLE 3.3

Propagation measurement 13 Aug. 1968

Transmitter: SA 9 Levell R-C-Generator, Savage-amplifier (75 v matching) 5 Rosenthal ceramic capacitors C_{tot} = = 30 nF, f = 6,68 kHz, I_A = 6,8 a_{eff} (Unigor 2s)

Receiver: FA 6 ("Plexifetantenna") Cascode preamplifier (non-selective) with transformer output, Marconi

point of measurement	r [m]	U_S	U_N	S/N
entrance	350	6 v	2 mv	3000
1	810	1,1 v	2 mv	500
2	870	0,9 v	1,5 mv	600
3	1160	220 mv	1 mv	220
4	880	0,7 v	2 mv	350
Landhaus	1600	92 mv	3 mv	30
Cafe Zillertal	3100	10 mv	2 mv	5

U_S ... Signal - (useful) voltage

U_N ... noise voltage (jamming transmitter and noise)

A series of measurements over distances as large as possible was made at a frequency of 2,74 kHz and an antenna current of 12 a. φ, the angle between the axis of the transmitting antenna and the radius vector is about 45° for all antenna points. The points of measurement lie along the Inn valley on a line connecting the mines of St. Gertraudi and Schwaz. The individual values of measurement are listed in Table 3.4.

TABLE 3.4

Propagation measurement 10 Dec. and 17 Dec. 1968

Transmitter: SA 9 decad. Levell R-C generator, impulser, Savage amplifier (50 v matching) 5 Rosenthal capacitors à 6000 pF, 4 cube capacitors à 380 nF, pot-type capacitor with 6 angles à 330 nF, f = 2,744 kHz, I_A = 12 a (Unigor 2s)

Receiver: FA 6 ("Plexifetantenna") Cascode preamplifier with resonance circuit, Marconi

Point of measurement	r [m]	U_S	U_N	S/N
Entrance	550	500 mv		
Landhaus	1600	22 mv	10 µv	2200
Cafe Zillertal	3100	14 mv		
junction Zillertal	3400	1,4 mv	10 µv	140
" Achensee	4300	0,6 mv	200 µv	3*)
Rotholz	5300	300 µv	20 µv	15**)
St. Margarethen	6400	70 µv	10 µv	7
Aral filling station (before Galzein)	7400	50 µv	10 µv	5
opposite Jenbacher Werke	7800	40 µv	8 µv	5
before entering Galzein road	8800	30 µv	8 µv	4
drive to mine of Schwaz	11.7km	20 µv	8 µv	2,5
behind Messerschmitt hall	11.3"	8 µv	4 µv	2

*) distance to the next high-voltage line

**) distance to the next power line about 20 m

The tables show that this measuring arrangement for the first time permitted measurement over a distance reaching from the mine of St. Gertraudi to the mine of Schwaz, i.e., 12 km were penetrated. Radio-communication between the two mines had been the aim of previous measurement, which, however, could not be attained, since the capacitor quality on the transmitter side was not high enough, and an adequate, low-noise receiver had to be built first. Very favorable for the measurement were the noise level which was very low at that time, the choice of frequency between two jamming stations, and the transmitter signal which was keyed.

The graphical representation of this series of measurements is shown in Fig. 3.6. Comparison is made with the theoretical curve for a conductivity of 10^{-4} mhos/m. It can clearly be seen that attenuation for the measured propagation is lower than the rock conductivity to be expected, since the measurement is not made continuously through rock. Zillertal causes a 3 km interruption, penetration into the ground afterwards being only partial. It shall be examined in later studies whether the signal propagation is a ground wave or skye wave. At a wavelength of about 100 km, it remains to be studied whether this is a case of wave propagation at all or whether it is a kind of open transformer.

3.4. Receiving device EA 7

In view of large distance propagation measurements and of the weak signals to be expected at measurements under difficult conditions, an extremely low-noise antenna preamplifier was constructed which was intended to have good noise properties and high electrical and thermal stability. For the input stage, very low-noise transistors were chosen: silicon NPN transistors

type BFY 77 having a characteristic noise factor of 0,6 db in a frequency range of 3 - 300 kHz. For fully utilizing this low noise factor, a cascode circuit [20] was chosen for the input stage. This type of circuit comparatively seldom described in literature, has some very interssting properties. For this reason, this circuit is going to be described hereinafter. The input circuit is shown in Fig. 3.7.

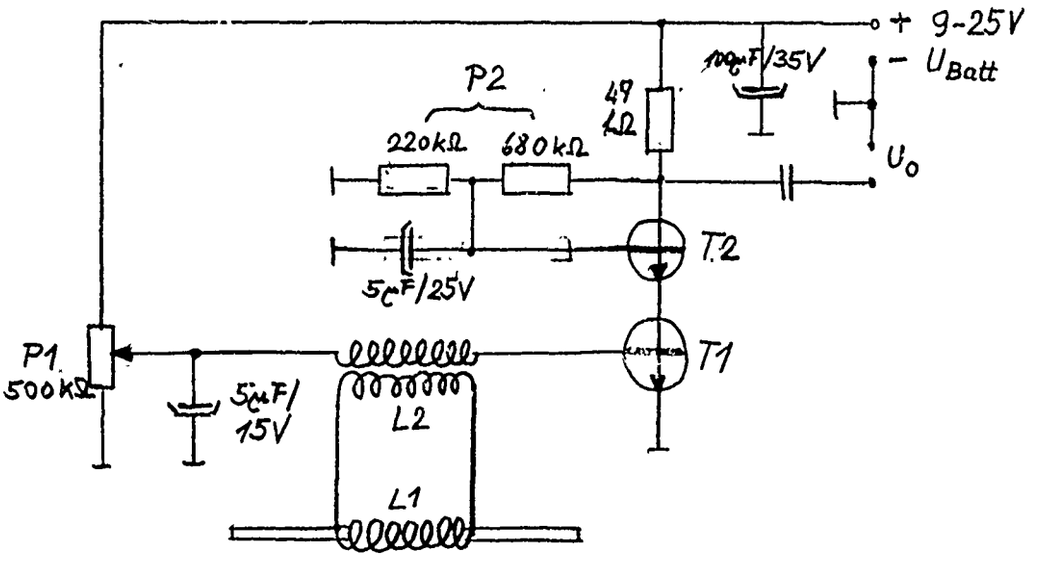

Fig. 3.7

In order to avoid coupling over a high-resistance input circuit (resonance circuit) which is disadvantageous for the noise level, inductive coupling was preferred. It has an input resistance of about 1,5 kΩ, its noise power being practically negligible. From the Nyquist formula, a noise voltage of 0,014 µv on this resistor was calculated for a receiver band width of 10 Hz (Marconi... 7 Hz). The potentiometer P1 of 500 kΩ which is used for adjustment of the base bias of the first transistor is short-circuited for a-c by a 5 µF capacitor. The voltage U_{CE} on transistor T_1 is very small. The latter therefore has only low

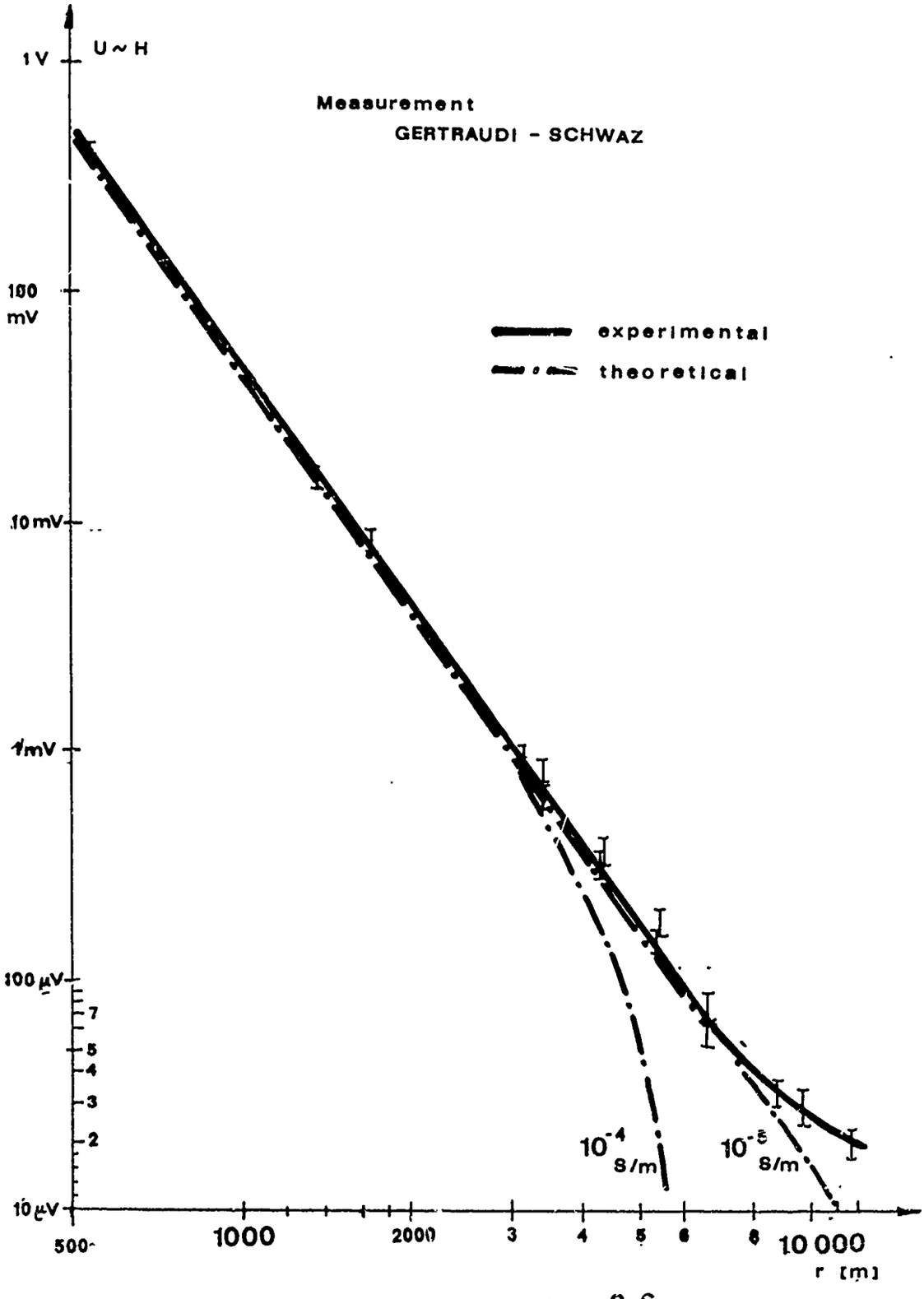
1 V
U ~ H
Measurement
GERTRAUDI - SCHWAZ
100 mV
experimental
theoretical
10 mV
1 mV
100 µV
10 µV
7
5
4
3
2
500
1000
2000
3
4
5
6
8
10 000
r [m]
10^-4 S/m
10^-5 S/m

Fig.: 3.6

amplification, but is very favorable with respect to its noise behavior. Actual amplification is due to transistor T_2 whose base can be adjusted via the potentiometer P_2 which in this circuit has been replaced by fixed resistors. The base of T_2 is grounded for a-c, i.e., the transistor T_2 operates in grounded base connection. The adjustment of potentiometer P_2 is uncritical in a relatively large region. If the base bias is driven too far toward positive battery voltage, the cascode circuit becomes unstable, tending to self-excited oscillations. Coupling of P_2 to the collector of the second transistor instead of the positive battery voltage, leads to negative feedback supporting the voltage stability. The most favorable battery voltage was 18 v, the amplification factor being v = 72. Table 3.5 gives the dependence of the amplification factor on the battery voltage.

TABLE 3.5

Amplification as dependent on U_{batt}

U_{batt} |v|	7	9	10	12	15	18	20	25
v_{rel}	0,5	0,8	0,9	0,96	1,0	1,0	1,0	1,1

It is remarkable that the amplification factor is almost constant in a very large voltage region (15 - about 22 v). This is due to the negative feedback of transistor T_2 via potentiometer P_2, and to the pentode characteristic of the total cascode stage. The signal passes through the cascode circuit undistorted in the entire region of voltages and frequencies.

Feeding the signal directly to the primary side of the input transformer L_2 in a suitable manner, the following frequency response can be measured:

600 Hz ... 150 kHz at -3 dB
900 Hz ... 100 kHz at -10%.

The cascode circuit with the values described in Fig. 3.7. has an input resistor of R_{in} = 1,5 kΩ and an output resistor of R_{out} = 25 kΩ. The demend for linear amplification limits the output signal at a maximum of 6 v_{ss} (measured with a Philips double-beam oscilloscope).

For testing the temperature stability, the temperature was measured by means of an iron - constantan temperature tester and an Unigor lp on the transistor case; high temperatures were reached by a hair-drier, low temperatures by means of a cold spray. Low temperatures were measured during the temperature rise. The following values were measured:

Temperature	10°C	amplification ratio v_t/v_{20} = 0,85
	16°C	0,86
	20°C	1
	30°C	1
	40°C	0,9 (operating point shifted)

Because of the comparatively high output resistance, high-resistance instruments had been used for the above measurement (oscillograph, vacuum tube voltmeter). For measurements with the selective level meter (Marconi) the input resistance of the meter was of the same order of magnitude as the output resistance of the circuit. This was very disadvantageous when the measuring range of the Marconi instrument was changed, as its input resistance depended on the range. At first, a single stage impedance transformer was connected with the cascode stage, amplification of this stage, however, proved too low for noise measurements.

In order to avoid a deterioration of the very favorable stability properties of this amplifier by connecting another amplifier stage in between, amplification was increased by a

resonance circuit which at the same time had the advantage of attenuating interfering signals at neighboring frequencies already in the preamplifier. The final preamplifier circuit is shown in Fig. 3.8. The input resistance of the simple emitter follower proved too small, i.e., the resonance circuit was attenuated too much so that a double emitter follower now forms the output circuit of the preamplifier. The resonance circuit L_3 was dimensioned according to optimum matching of resistance. The input resistance of the double emitter follower stage is about 2,5 MΩ so that there is a resistance formation of 1 : 100 from the output of the cascode stage to the input of the emitter follower. This requires a turn ratio on the transformer of 1 : 10 . The inductance depended on the desired frequency region: Secondary 2,6 H yielded a frequency variation of 2,5 - 13,5 kHz with a three-fold variable capacitor (1500 pF - 30 pF). This inductance was reached by means of a pot-type core without an air gap with n_2 = 1000 turns. The primary number of turns thus was determined as n_1 = 100. The output resistance of this circuit is now smaller than 1kΩ, mainly depending on the emitter resistance of the last transistor.

Table 3.6a gives the frequency behavior of the preamplifier plus the resonance circuit.

TABLE 3.6 a

f [kHz]	2,5	3	5	10	12
v_{Res}	210	225	230	230	235

In order to examine the noise behavior of the preamplifier, a calibration field was produced with a calibration coil (area 1290 cm^2, ω = 10, I = 0,5 ma) at a distance of 3 m. This field mainly served the purpose of adjusting to the same frequency the preamplifier

and the selective transmission level meter. When the calibration field was switched off, the level of atmospheric disturbances could be measured, i.e., the input noise of the transistor could be measured when replacing the antenna rod by a pot-type core of equal inductance. For measuring the noise potential correctly, an effective voltmeter would have been necessary with an adequate time constant. This, however, was not available at the time of measurement, so it was carried out with an apparatus that is used in measurement work. The values for the noise voltage are values visually integrated over a certain period of time on the indicating instrument of the selective transmission level meter. Thus, however, the noise level can be estimated but roughly, especially since the peaks which often are a multiple of the measured noise level, are not taken into account. Yet, this method is admissible for noise level comparisons, since the signal is to be measured under the same conditions and need only be distinguished clearly from the noise level. Tab. 3.6b shows various measured values on the noise behavior of the preamplifier, where

- f = resonant frequency to which the preamplifier circuit is matched
- U_a = output voltage at switched-on calibration coil
- U_N = voltage of all noise signals with the calibration coil being switched off
- U_O = voltage at open input (ferrite antenna disconnected)
- U_L = ferrite antenna replaced by a pot-type core of equal inductance (pot-type core shielded against external radiation)
- U_k = input short-circuited

TABLE 3.6 b

f	U_a	U_N	U_o	U_L	U_K
3 kHz	1,8 mv	100 µv	< 6 µv	< 5 µv	5 µv
5 kHz	2,2 mv	100	< 8 µv	< 7 µv	< 8 µv
10 kHz	2,2 mv	70 µv	15 µv	15 µv	12 µv

The given voltages refer to the output of the preamplifier, the voltage at the input being calculated by dividing by the respective amplification factor.

For enlarging the frequency region of the preamplifier, it is planned to connect the inductance L3 (Fig. 3.8) in several stages, with the ratio of turns of 1:10 (resistance matching!) being preserved. Thus, the entire frequency region of the cascode stage is to be utilized (even when an antenna of higher frequency has to be taken into account).

Total circuit of the antenna preamplifier

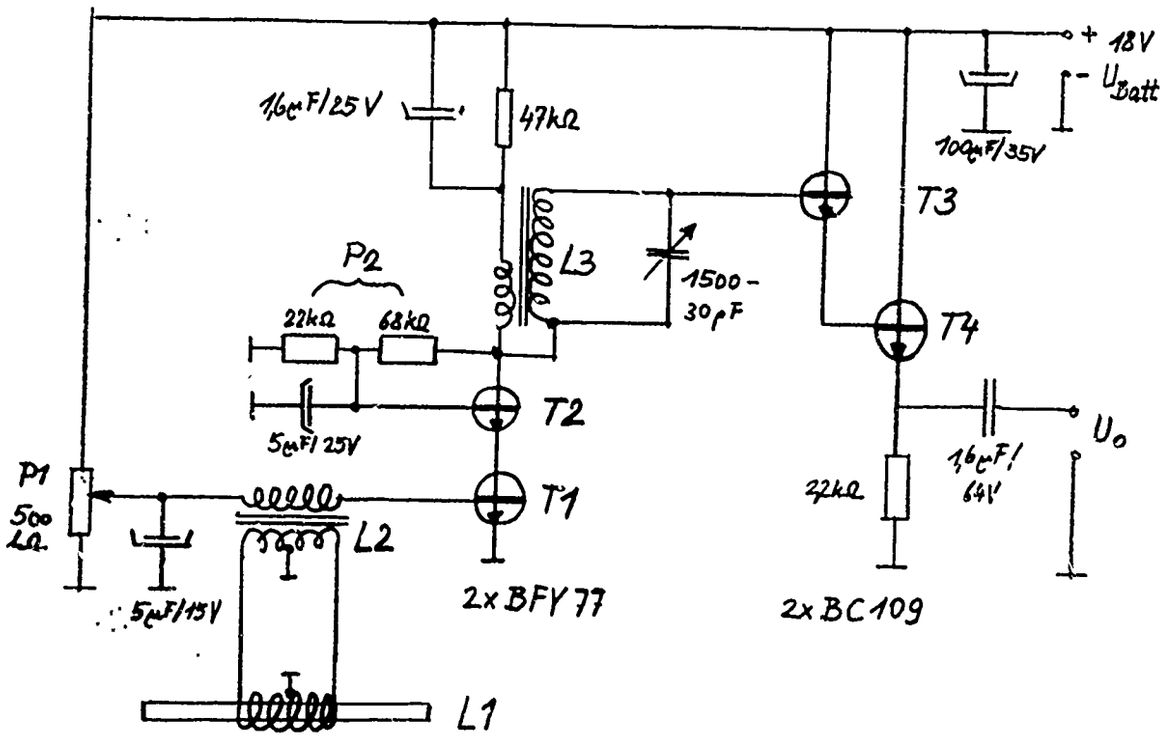

L_1 ... ferrite rod antenna FA 6 x length 1 m, circuit 1 300 turns

2 300 "
4 300 " } 160 mH } 0,58H
6
7 300 "

L_2... pot coil core transformer 58T3, material 1100N22, without air gap

prim 0,11 H, 10Ω

sec 0,24 H, 15 Ω

L_3 ... pot coil core transformer 58T3, material 1100 N 22, without air gap

prim 20 mH, 100 turns

sec 2 x 0,66 H, 2 x 500 turns

2,6 H 1000 turns

Fig. 3.8

4. ELECTRICAL ROCK CHARACTERISTICS FROM THE FIELD STRUCTURE OF A MAGNETIC DIPOLE IN A CONDUCTING MEDIUM

This report reviews the studies so far conducted on the above subject. Besides a brief discussion of the theoretical principles, which have been reported in detail before [9], some results are given of measurements which shall be published in the near future. A scientific report giving detailed information on this subject is now being prepared.

4.1. Introduction

Studying the propagation of electromagnetic waves through rock, two fundamental problems arise concerning the medium.

1) May the rock be considered as a homogeneous, isotropic medium?
2) If so, how large are the mean values of conductivity and dielectric constants?

In order to answer these two questions, propagation measurements will have to be studied, since in the first problem only homogeneity with respect to propagation of electromagnetic waves is being discussed. The second problem cannot be solved by measuring σ and ε_r on rock samples, since

1) there exist difficulties of simulating the in situ conditions (pressure, temperature, humidity). This has already been stated by L.A. Ames et al. [22],
2) there is no hint as to how values decisive for propagation might be obtained from samples even when measured under in situ conditions,

3) electrode polarization at low frequencies disturbs the ε_r measurement [8] (for VLF propagation processes, however, then usually $\sigma >> \omega\varepsilon_r\varepsilon_o$ so that the exact value of ε_r is insignificant.)

The method of measurement used by O. Gröbner [23] and technically improved by N. Nessler [18] was applied without any changes. In this method, a magnetic dipole with a horizontal axis is used as a transmitting antenna which is rotated in certain angular positions, the magnetic field strength components being measured at the point of reception. The methods described by R. Hommel [17] and N. Nessler [18] permit the determination of σ and ε_r, but give no information on the problem of homogeneity. In these cases it may occur for example that some conductivity is measured which is incorrect by several orders of magnitude, since the conditions of measurement have not been fulfilled. Therefore it is necessary that a method should be applied in which each measured angular position of the transmitting antenna is evaluated so that information is obtained to what extent the experiment is described by the theory.

4.2 Theory

The following conditions are assumed:

1. The medium be
   a) homogeneous
   b) isotropic
   c) unbounded.

At a time factor of exp ($+i\omega t$) it is characterized by the complex wave number k:

$$k = k_1 - ik_2 = \omega \sqrt{\varepsilon\mu\left(1 - i\frac{\sigma}{\omega\varepsilon}\right)} \; . \qquad (4.1)$$

σ = conductivity $[\Omega^{-1}m^{-1}]$, $\omega = 2\pi f$, f [kHz] ... frequency

$\varepsilon = \varepsilon_r\varepsilon_o$ ... dielectric constant [as/vm]

μ ... permeability [vs/am],

$\mu = \mu_o$ is being assumed

2.)J.R. Wait [24],[25] showed that the influence of an air-filled spherical cavity in which the transmitter is immersed is negligible if

$$k_o a \ll 1 \quad \text{and} \quad |ka| < 0{,}2.$$

a ... radius of cavity

k_o ... wave number in air ($k_o = 2\pi/\lambda_o$)

3.) Let b be the maximum dimension of transmitting or receiving antenna, then

$$b \ll r \quad (r = \text{transmitter - receiver distance})$$

and

4.) $b \ll \lambda_o$.

The conditions of pos. 2 and 4 determine an upper frequency limit. The size of the region considered as being homogeneous in connection with the fact that a useful accuracy is reached only if $k_r > 0{,}3$, give the lower frequency limit.

Under the above conditions, the expressions for the magnetic field strengths of the magnetic dipole in spherical coordinates [26]

$$H_r = \frac{n\,I\,F}{2\pi r^3}(1 + ikr)e^{-ikr}\cos\vartheta \qquad (4.2)$$

$$H_\vartheta = \frac{n\,I\,F}{4\pi r^3}(1 + ikr - k^2r^2)\,e^{-ikr}\sin\vartheta \qquad (4.3)$$

I ... transmitting current
F ... area of the transmitting antenna
n ... number of turns
r, ϑ, φ ... spherical coordinates.
Defining

$$G = \left|\frac{H_r}{H_\varphi}\right| \tan \varphi \qquad (4.4)$$

with δ = phase difference between H_r and H_φ
We can derive formulas from (4.2) and (4.3) for G and δ :

$$G = G(x,p) \qquad (4.5)$$
$$\delta = \delta(x,p) \qquad (4.6)$$

where

$$x = k_1 r \qquad (4.7)$$

$$p = \frac{k_2}{k_1} \qquad (4.8)$$

The quantities G and δ are measured, the equations (4.5) and (4.6) are solved for x and p, the complex wave number thus being determined. From (4.1) we obtain for σ and ε_r

$$\sigma = 2{,}533 \cdot 10^5 \frac{k_1 \cdot k_2}{f} \quad [\Omega^{-1} m^{-1}] \qquad (4.9)$$

$$\varepsilon_r = 2{,}280 \cdot 10^{15} \frac{k_1^2 \cdot k_2^2}{f^2} \quad [1] \qquad (4.10)$$

G and δ are determined from measurements on polarization ellipses, thus confining the distance region for the measurement. Polarization ellipses are known to occur in the transition zone between the quasistatic field ($kr \ll 1$) and far field ($kr \gg 1$), hence kr must have the order of 1 for such measurements.

If the frequency, distance and the angle ϑ are known, σ and ε_r can be determined from one polarization ellipse. Of the polarization ellipse only the axial ratio v and ψ and the angle between radius vector and large principal axis are required.

If the receiving device operates linearly, like in the case of the ferrite rod antennas developed by W. Bitterlich [16], the receiving antenna need not be calibrated for determining σ and ε_r. A calibrated receiving antenna, however, can be used for an additional control by substituting in (4.2) and (4.3) the value obtained for the complex propagation constant, and comparing the result with the field strength value measured directly.

4.3. Experiment

At the beginning of the measurements, the device built by N. Nessler [18] could be used. In order to find the upper frequency limit for the applicability of theory, a valve transmitter of 50 w, 140 - 1000 kHz was built. A preamplifier for the receiving device for higher frequencies was built by R. Lukavec (see chap. 1.4). Furthermore, two circular frame antennas with one turn were constructed, one being made as a shielded loop. Both have a diameter of slightly less than 1 m so that they are easy to set up in the mine.

Measurements were made in the mine of St. Gertraudi (Tyrol) for frequencies of 120 - 1000 kHz and transmitter-receiver distances which usually were below 100 m.

The transmitting antenna is rotated from $\vartheta = 0^\circ$ to $\vartheta = 180^\circ$ in steps of 15°. For each angular position of the transmitting antenna (except for $\vartheta = 0^\circ$ and $\vartheta = 90^\circ$), the polarization ellipses yield a G value and a δ value.

In contrast to theory, experiments showed that these values were not independent of the angular position of the transmitting antenna. Repeating the measurements, this fact could be proved by means of variance (F) test [27] . The method of determining σ and ε_r thus is affected by a considerable systematic error whose influence can be estimated by the scattering of G values and δ values.

In favorable cases, this error was about 25% for the σ measurement and about 60% for the ε_r measurement.

A possible cause for the field distortions was the immediate neighborhood of the transmitter (instruments). Various transmitting antennas were compared under equal conditions (place and time of measurement, frequency), with the transmitting device being set up differently. The F test yielded no significant differences between the different antennas. A significant difference however was found in the field symmetry with respect to the line connecting transmitter and receiver. Since a long and straight gallery is unlikely to produce such an unsymmetry (transmitter and receiver were located in such a gallery at visual range), there remains only the possibility that a geological disturbance causes a field distortion. In fact, there exists such a disturbance near the point of reception. Since there exists no theory for such cases, a clear relation between a geological disturbance and field distortion could not be proved.

4.4. Conclusion

It was shown that the described kind of measurements

1. permits testing of the electromagnetic homogeneity of the region surrounding the distance transmitter - receiver,

2. yields mean values of σ and ε_r.

The accuracy of the σ and ε_r measurement largely depends on how far there actually exists homogeneity. The measurements showed that this assumption can be refuted, but if the field is not too much distorted, mean values of σ and ε_r with a reasonable error can be obtained.

5. PRELIMINARY WORK FOR MEASURING THE ELECTRICAL PROPERTIES OF ORES

5.1. Complex electrical conductivity of ores at low frequencies

5.1.1. Introduction

This report reviews in brief examinations of electrical properties of ores, made recently by various German and American authors. Current studies in this field made at Innsbruck are based on the above studies. Within the framework of research on the propagation of electromagnetic waves through rock it was of interest on the one hand to give values for the electrical rock parameters (conductivity and dielectric constant) used in theory, and on the other hand, compare them with quantities derived from values of field strength measurements and field structure examinations. Furthermore it is of great interest for geoelectric prospection to obtain accurate information on the electrical properties of certain sulfide ores and their complex dependence on various factors.

5.1.2. Conductivity and apparent dielectric constant of water-saturated rock

O. Wörz [19] at first made d-c conductivity measurements on solid rock, using a Wenner electrode arrangement. The work comprising also drill cores was continued by H. Wöbking [8] at frequencies ranging from 30 Hz to 300 kHz. He especially studied the influence of the pore water on the frequency dependence of conductivity and dielectric constant. The rock samples were cut

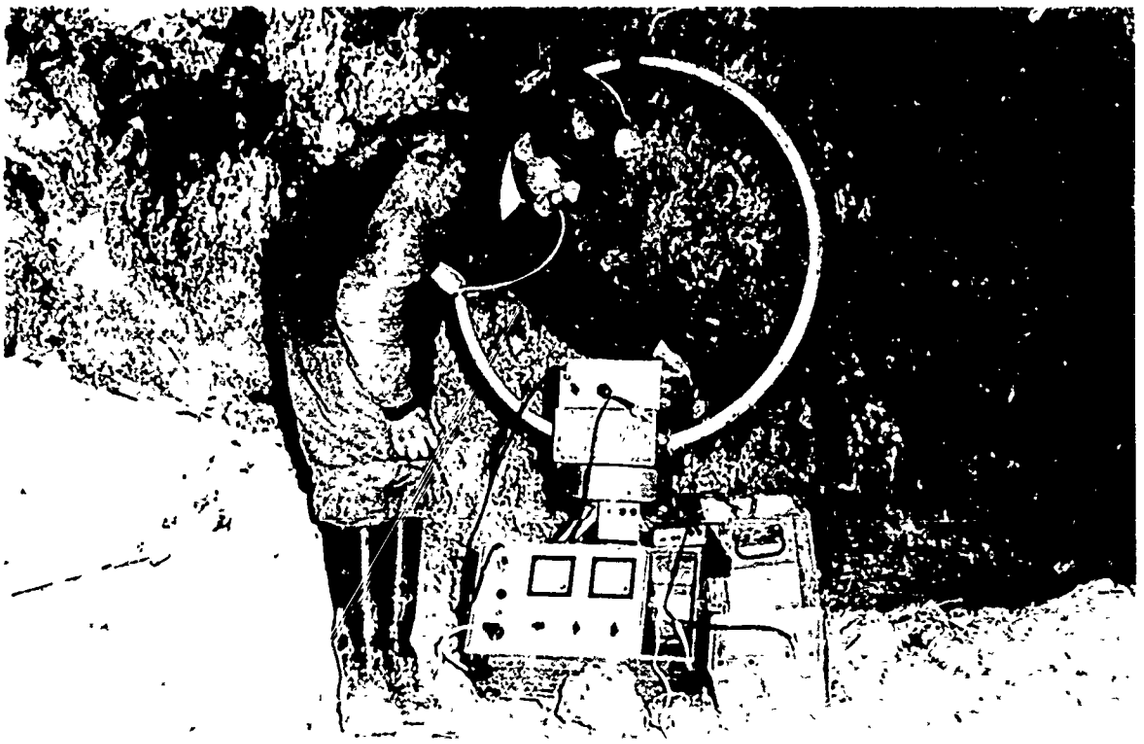

BILD III

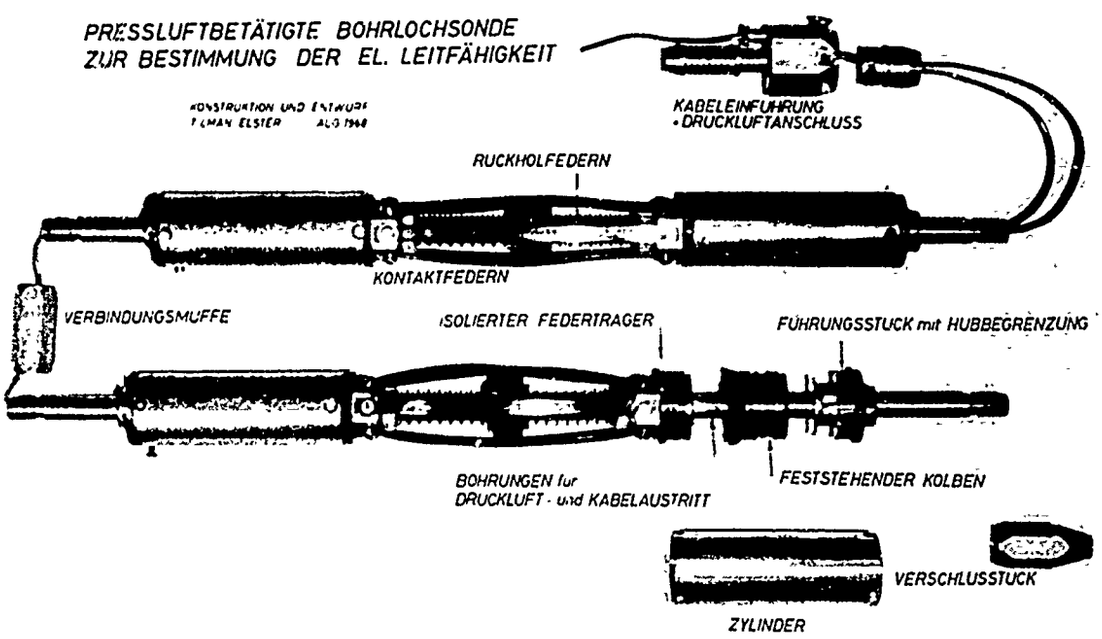

BILD IV

off from drill cores in the form of thin disks and studied as a lossy dielectric in a plate capacitor at different degrees of water saturation. A capacitance bridge was used for determining the parallel capacitance and parallel resistance from which the apparent dielectric constant and the specific conductivity were calculated. As expected, both quantities were found to depend largely on frequency. The parallel capacitance increased rapidly as the frequency decreased so that values up to 10^5 were obtained for the apparent dielectric constant ε at frequencies of about 30 Hz. The specific conductivity increased easily with frequency. These dispersion curves were taken of all rock samples at several degrees of saturation and thus at different absolute water contents depending on the porosity. The results showed that possible characteristic features of the individual kinds of rock are superimposed almost completely by the great influence of the water content.

The very high ε values at low frequencies were explained by the theory of space charge polarization. It takes into account the fact that ions providing charge transportation in the pore liquid have to overcome a potential threshold on the metal electrodes when transferring their charge. The resulting local accumulation of ions in front of the electrodes causes a frequency-dependent space charge polarization simulating a high dielectric constant of the rock. The assumption of space charge polarization in the immediate electrode neighborhood originally was developed for liquid electrolytes by Jaffe [28] . Wöbking extended the theory calculated by Friauf [29] to the pore water - rock system. For this purpose an equivalent circuit diagram was chosen by which it is attempted to explain the measured values by the combined effect of a barrier on the electrode - pore water interface, the pore water itself and the contribution of dry rock.

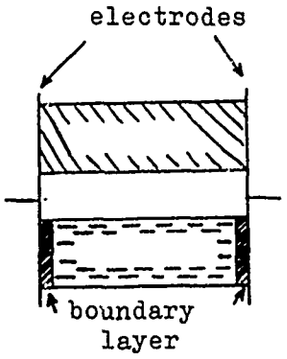

Schematic representation of a water-saturated rock sample in a plate capacitor

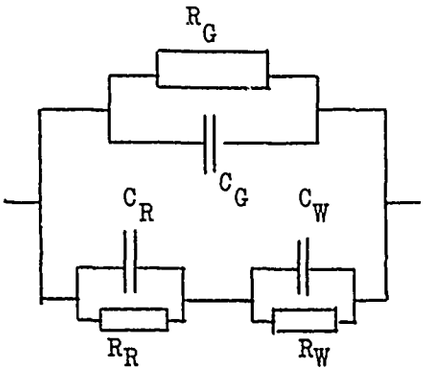

equivalent circuit diagram

R_G = rock resistivity

C_G = capacitance of dry rock

C_R = barrier capacitance

R_R = barrier resistivity

C_W = capacitance of pore water

R_W = water resistivity

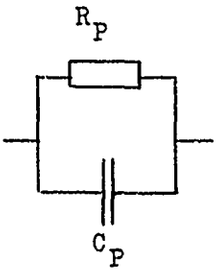

measured quantities

The frequency at which the space charge zone in front of the electrodes is built up and breaks down in "resonance", is called relaxation frequency. In this region, which according to the theory used in [8] lies below 50 Hz, the dispersion curves of the dielectric constants should show their greatest gradient. Because of the restriction to frequencies > 30 Hz (due to technical reasons) the relaxation frequency in most cases could not be clearly proved. Yet the empirically obtained law for the conductivity of water-saturated rock

$$\sigma = B \cdot f^A$$

could be explained by space charge polarization as well as the dependence of the quantities A and B on the water content and the geometrical shape of the pore channels. Although agreement of the frequency curves of conductivity and parallel capacitance with the theoretically assumed trend usually is only qualitative, the theory modified for the rock samples yet can give a general

explanation of the effects that occur with the measuring arrangement used. Certainly, the schematic division into two independent current paths, dry rock body and pore water, is not admissible, since ion absorption and ion exchange between rock and pore water ought to be taken into account too.

5.1.3. The electrical behavior of ores

The studies commenced in 1968 in the geophysical field of the VLF project work are mainly dedicated to the electrical behavior of rock containing ore. Rock containing metallically conductive ore particles besides the electrolytically conductive pore water exhibits effects on all ore particle/pore liquid interfaces that correspond to electrode polarization when current flows. The electrolytical potential differences which exist between ore grains and pore water already without any current, are displaced when an external field is applied. Generally, the changes that occur in the negative or positive areas are opposite, the ore particles therefore appear to be polarized. Polarization is caused by the flow of current and is therefore called "galvanically induced polarization". It is not quite clear how the polarization voltages occur; there exist several types having different causes. Essentially, however, they depend on the type of pore liquid, on the ore and the local current density. The formation and decrease of polarization voltages show a certain displacement in time with respect to the amplitude of current density. Macroscopically, induced polarization therefore can be observed in two ways: After switching off a current impulse, there still exists a residual voltage between two points of the rock, which drops down to zero within several seconds. Its shape can be made visible, e.g., on an oscilloscope screen. Furthermore, a frequency-dependent complex conductivity is caused by electro-

chemical energy accumulation in a metallically mineralized zone when using a-c. Because of the large time constants of electrochemical processes, the region of maximum dispersion is to be expected at very low frequencies.

According to the two types of induced polarization, various quantities are calculated for characterizing rock that contains metals. When using d-c impulses, the decreasing residual voltage is measured at certain moments in the current breaks, and compared with the voltage applied externally. The ratio is then given in mv/volt or in mv. sec/volt, when integrating the drop voltage over a long period of time. The effective interfacial capacitance and the mean conductivity can be determined from the resulting time constants.

The second possibility lies in plotting the frequency curves of complex conductivity, with the real part and imaginary part or only the phase angle being measured. The quantity of polarization owing to metal orification is expressed by the increase of conductivity in percents at a certain frequency as compared to the d-c value. It is called "frequency effect":

$$\text{frequency effect} = \frac{Z(DC) - Z(AC)}{Z(DC)}$$

Z(DC) = d-c resistivity
Z(AC) = a-c resistivity

For the attempt of explaining theoretically the frequency curves of complex conductivity, schematic simplifications for the rock must be found and the respective electrical equivalent circuits. It is then possible to convert the values obtained from the time trend of the polarization voltage into quantities of the frequency behavior by means of a Fourier transformation.

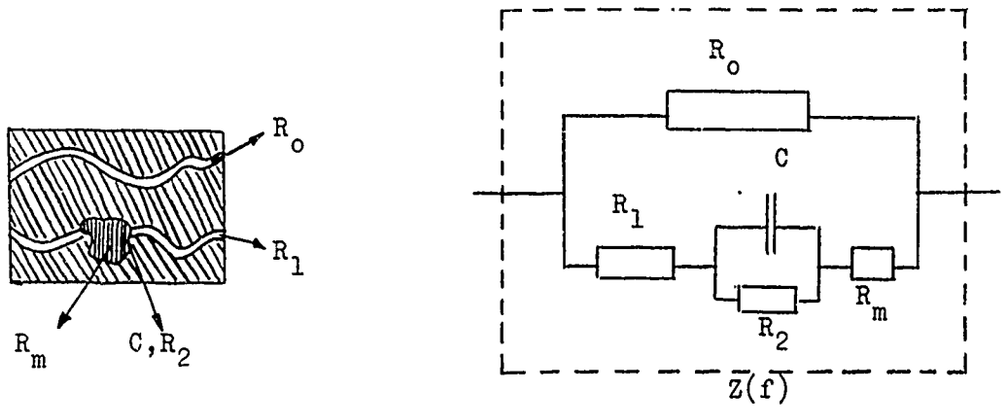

Schematic representation and equivalent circuit diagram according to Madden and Marshall [32] .

This diagram is based on the assumption that an ore sample contains channels that may go right through and are filled with pore liquid, others being interrupted by ore minerals. Pores that are completely blocked up by electron conductors represent a so-called "Warburg" impedance [35] owing to an electrochemical ion accumulation . Since an ion excess is compensated only by diffusion, such impedances show a frequency dependence of $\sim f^{-1/2}$. Rock which consists mainly of mineral grains contains mainly pore channels in which only part of the wall is formed by metallic minerals. Such combined current paths according to Madden and Cantwell [36] show a frequency dependence of $\sim f^{-1/4}$. Under certain restrictive assumptions that seem to be justified by numerous measurements, these authors obtain the simplified formula of "frequency effect"

$$\text{frequency effect} \simeq \frac{\frac{R_o}{Z_m} f^{1/4}}{1 - \frac{R_o}{Z_m} f^{1/4}}$$

in which R_o is the resistance of the pure ion paths, f is the measuring frequency and Z_m the electrochemically caused resistance of the blocked-up pores. In some cases, the frequency behavior of induced polarization could be represented by means of the

above formula down to frequencies of 0,1 Hz. An essential part apparently is played by the ratio of the impedances of current paths having pure ion conduction and those with a combined ion/electron conduction. The polarization effect caused by a certain part of volume of polarizable ore particles, thus entirely depends on their grain size and geometrical distribution within the pore volume. The insufficient consideration of this fact by the simple model is possibly one reason why it failed at low frequencies. Even if the model is used for explaining the time trend of the induced residual voltage, considerable differences are found with respect to the assumed value, if the voltage is measured some time after the exciting current impulse (this corresponds to lower frequencies). Collet [37] in his experiments with artificial samples found good agreement with small ore grains and considerable deviations in large ore grains. The used voltage, however, was so high that the electrochemical processes certainly were outside the linearity region.

Ores that show induced polarization, have about the same behavior during impedance measurements in a measuring capacitor as a dielectric with an extremely high dielectric constant. Polarization effects, however, occur at frequencies that are much too low for normal dielectric displacement currents. The expression "dielectric constant" therefore is slightly misleading since it suggests unusual dielectric phenomena. Actually, the high values (order of magnitude of 100 $\mu F/cm^2$) for the capacitances used in the equivalent circuit diagrams are due to the extremely low thickness of the electrochemical double layer.

5.1.4. Application of induced polarization in geological prospection

The effect of galvanically induced polarization for some time has been used in applied geophysics for prospecting sulfide ores [30], [31], since it might permit the distinction between highly conductive humid soils (disturbing inclusions in pure resistivity prospection) and highly conductive ore zones. Difficulties arise, however, by the fact that induced polarization is caused not only by electrochemical energy storage on electrolyte/metal interfaces, but also by mechanical (streaming potentials), thermal and electromagnetic storage, being expressed also in the existence of residual voltages after current has been switched off. Theoretical considerations by D.J. Marshall and T.R. Madden [32], however, showed that in rock only electrode polarization and membrane polarization contribute noticeably to galvanically induced polarization. Electrode polarization in the described way would suggest ore deposits, whereas the socalled membrane polarization occurs always when there are adjacent zones of mean transport numbers that are different for cations and anions in one rock complex. Almost all rocks absorb negative ions on their area of contact with pore liquid. Hence, there occurs an increased concentration of positive ions in a thin boundary layer. If the diameter of pore channels has the order of magnitude of the boundary layer thickness, the entire current is carried almost completely by positive ions. Polarization effects however occur only if such selective zones and opposite or neutral zones alternate with each other. These conditions can be found anywhere in nature, e.g., in loamy sand (large pore spaces between the sand grains, small pores in loam). Detailed examinations of membrane polarization during prospection for ground water were conducted by R.H. Frische et al [33] and V. Vacquier et al. [34].

5.1.5. Theory of induced polarization by W. Buchheim

Complex conductivity of a rock sample that contains finely distributed metallic inclusions, can be derived theoretically by still another method. W. Buchheim [38] and I.R. Wait [42] were the first to describe this theory which shall now be given in detail. Since in this theory the influence of the grain size and the volume portion of the ore grains is clearly demonstrated, we are going to compare it with the results of our own current experiments on artificial samples.

A suspension of metallically conductive spheres in an electrolytically conductive surrounding is used as a model.

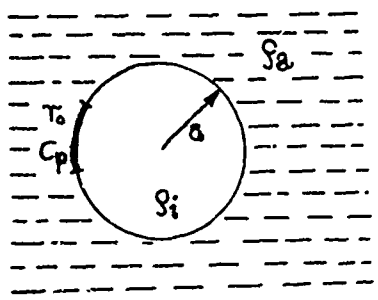

ρ_i [Ωm] specific resistivity of the spheres

ρ_a [Ωm] specific resistivity of the electrolyte

a [m] radius of the spheres

r_o [Ωm²] transition resistivity of the unit area

C_p [Fm⁻²] polarization capacitance of the unit area

j [am⁻²] current density

According to Buchheim [31], there exists the following potential difference transversal to the electrolyte - ore sphere interface if the current density is sufficiently small:

$$V(t) = V_o + r_o j(t) + \frac{1}{C_p} \int_{-\infty}^{t} j(t') \cdot N(t-t')dt'$$

where V_o is the potential difference between the metal and the electrolyte which exists always even without current flow. (Nernst). The term $r_o j(t)$ stands for the "resistance polarization", being a purely ohmic voltage drop owing to the poorly conductive boundary

layer (oxide film, discharge inhibition) at the ore grain surface. The integral term contains all the other kinds of polarization such as concentration polarization, activation polarization etc, in a phenomenological manner. The residual induction factor $N(t-t')$ describes the fact that after a current impulse, the polarization voltage gradually decreases to zero, i.e., that a charge element $j\,dt$ has less influence the further back it lies. Its accurate time function is not known in detail, it however depends on the number and kind of reactions that take place in the electrochemical boundary layer. Mathematically, it must have the following properties:

$$N(0) = 1 \qquad \frac{dN}{d\tau} < 0 \qquad \lim_{\tau \to \infty} N(\tau) = 0 \qquad t-t' = \tau$$

Esperiments by I. Schrage [39] showed only that the residual induction cannot be described by the simple formulation of

$$N(\tau) = \text{const.}\ e^{-\lambda\tau}$$

A more general form would be

$$\frac{1}{C_p} N(\tau) = \sum_i \frac{1}{C_{p_i}} e^{-\lambda_i \tau} .$$

where the quantities C_{p_i} and λ_i represent the capacitances and drop constants characteristic of the individual types of polarization.

From the boundary conditions, steadiness of the normal components of the current and potential drop, Buchheim [38] calculated the electric moment which such a polarized sphere assumes in a sinusoidal alternating field

$$m = a^3 E_o e^{i\omega t} \frac{\rho_a - \left(\rho_i + \frac{r_o}{a} + \frac{\int_o^\infty N(t) e^{i\omega t} dt}{aC_p}\right)}{\rho_a + 2\left(\rho_i + \frac{r_o}{a} + \frac{\int_o^\infty N(t) e^{i\omega t} dt}{aC_p}\right)}$$

If we compare it with the electric moment of a non-polarizable sphere,

$$m = a^3 E_o e^{i\omega t} \frac{\rho_a - \rho_i}{\rho_a + 2\rho_i}$$

the galvanically polarized sphere can be attributed the effective, complex, specific internal resistance

$$\rho_i^* = \rho_i + \frac{r_o}{a} + \frac{\int_o^\infty N(t) e^{i\omega t} dt}{aC_p} \quad .$$

According to Maxwell's considerations [43] the effective mean specific resistivity $\bar{\rho}$ of a suspension that consists of n^*/cm^3 polarizable spheres, is obtained by putting the electric moment of an assumed sphere cut out of a suspension equal to a homogeneous sphere of the same size which has exactly the desired specific resistivity $\bar{\rho}$. It must, however, be taken into consideration that the individual dipoles affect each other when the volume portion of the ore particle increases. Then not the outer field E_o acts upon each sphere, but the field

$$E = E_o + \frac{4\pi}{3} P = E_o + \frac{4\pi}{3} n^* a^3 \frac{\rho_a - \rho_i^*}{\rho_a + 2\rho_i^*} E$$

$$E = \frac{E_o}{1 - \frac{4\pi}{3} n^* a^3 \frac{\rho_a - \rho_i^*}{\rho_a + 2\rho_i^*}}$$

owing to polarization of the neighboring spheres. The mean, effective, specific resistivity of the suspension is thus obtained from the dipole moment

$$M_{suspension} = \frac{\frac{4\pi A^3}{3} n^* a^3 \frac{\rho_a - \rho_i^*}{\rho_a + 2\rho_i^*} E_o e^{i\omega t}}{1 - \frac{4\pi}{3} n^* a^3 \frac{\rho_a - \rho_i^*}{\rho_a + 2\rho_i^*}} = A^3 \cdot \frac{\rho_a - \bar{\rho}}{\rho_a + 2\bar{\rho}} E_o e^{i\omega t}$$

with

$$\bar{\rho} = \rho_a \frac{\rho_a(1 - 2v) + \rho_i^*(2 + 2v)}{\rho_a(1 + v) + \rho_i^*(2 - v)}$$

where $v = \frac{4\pi a^3}{3} n^*$ (volume of ore particles per cm^3). The latter formula according to the described theory holds for the model of a rock whose pore space contains an electrolyte with the specific resistivity ρ_a and in which metallically conductive ore particles are regularly distributed. In natural ore, the particles hardly ever occur in spherical shape. R. Rösler [41] therefore extended Buchheim's theory to rotation elliptic grains by developing the polarization potentials by the harmonic functions of the elongated, split-off rotation ellipsoid. In the limiting case, needle shaped and disk-like grains are also comprised. Rösler found out that for each shape and orientation of ore particles with respect to the outer field, an equivalent suspension of spheres can be given which has the same mean specific resistivity as the suspension of rotation elliptic particles.

5.1.6. Experiments on artificial ore samples

Naturally, the assumption of a suspension of polarizable particles in an electrolyte, on which theory is based, represents only a partial approximation to natural impregnation ores; but as experiments by W. Anders [40] showed, at least some effects of induced polarization can be made understood. In order to be able to interpret results of measurements made on natural ore samples, e.g., drill cores or field measurements, it is necessary to check the validity region of the model assumption on natural samples. For this purpose, artificial samples must be used, since here parameters such as:

specific resistivity of the pore liquid
pore volume
portion of ore volume
grain size of ore and gangue minerals

can be changed in a defined way. Thus, the values for r_o, C_p and $N(\tau)$ can be obtained and statements can be made on the grain size and portion of volume of unknown samples. The rock model used by W. Anders [40], a liquid mixture of sand, sulfuric acid and galena grains satisfied the model assumption fairly well, but does not coincide with the geometry of natural rock. We shall therefore examine artificial ore samples that permit variation of parameters occurring in theory, but are much closer to natural ore-containing rock. Samples that meet these requirements, are made of concrete, dolomite or quartz sand and ore grains of varying size. The resulting solid rock structure has an accurately defined porosity containing ore particles of known grain size in various portions of volume. The porosity and thus the ratio between electrolytic current paths and metallic conductors is affected by the choice of the water-cement factor and the size of sand grains. The ore we chose first was copper pyrite $CuFeS_2$, since there

exist plenty of natural samples of this ore, with which the artificial samples can be compared. At the same time, various a-c conductivity measurements are made in drill holes by methods that shall be used in the copper mine of Mitterberg, Salzburg. Further experiments are scheduled for samples containing galena PbS, and zinc blende ZnS.

The time constant of the electrochemical processes on the phase boundaries of water and ore lie partly in the order of seconds. Hence, impedance measurements shall be made at frequencies of down to 0,01 Hz. For the frequency range of 30 Hz - 300 kHz, an impedance bridge (General Radio) is available whose measuring range had to be extended up to 10 mhos by a conductance decade, because of the high ore conductivity. Frequencies < 30 Hz require the construction of a new bridge arrangement permitting the measurement of impedances with real parts of up to 10 mhos and imaginary parts of up to 1000 µF at frequencies ranging from 0,01 Hz to 1 kHz. The artificial ore samples of the above-mentioned composition are made in the form of thin disks and are then studied in the measuring capacitor described in [19] . The frequency behavior of liquids used for filling up the pore space, is determined in a specially constructed measuring cell that permits a continuous change of electrode spacing and the use of various electrode materials.

At present, the number of measurements is too small as to justify the report on details of the experiments and their results at this moment.

5.2. Construction of an electrode

When determining the electrical conductivity of rock in drill holes, certain difficulties of contacting arose which required the observation of various conditions. The contact area on the wall of the drill hole should be as small as possible so that a high specific pressure per unit area is attained which makes it possible that pollutions on the surface to be contacted can be pushed through as the device with the electrodes advances. The pressure per unit area must be variable so that the probe can be advanced also at places where the surface is very rough and where the wall of the drill hole is broken out or has small cavities. In order to obtain a definite point of contact, only the part used for contacting may have voltage, all other parts of the mechanism must be insulated. For the case of a possible failure of power for the required pressure, the probe must assume automatically its minimum diameter so that it can be saved. It must be constructed so that it does not catch on wall protrusions or get stuck on the way. Naturally, the probe must have a certain mechanical strength, being unaffected by humidity, pollution and rough handling.

In order to meet these requirements it is recommended that compressed air should be used for operating the probe. It is available in almost any mine, dosage is easy, and being fed through a sufficiently dimensioned hose, it may be simultaneously used for moving the probe. Experience we gathered during measurements with various test probes in Bleiberg, Kärnten in fall 1967, was utilized for developing and designing a new device last summer. In this device, all mobile parts except for the electrodes are inside metal cylinders. The diameter of the instrument was reduced to a minimum as to permit measure-

ments also in drill holes of small size.

On the whole, the probe consists of two cylinders that can be moved on a supporting tube. Between their front surfaces that face each other, there are six flat bands mounted symmetrically and parallel to the longitudinal axis. If the cylinders approach each other, the flat bands bend outwardly, contacting the wall of the drill hole.

Fig. 5.1 shows a section through such a cylinder. A brass tube -B- 35 mm in diameter and with a wall thickness of 2 mm is firmly connected with the front end pice -F- and the rear end pice -H-. Piston -K- is mounted firmly on the supporting tube, being sealed off with a leather sleeve -L 1- which is held and centered by a brass ring -C-. The parts G, H and K are made of insulating plastic. Compressed air can be filled into the space between the piston -K- and the front end pice -F- through holes in the supporting tube, thus moving the cylinder toward the front end piece. Current supply also goes through this tube with an insulated cable -D- which enters the cylinder space through one of the air holes, contacting one of the longitudinal screws. These screws hold the hexagonal band electrode carrier -G- (made of brass) on part -F-, pressing at the same time the sealing sleeve -L 2- against the supporting tube by means of a ring -E-. The rear end pice -H- runs on a cylinder -I- which is mounted adjustably on the supporting tube, having a disk -J- on its inner front face by which part -H- is stopped during the working stroke. The bridge -A- connected with -I- runs in a groove cut into -H- so that the cylinder cannot be twisted with respect to the supporting tube. The six spring plates -M- which are used for contacting, are screwed on the carrier -G- and can easily be exchanged. Inside the spring plates there lies a compression spiral spring which brings the cylinders back into their original position when there is no compressed air pressure. A distance piece in the middle between the two cylinders stops the spring plates from

bending inward.

There are threads on either side of the supporting tube. On one side a connecting piece can be put on by which the electric cables are tightly guided into the tube and which carries a connection for the compressed air tube. The other side can either be sealed with a cap nut or another such probe system can be connected, thus forming a second contacting plane. The cable for the second system up to the inlet piece runs also inside the supporting tube. The distance between the two probes can be varied by intermediate tubes of adequate length.

6. FIELD STRENGTH RECORDINGS

The field strengths of NAA and GBR were recorded continuously above ground at the Aldrans station near Innsbruck and below ground with interruptions in the mine of Großkogl, end of Südostschlag. The recordings on a multicolor dotted line strip chart recorder so far have been made in linear amplitude scale. An evaluation is very time consuming especially when mean values are to be taken over large periods of time and when comparing various records. It is practically impossible to study the collected material with the desired thoroughness, for example with respect to seasonal or climatic influences by means of statistical methods. Preparations have therefore been made to proceed to logarithmic representation.

An estimation of the existing records showed that a span of about 30 dB f.s. would be the most suitable compromise between resolution and necessary range reserve. For this comparatively small range it proved favorable not to utilize the usually applied logarithmic relation between reverse current and voltage of a pn-junction as a logarithmic element, but to use selected diodes in the forward direction. However, the relation between forward current and forward voltage is strictly logarithmic only in a much smaller range, namely nc more than 40 - 50 dB as compared to an exactly logarithmic region of up to 100 dB with special logarithmic diodes in off-direction. The useful on range lies at currents of about 10^{-4} to 10^{-2} a, thus being highly favorable for use in transistorized circuits. This is especially true with respect to the impairing climatic conditions under which the instruments operate at times. Here, instead of the temperature dependence of the reverse current, on the whole we have that of the forward voltage, i.e., practically that of diffusion voltage of the junction. The

which is much less subject to exemplary variations, changes practically linear with temperature in the temperature range of interest, yielding much simpler possibilities of temperature compensated circuits. The developed circuit despite its striking simplicity has a conformity and constancy that is higher than fractions of a dB. There exists an unavoidable deviation from linear response in the existing dotted line strip chart recorders because of the tangent errors, as well as in continuous line recorders despite the elliptic pen guide system. As this deviation is noticeable especially when comparing continous line and dotted line recorders, an improvement of the circuit properties would not be highly advantageous. However, in the medium recording range, the accuracy of direct comparison is still better than 1 dB, even when comparing the records of various recorders.

The hitherto used method of amplitude measurement of keyed signals by means of peak rectification and carefully tested rise time and fall time constants shows a satisfactory amplitude response when keying is changed (especially A_1 - F_1). When comparisons at the same geographical location are made, it also shows an apparently sufficient independence of various noise levels. A detailed examination, however, showed that there occur inadmissible deviations when there are differences in the signal-to-noise ratio which is the case especially when records above ground and below ground are made and compared. Intensive studies for improvement have therefore been made. The obtained solution shall be published in the near future in a separate Scientific Report. It brings a considerable improvement especially when the noise shows high peaks frequently caused by atmospherics and by nearby man made interference. It is based on the following principle: The signal is being rectified in a peak rectifier whose rise time is short enough as to reach full charge within the time period of one Morse dot. The fall time has been chosen so that the breaks between the dots are bridged without great voltage drops. The voltage on

the charging capacitor is then at least as high as the peak voltage of the signal. It is superimposed by sporadic peaks of the noise which have different abundance and amplitude. Another inversely poled diode which is connected via an impedance transformer, scans the voltage minimum of the peak rectifier, which corresponds to the signal voltage and is independent of the number and height of noise pulses. The time constant of the second rectifier may be a multiple of that of the signal rectifier and can be chosen at optimum for the used recorder.

The used ferrite antennas were made even less sensitive to nearby interference by careful balancing, especially with the use of bifilar windings. A separate examination on the attainable basic limiting sensitivity of magnetic pick-ups connected to different amplifiers was made and will be described in a Scientific Report. The result permits the following conclusions: for measuring the field strength of our own or of alien transmitters, the field strength of the expected noise above ground is always (and below ground almost always) so high that it induces a voltage that lies far above the noise of a carefully constructed input stage. If, however, the noise field intensity itself is to be studied, it will be necessary to utilize the limiting sensitivity as much as possible. Based on available active components for the input stage and ferrite rods for the antenna, we get clear conditions for optimizing the antenna winding and the transformer. Since the distinct directivity of the ferrite rod antenna has a disturbing effect on some experiments, the suitability of a short electric dipole was studied with respect to the noise. Surprisingly enough, its theoretical limiting sensitivity is almost two powers of ten better, proceeding again from materializable techniques. In practical use, however, it cannot be utilized, since there are too many man-made interferences in the near region at VLF wavelengths which at the point of reception are

received mainly in the form of electric noise field strengths. The equivalence between magnetic field strength and electric field strength in wave propagation described by the characteristic impedance of the vacuum (or air) holds only for remote sources, i.e., for an almost plane wave and propagation through air.

For measuring the field strength and field direction of the incident waves from remote source, depending on the point below ground, a fully transistorized portable receiver was built which is equipped with a single-track line recorder and all necessary devices such as BFO and calibration generator. It also permits to make an exact time comparison of field strength fluctuations against records from an above ground station.

7. WHAT HAPPENED IN 1968 ?

This is to give a brief chronological review of events and work of the project year of 1968 not included in the scientific part of the present report.

At the end of February, Mr. Norbert N e s s l e r got his doctor's degree (Ph.D.). The subject of his thesis was "The propagation of long electromagnetic waves through homogeneous and inhomogeneous solids".

In the middle of March, Dr. Wolfram B i t t e r l i c h, head of the VLF project, made his habilitation in the field of electronics. Besides a number of related studies, his habilitation work entitled "Propagation of VLF waves through the interior of the Earth" was published in Acta Physica Austriaca (26, 1967).

Mr. B l a c k s m i t h (AFCRL) who visited us in the middle of March for discussing the project work, during an excursion into the mine of Großkogl, was able to check the progress of our studies.

On the occasion of a visit to Siemens Halske in Munich by our co-workers Dr. N. N e s s l e r , W. K e l l n e r and R. L u k a v e c , a special order was given to have special ferrite cores made for transmitter output stages in the LF-region. They were delivered completely free of charge.

R. L u k a v e c together with T. E l s t e r gave an interim report about the work on helical antennas in Scientific Report Nr. 6, "Some Properties of Helical Antennas at Low Frequencies".

In Scientific Report Nr. 7 Dr. N. N e s s l e r reported on a chapter of his thesis: "Measurement of the conductivity and dielectric constant by means of wave propagation". For test drilling for geoelectrical examination, comprehensive preparations had to be made as to adapt the geological desires to the

technical possibilities. For meeting the great demand for compressed air of the drilling machine, the mine compressor was used and in addition, an electrical compressor for 6 m^3/min at 6 atm plus air vessel had to be transported into the mine where it was connected. This device was lent by Messrs. Innerebner u. Mayer. The above devices were supplemented by a compressor (Diesel) borrowed from Jenbacher Werke.

The drill work was performed by a team of the copper mine of Mitterberg (Salzburg) (core drilling 47 mm ∅ outside and 28 mm core ∅). During the two weeks of drilling, our team members T. E l s t e r and Chr. G r i s s e m a n n were of great technical help. The cable from the transformer to the electric compressor (40 kw motor!) for example proved too weak and had to be reinforced (4 × 25 mm^2, 300 m long, borrowed from TIWAG) or , another example, the thick-walled plastic hoses used for compressed air withstood a pressure of 6 atm. only at low temperatures so that a large radiator had to be built in.

Despite the numerous difficulties, a total of 76 m core drilling of 47 mm ∅ was attained.

Dr. R. S t e i n m a u r e r , Univ. Prof. and head of the Physics Institute, and Dr. J . K o l b , Univ. Prof. (second department of experimental physics) visited us during the drilling period in the mine of Großkogl and at the same time had a look at the new transmitter, above all the new underwater antenna.

For conducting measurements in the drill holes, Chr. G r i s s e m a n n and T. E l s t e r designed and constructed special probes, the technical construction and mechanical work being made by Mr. E l s t e r.

During the period of report, Dr. N. N e s s l e r started again studies with the large transmitting antenna SA 9. The antenna, size 40 x 40 m, had been built in 1964 and had not been changed since then. Careful repair work was therefore necessary. The insulators had to be cleaned, some of them replaced. This work was very hard, especially in the vertical shafts.

The use of new high quality capacitors for tuning to resonance resulted in a flash-over at the humid insulators, thus causing failures and time consuming repair work.

At the same time, high-stability low-noise antenna pre-amplifiers were developed. A detailed report on this subject and on the propagation measurements is given in the scientific part of the present report.

On 30 July, Mr. L.N. M o l n a r and Mr. R. W. S t r i c k l a n d came to Innsbruck (EOAR, American Embassy Brussels) for discussing various project problems, and they also had a look on our work in the mine. Mr. J. P. W i l k e visited us on 1 October.

In the middle of September, W. K e l l n e r and R. L u k a v e c attended the 1968 IEEE International Antennas and Propagation Symposium and 1968 Fall-URSI Meeting in Boston where they reported on their work. W. K e l l n e r gave a report on "Electric rock characteristics from the field structure of a magnetic dipole immersed in a conducting medium" and R. L u k a v e v on "Measured properties of small self-resonant helical antennas for application in a dissipative medium".

At the ÖSTERR. PHYSIKERTAGUNG (Austrian Symposium on Physics) in Graz at the end of September, Dr. N. N e s s l e r gave a report on "The measurement of dielectric constants and conductivity on solid rock by means of wave propagation."

At the beginning of October, Dr. N e s s l e r and T. E l s t e r took down an inventory record of all project property (instruments, components, etc.).

In an interview by the Austrian Radio (Ö 1), end of October, Dr. N e s s l e r was given the opportunity to report on the project work in the series "The research work of our Universities".

Dr. N. N e s s l e r , W. G r a d l, W. K e l l n e r and R. L u k a v e c visited the electronic exhibition in Munich, beginning of November, where they gathered information

on the most recent achievements in electronics.

In Scientific Report Nr. 8, R. L u k a v e c reported on the most recent results of his work with the helical antenna, under the title of "Measured properties of small self-resonant helical antennas for application in dissipative media."

H. W ö b k i n g handed in his thesis on "The frequency response of the dielectric constant and the electric conductivity of rock and on the importance of the electric rock parameters for determining rock fabric quantities". We congratulate him to his successful exams. He is now working for the Montanwerk Brixlegg, but will still be available also for project work.

T. E l s t e r left the project team for professional reasons on 15 October 1968. We thank him for his assistance.

§. REFERENCES

[1] Scientific Report No. 6: Some Properties of Helical Antennas at Low Frequencies. Contract No. 61(052)-902, 20 April 1968.

[2] H. HEYNISCH: Die Ausbreitung von Mikrowellen und langen Wellen auf einer Wendelleitung mit Dielektrikum und koaxialem Außenleiter. A.E.Ü. vo. 17 (1963) Nr. 5.

[3] I.A. DOMBROWSKI: Antennen. Verlag Technik, Berlin, Porta Verlag München, 1957, p. 37.

[4] I. A. STRATTON: Electromagnetic Theory. McGraw Hill Book Co. Inc. New York 1941.

[5] Charles L. MARQUANT: The Near Electromagnetic Field. Electro-Technology Nr. 61, Jan 1964.

[6] 2nd Technical Annual Report: On the propagation of VLF waves in solids, 61(052)-490 Dec. 1962.

[7] K. BLANK: Raumladungserscheinungen in flüssigen und festen Ionenleitern. Nachrichtentechnische Fachberichte (NTF) 29 pp. 41-50 (1964).

[8] Hans WÖBKING: Über den Frequenzgang der Dielektrizitätskonstante (DK) und der elektrischen Leitfähigkeit (LF) bei Gesteinen und über die Bedeutung der elektrischen Gesteinsparameter für die Bestimmung gefügekundlicher Größen. Dissertation, Universität Innsbruck, Juni 1968. (Doctor's thesis at Innsbruck University, June 1968).

[9] Scientific Report No. 4. Determination of the Mean Values of Conductivity and Dielectric Constant from The Field Structure of A Magnetic Dipole. Contract No. 61(052)-902. 20 June 1967.

[10] Walter A. KELLNER: Electrical Rock Characteristics from the Field Structure of a Magnetic Dipole in a Conducting Medium. Paper presented at the '68 G-AP Symposium in Boston, Mass.

[11] Univ. Doz. Dr. Wolfram BITTERLICH: Die Ausbreitung von VLF-Wellen durch das Erdinnere. Acta Physica Austriaca. Bd. XXVI, 1967 Heft 2-3.

[12] Frank M. GREENE: The Near-Zone Magnetic Field of a Small Circular Loop Antenna. Journal of Research of the National Bureau of Standards Section C.- Engineering and Instrumentation. Vol. 71C. No. 4, October-December 1967 pp. 329-326.

[13] Harold A. WHEELER, Fellow IRE: Fundamental limitations of small antennas. Proceedings of the IRE. December 1947; pp. 1479 - 1484.

[14] Scientific Report No. 5: Frequency Dependence of the Field Strength Components of a Dipole Embedded in a Conducting Medium. 30 November 1967. Contract Nr. 61(052)-902.

[15] Fourth Annual Report (Vierter technischer Jahresbericht): On the propagation of VLF waves in solids (Über die Ausbreitung von VLF-Wellen in Festkörpern). December 1964, Contract Nr. 61(052)-490, Dr. W. Bitterlich, Innsbruck.

[16] Scientific Report Nr. 10: Magnetic dipole antennas for receivers. Contract Nr. 61(052)-490, Dr. W. Bitterlich, Innsbruck, Sept. 1964.

[17] Technical Note Nr. 3: Determination of rock conductivity from VLF propagation measurements. R. Hommel. Contract Nr. 61(052)-490, July 1963,

[18] N. NESSLER, Die Ausbreitung langer elektromagnetischer Wellen durch homogene und inhomogene feste Medien, Dissertation Oktober 1967 (Thesis) , Universität Innsbruck.

[19] O. WÖRZ: Über die Leitfähigkeit σ und die Dielektrizitätskonstante ε von Gesteinen Dissertation (Thesis) Mai 1965, Universität Innsbruck.

[20] W. BITTERLICH: Einführung in die Elektronik, Springer Verlag 1967

[21] Final Scientific Report: On the propagation of VLF waves in solids. Contract 61(052)-490, December 1965, Dr. W. Bitterlich, Innsbruck.

[22] L.A. AMES, J.W. FRAZIER, A.S. ORANGE: Geological and geophysical considerations in radio propagation through the Earth's crust. IEEE Trans. AP-11, 3, 369-371 (May 1963)

[23] O. GRÖBNER: Über die Ausbreitung sehr langer (VLF) Wellen im Gestein. Diss. Innsbruck, July 1964 (Thesis)

[24] J.R. WAIT: The magnetic dipole antenna immersed in a conducting medium. Proc. I.R.E. 40, 1244-45 (Oct. 52)

[25] J.R. WAIT: Insulated loop antenna immersed in a conducting medium. Journ. Res. N.B.S. 59, 2, 133 - 137 (Aug. 57).

[26] J.A. STRATTON: Electromagnetic theory, McGraw Hill, New York, 1941

[27] A. LINDER: Statistische Methoden, Birkhäuser, Basel 1964

[28] G. JAFFE: Ann. Physik 16 (1933) S. 217 ff.

[29] R.J. FRIAUF, Polarization effects in the ionic conductivity of silver bromide. J. Chem. Physics, 22 1329-1338 (1954)

[30] D. BLEIL: Induced Polarization, a method of geophysical prospecting. Geophysics, 18 (1953) pp 636.

[31] W. BUCHHEIM: Theoretische Betrachtungen und Versuche zur Unterscheidung elektrolytischer und metallischer Stromleitung im Boden beim Schürfen auf Sulfiderze. Geologie 3 (1954) S. 1009-1035.

[32] D.J. MARSHALL and T.R. MADDEN: Induced polarization, a study of its causes. Geophysics 24 (1959) pp 790-816.

[33] R.H. FRISCHE and H. BUTTLAR: A theoretical study of induced electrical polarization. Geophysics 22 (1957) pp 688 - 706.

[34] V. VACQUIER et al.: Prospecting for ground water by induced electrical polarization. Geophysics 22 (1957) pp 660 - 687.

[35] E. WARBURG: Annalen der Physik (1899) S. 493 ff.

[36] T.R. MADDEN, T. CANTWELL: Induced polarization, a review preprint from SEG Mining Geophysics volume (1963).

[37] L.S. COLLET: In overvoltage research and geophysical applications, Pergamon Press, Chap. 5 (1959).

[38] W. BUCHHEIM: Zur Theorie der induzierten galvanischen Polarisation elektrisch aktiver Imprägnationserze. Freiberger Forschungshefte C 28 (1956).

[39] J. SCHRAGE: Experimentelle Untersuchungen zur induzierten galvanischen Polarizsation an Sulfiderzen. Freiberger Forschungshefte C 28 (1956)

[40] W. ANDERS: Versuche zur induzierten galvanischen Polarisation an Gesteinsmodellen. 426 Bergakademie 8/1958.

[41] R. RÖSLER: Die galvanisch induzierte Polarisation an Dispersionen rotationselliptischer Teilchen, Freiberger Forschungshefte C 67 (1959).

[42] I.R. WAIT: A phenomenological theory of induced electrical polarization, Can. J. Phys. vol. 36 (1958).

[43] I.C. MAXWELL: Lehrbuch der Elektrizität und des Magnetismus. Deutsche Ausgabe von B. Weinstein (Berlin 1883) Bd. 1.

INHALTSVERZEICHNIS DES JAHRESBERICHTES 1966

INHALTSVERZEICHNIS DES JAHRESBERICHTES 1967

Liste der Scientific Reports
1966-1968

Scientific Report No. 1, 1 March 1967: The Helical Antenna And Its Problems

Scientific Report No. 2, 15 April 1967: Propagation of Long Electromagnetic Waves Through Rock

Scientific Report No. 3, 25 April 1967: The Frequency Dependence of the Dielectric Constant And Conductivity of Rock And Its Relation to Quantities of Rock Fabric

Scientific Report No. 4, 20 June 1967: Determination of The Mean Values of Conductivity And Dielectric Constant from The Field Structure of A Magnetic Dipole

Scientific Report No. 5, 30 Nov. 1967: Frequency Dependence of The Field Strength Components of A Dipole Embedded in A Conducting Medium.

Scientific Report No. 6, 20 April 1968: Some Properties of Helical Antennas at Low Frequencies

Scientific Report No. 7, 25 July 1968: Measurement of The Conductivity And Dielectric Constant of A Homogeneous Medium By Means of Wave Propagation

Scientific Report No.8, Dec. 1968: Measured Properties of Small, Self-resonant Helical Antennas at Low Frequencies for Application in Dissipative Media.

CONCLUSIONS,
RECOMMANDATIONS

The studies on helical antennas show relations between the geometrical dimensions and electric properties.

Various methods of measuring rock parameters and radiation characteristics of frame antennas contribute to a better understanding of the propagation mechanism of VLF and LF waves, giving clues for the continuation of theoretical calculations.

Artificial orifications yield nclear conditions of measurement for the geoelectrical studies on samples and bore holes planned for the near future. Measurements over large distances are informative despite the considerable technical difficulties, offering a large field for attenuation and polarization studies.

Continuous records of remote VLF transmitters (GBR, NAA etc.) supplement our field of work comprising near field measurement and global radio communication.

In continuation of this program, theoretical and experimental examinations are scheduled on small helical antennas and frame antennas; far field measurements are also to be extended.

DOCUMENT CONTROL DATA - R&D

AD 687751

1. ORIGINATING ACTIVITY (Corporate author)
University of Innsbruck
Innsbruck, Austria
Univ. Doz.Dr. W. BITTERLICH
VLF Project

2a. REPORT SECURITY CLASSIFICATION

2b. GROUP

3. REPORT TITLE

VLF PROPAGATION THROUGH SOLID AND LIQUID MEDIA

4. DESCRIPTIVE NOTES (Type of report and inclusive dates)
Scientific, Final Report

5. AUTHOR(S) (Last name, first name, initial)
Univ. Doz. Dr. W. Bitterlich, W. Gradl, Chr. Grissemann, W. Kellner, R. Lukavec, T. Elster, Dr. N. Nessler

6. REPORT DATE	7a. TOTAL NO. OF PAGES	7b. NO. OF REFS
31 December 1968	121	43

8a. CONTRACT OR GRANT NO.
AF 61(052)-902
b. PROJECT AND TASK NO.
4600-10
c. ELEMENT
6240545 F
d. SUBELEMENT
671600

9a. ORIGINATOR'S REPORT NUMBER(S)

9b. OTHER REPORT NO(S) (Any other numbers that may be assigned this report)

10. DISTRIBUTION STATEMENT

THIS DOCUMENT HAS BEEN APPROVED FOR PUBLIC RELEASE AND SALE; ITS DISTRIBUTION IS UNLIMITED

11. SUPPLEMENTARY NOTES
Tech, Other

12. SPONSORING ACTIVITY
UNITED STATES GOVERNMENT

13. ABSTRACT

Impedance, current distribution and radiation characteristics were measured on various types of antennas in air and in water in continuation of examinations on small self-resonant helical antennas.

Two methods of determining the conductivity and dielectric constant of a dissipative medium with graphical evaluation are described as an example of applying measurements of frame antenna directivity patterns.

Radio communication was reached between the mine of Schwaz and the mine of St. Gertraudi by means of a 1600 m² frame antenna and a new low-noise receiving amplifier.

Preliminary examinations were made for geoelectric ore examinations, and a measuring probe was built for drill hole examinations.

1473

14. KEY WORDS	LINK A		LINK B		LINK C	
	ROLE	WT	ROLE	WT	ROLE	WT
Small helical antennas						
Low frequencies						
Network model						
Lossy media						
Electrical properties of fresh water						
Propagation of electromagnetic waves						
Rock conductivity						
Dielectric constant of rock						
Measurement of rock parameters						
Measuring accuracy for ϵ and σ						
Gaussian positions						
Noise measurements						
Long period registration						
Registration of N&A and GBR						